Cosmic Reionization and the End of the Dark Ages

Paul R. Shapiro

University of Texas at Austin

"The Standard Model of the Universe,"

12th Paris Cosmology Colloquium, Ecole Internationale Daniel Chalonge,

Observatoire de Paris

July 18, 2008

Cosmic Reionization and the End of the Dark Ages

Paul R. Shapiro

University of Texas at Austin

Collaborators:
Ilian Iliev (U. Zurich)
Ue-Li Pen, J. Richard Bond, Patrick McDonald (CITA/U.Toronto)
Garrelt Mellema (Stockholm U.), Hugh Merz (U. Waterloo)
Kyungjin Ahn (Chosun U./Korea), Leonid Chuzhoy (U.Chicago)
Marcelo Alvarez (KIPAC/Stanford), Benedetta Ciardi (MPA),
Eiichiro Komatsu, Jun Koda, Elizabeth Fernandez (U. Texas)

The Epoch of Reionization

- Absorption spectra of quasars have long shown that the intergalactic medium at redshifts $z < 6$ is highly ionized, with a residual neutral H atom concentration of less than 1 atom in 10^4 .

  ===> universe experienced an “epoch of reionization” before this.

The Epoch of Reionization

- Absorption spectra of quasars have long shown that the intergalactic medium at redshifts $z < 6$ is highly ionized, with a residual neutral H atom concentration of less than 1 atom in 10^4 .

  ===> universe experienced an "epoch of reionization" before this.

- Sloan Digital Sky Survey quasars have been observed at $z > 6$ whose absorption spectra show dramatic increase in the H I fraction at this epoch as we look back in time.

  ===> epoch of reionization only just ended at $z \gtrsim 6$.

SDSS quasars show Lyman α opacity of intergalactic medium rises with increasing redshift at z = 6 ➔ IGM more neutral ➔ reionization just ending?

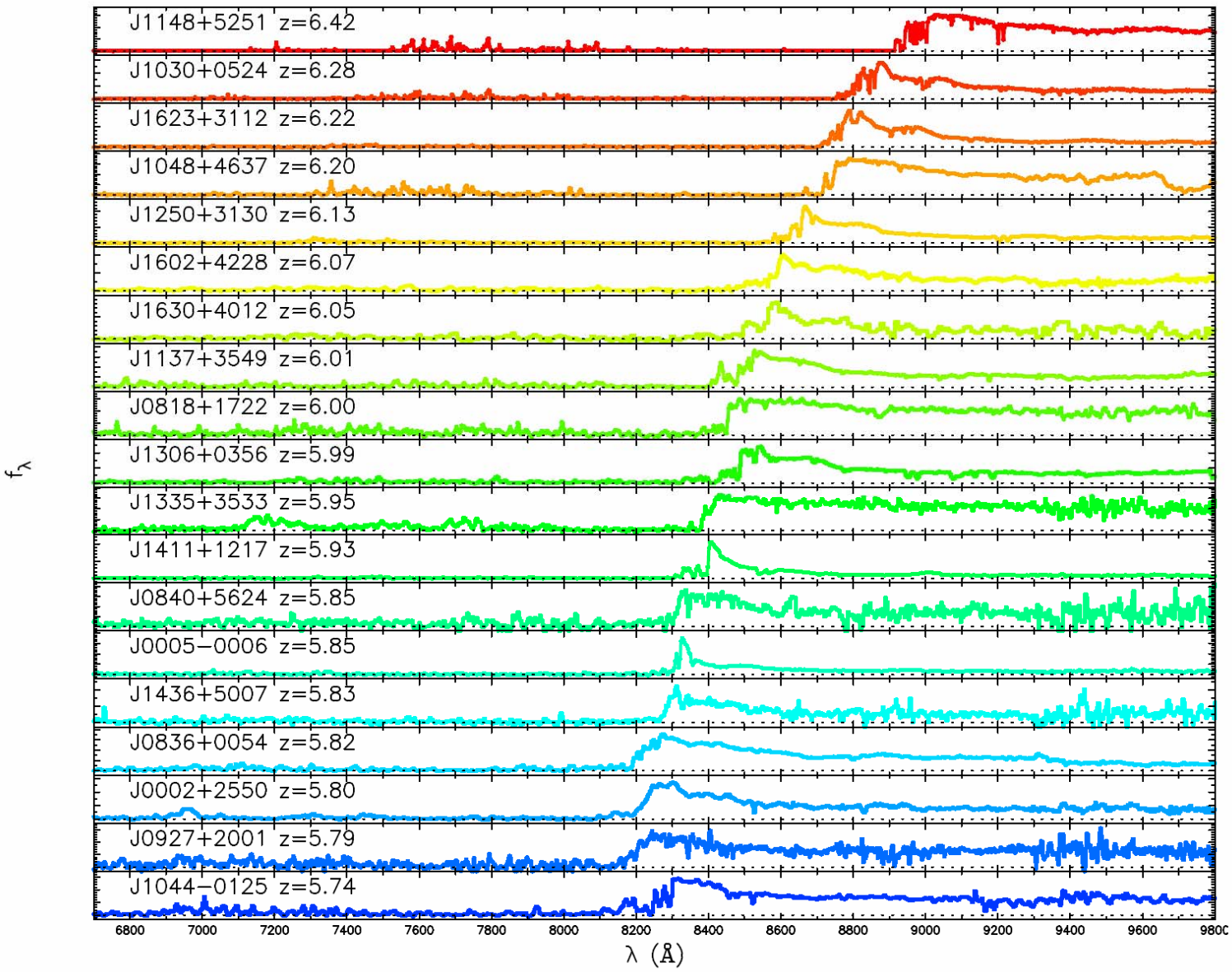

Fan et al (2005)

The Epoch of Reionization

- Absorption spectra of quasars have long shown that the intergalactic medium at redshifts $z < 6$ is highly ionized, with a residual neutral H atom concentration of less than 1 atom in 10^4 .

  ===> universe experienced an "epoch of reionization" before this.
- Sloan Digital Sky Survey quasars have been observed at $z > 6$ whose absorption spectra show dramatic increase in the H I fraction at this epoch as we look back in time.

  ===> epoch of reionization only just ended at $z \gtrsim 6$.
- **The cosmic microwave background (CMB) exhibits polarization which fluctuates on large angular scales; WMAP finds that almost 10% of the CMB photons were scattered by free electrons in the IGM**

  ===> IGM must have been ionized much earlier than z = 6 to supply enough electron scattering optical depth

  ===> reionization already substantial by $z \gtrsim 11$

EoR Probes the Primordial Power Spectrum on the Smallest Scales

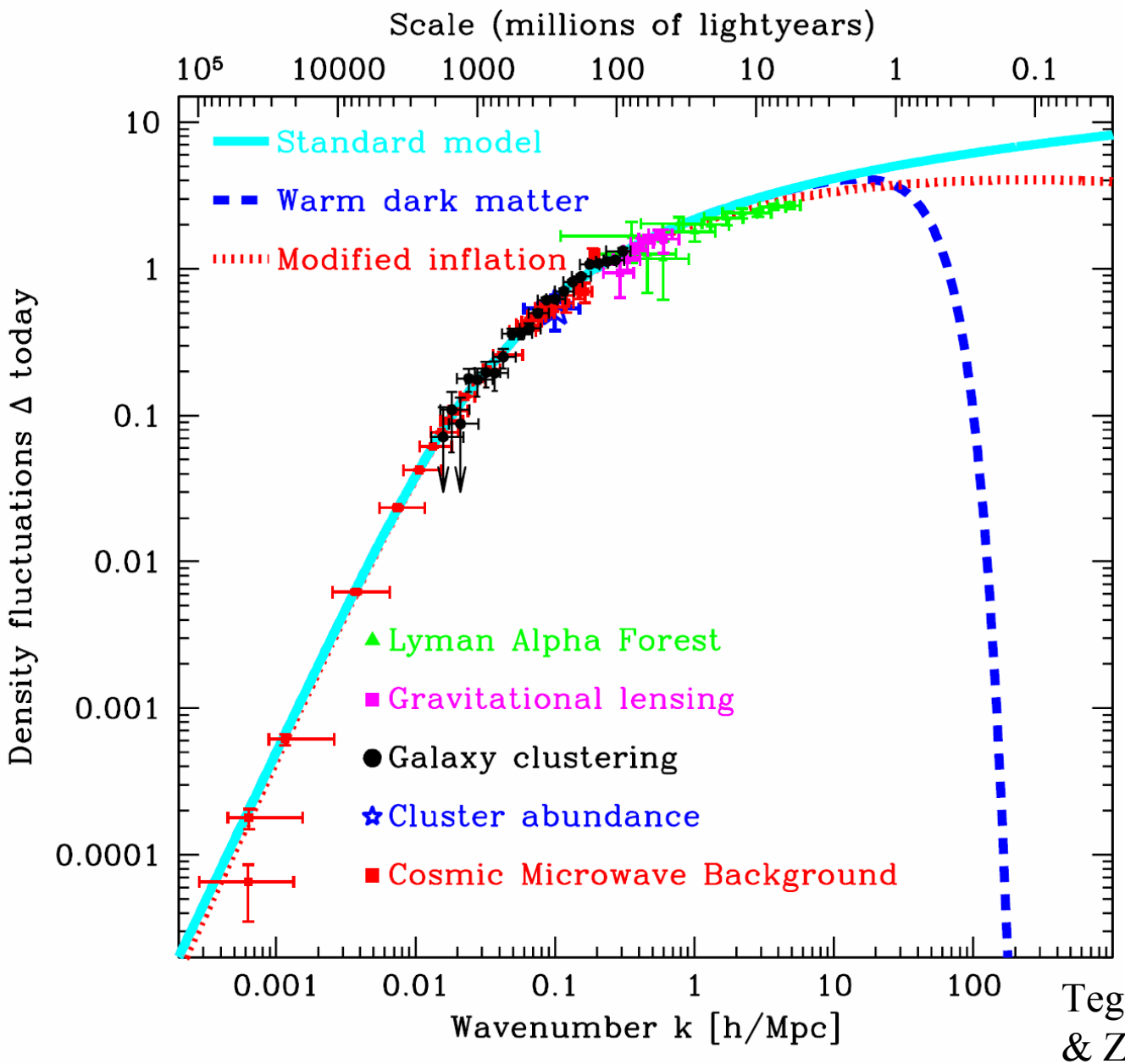

Tegmark
& Zaldarriaga (2008)

Structure formation in ΛCDM at z = 10

simulation volume = $(100\ h^{-1}\mathrm{Mpc})^3$, comoving

1624^3 particles on 3248^3 cells

Projection of cloud-in-cell densities of 20 Mpc slice

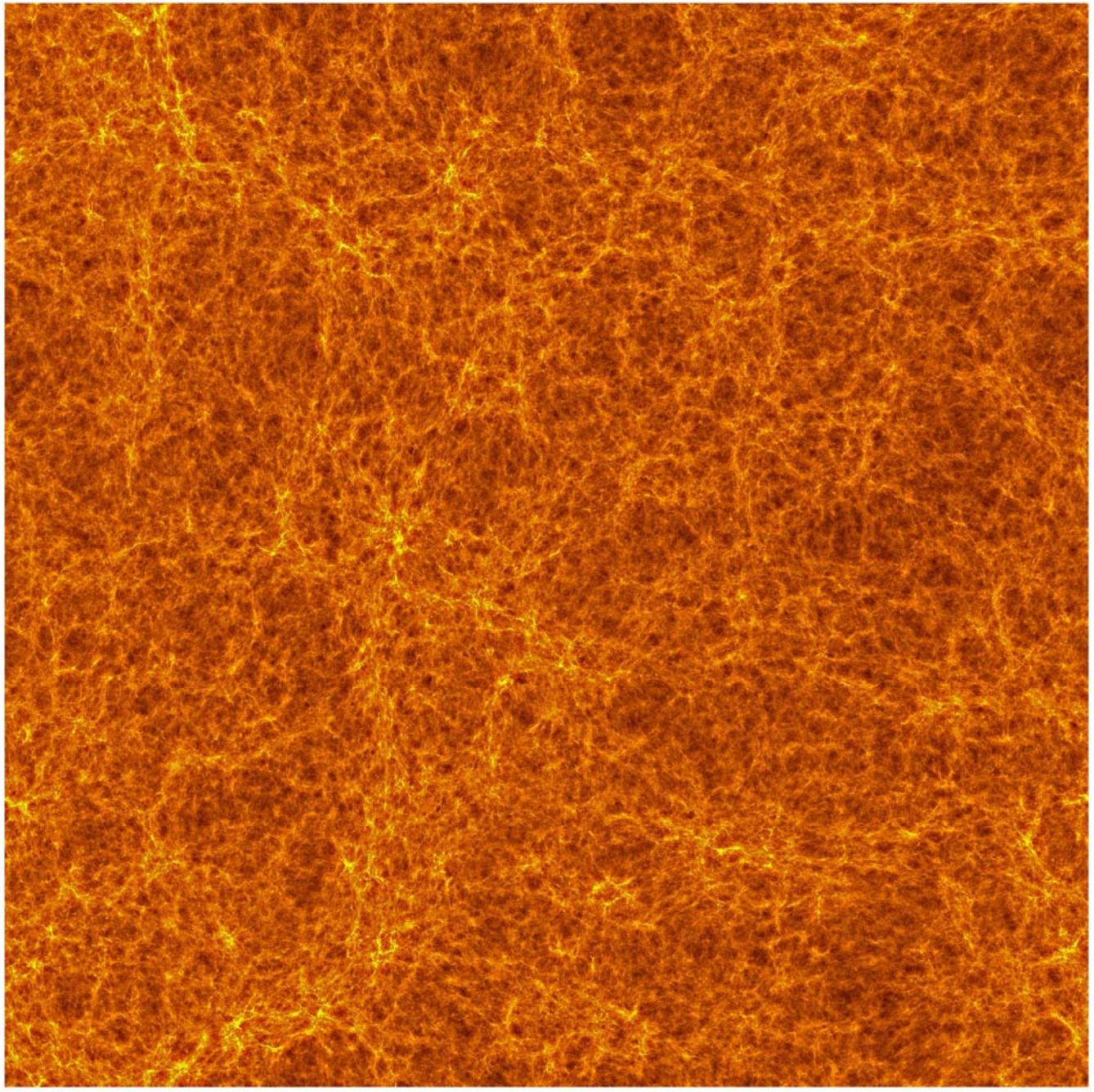

A Dwarf Galaxy Turns on at z=9

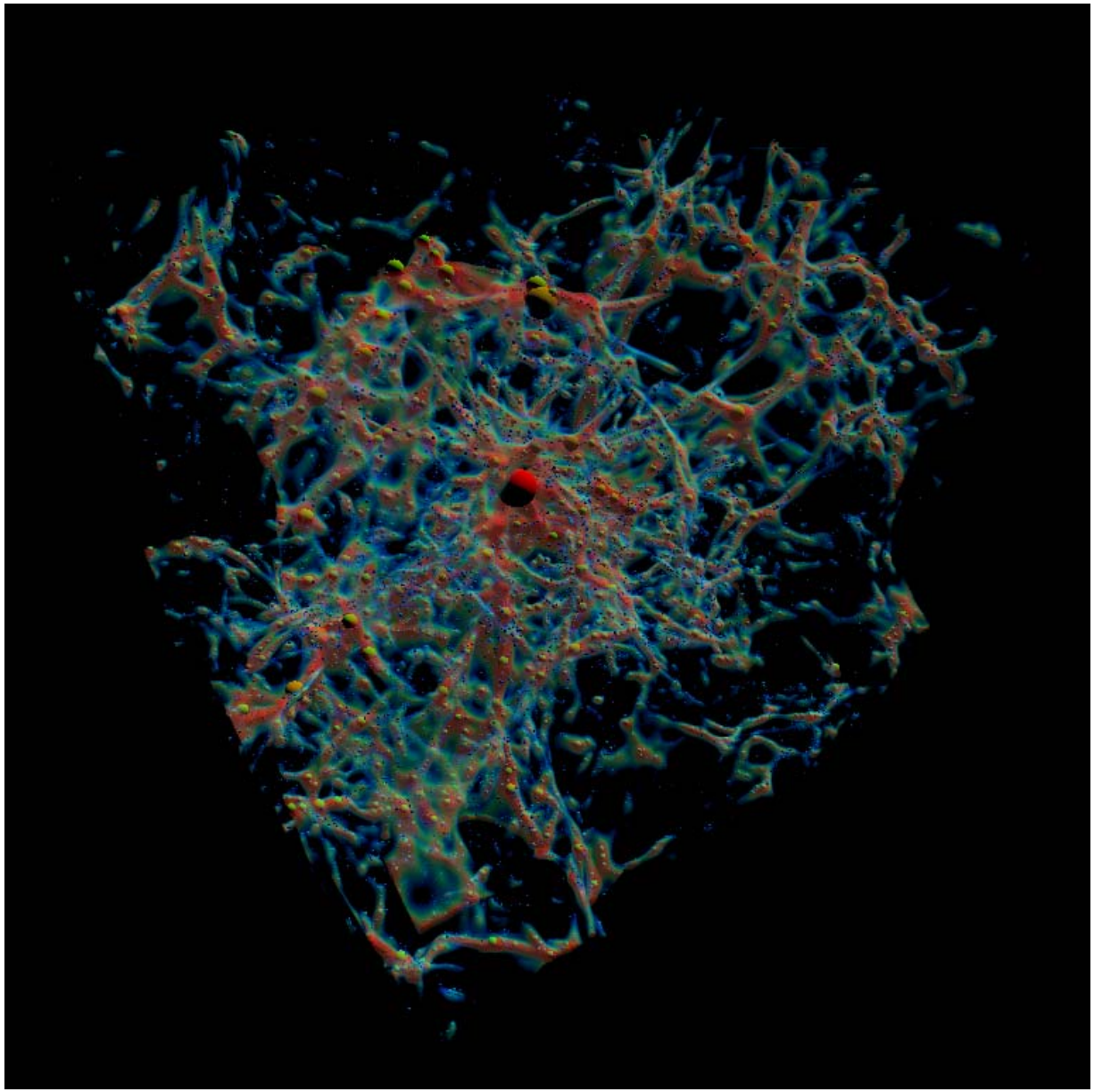

THE PHOTOEVAPORATION OF MINIHALOS OVERTAKEN BY COSMOLOGICAL I-FRONTS

(Shapiro, Iliev & Raga 2004, MNRAS, 348, 753;
Iliev, Shapiro, & Raga 2005, MNRAS, 361, 405)

- We performed radiation-hydrodynamical simulations of the photoevaporation of a cosmological minihalo overrun by a weak, R-type I-front in surrounding IGM, created by external source of radiation.
- 2D, axisymmetric, Eulerian hydro code with Adaptive Mesh Refinement and the van Leer flux-splitting algorithm, including radiative transfer (H, He bound-free opacity).
- Nonequilibrium ionization rate equations: H, He + (C, N, O, Ne, S) @ 10-3 solar abundance

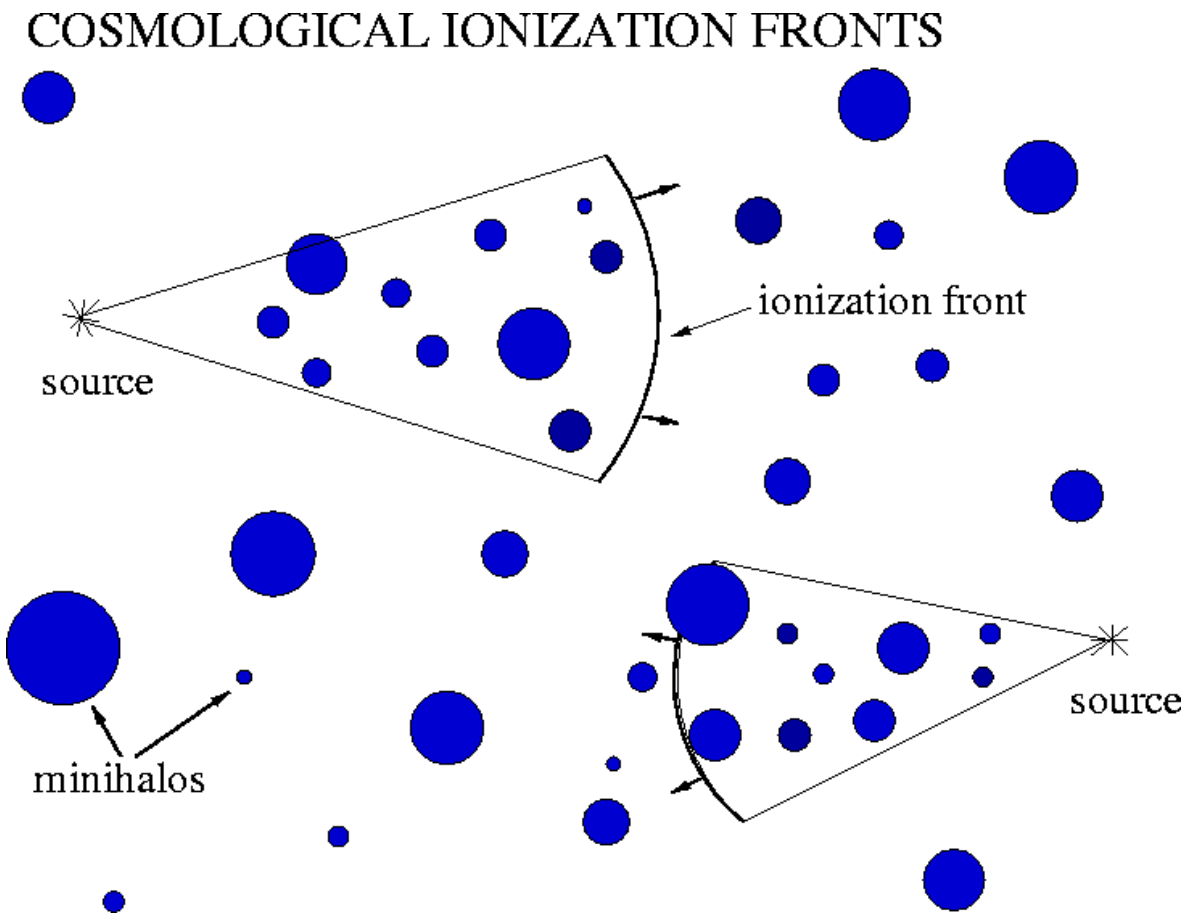

Temperature at times t = 0.0, 0.2, 2.5, 10, 60, 150 Myrs.

(M_{halo}, $z_{initial}$, F_0) = ($10^7 M_{sun}$, 9, 1).

Pop II source.

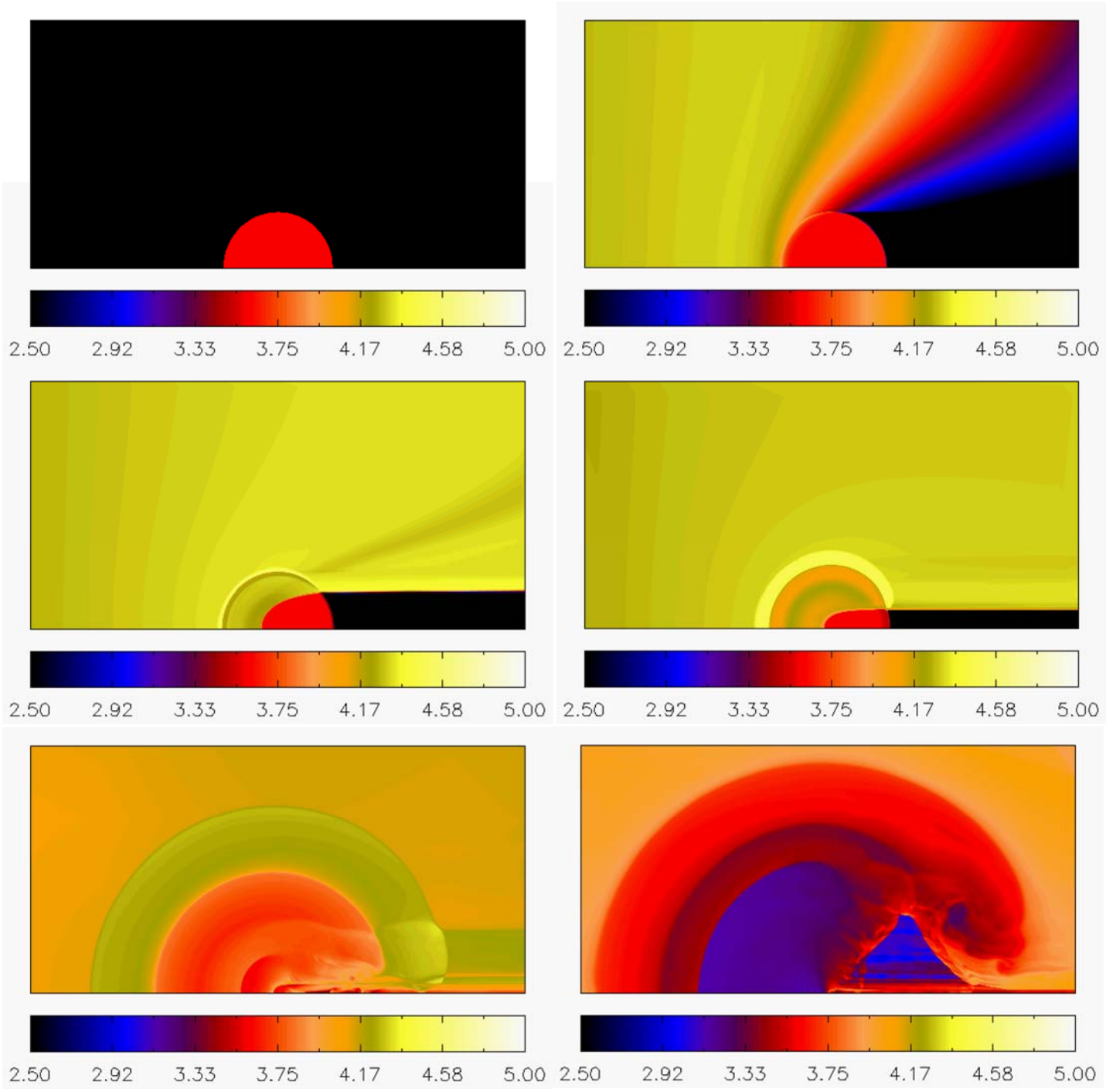

ANIMATIONS

Pop II

- **TEMPERATURE**
- **DENSITY**
- **H I**
- **He II**
- **C IV**

Pop III

- **TEMPERATURE**
- **DENSITY**
- **H I**
- **He II**
- **C IV**

Simulating Cosmic Reionization at Large Scales I. : The Geometry of Reionization

Iliev, Mellema, Pen, Merz, Shapiro & Alvarez (2006)
MNRAS, 369, 1625 (astro-ph/0512187)

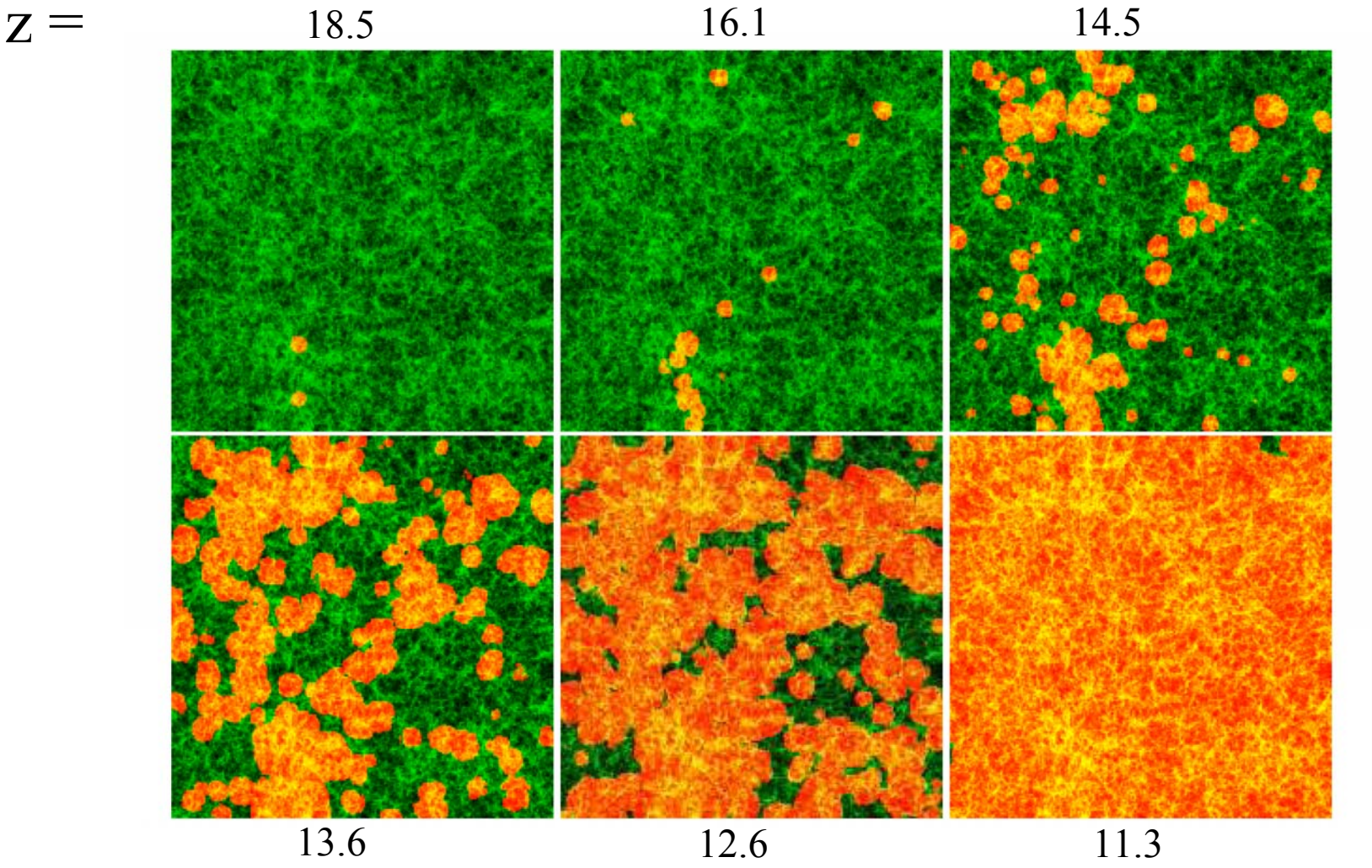

N-body + Radiative Transfer ➔ Reionization simulation

- **N-body simulation yields the density field and sources of ionizing radiation**
  - **PMFAST** code (Merz, et al. 2005) with
    1624^3 = 4.28 billion particles, 3248^3 cells,
    particle mass = $2.5 \times 10^7 M_{sun}$ (100 h^{-1}Mpc box),

  - Halo finder "on-the-fly" yields location, mass, other properties of all galaxies,
    $M \geq 2.5 \times 10^9 M_{sun}$ (100 h^{-1}Mpc box),

e.g. N_{halo} ~ 4×10^5 by z ~ 8 (WMAP1)
~ 3×10^5 by z ~ 6 (WMAP3)

N-body + Radiative Transfer ➔ Reionization simulation

- **Radiative transfer simulations evolve the radiation field and nonequilibrium ionization state of the gas**

  - New, fast, efficient **C^2-Ray** code (**C**onservative, **C**ausal **R**ay-Tracing) (Mellema, Iliev, Alvarez, & Shapiro 2006, *New Astronomy*, 11, 374) uses short-characteristics to propagate radiation throughout the evolving gas density field provided by the N-body results, re-gridded to $(203)^3$ and $(406)^3$ cells, for different resolution runs, from each and every galaxy halo source in the box.

e.g. N_{halo} ~ 4 x 10^5 by z ~ 8 (WMAP1)

~ 3 x 10^5 by z ~ 6 (WMAP3)

Every galaxy in the simulation volume emits ionizing radiation

- We assume a constant mass-to-light ratio for simplicity:

f_γ = # ionizing photons released by each galaxy per halo baryon

$= f_* \ f_{esc} \ N_i$,

where f_* = star-forming fraction of halo baryons,

f_{esc} = ionizing photon escape fraction,

N_i = # ionizing photons emitted per stellar baryon over stellar lifetime

e.g. $N_i = 50{,}000$ (top-heavy IMF), $f_* = 0.2$, $f_{esc} = 0.2$ ➔ $f_\gamma = 2000$

Every galaxy in the simulation volume emits ionizing radiation

- We assume a constant mass-to-light ratio for simplicity:

f_γ = # ionizing photons released by each galaxy per halo baryon

$= f_* \ f_{esc} \ N_i$,

where f_* = star-forming fraction of halo baryons,

f_{esc} = ionizing photon escape fraction,

N_i = # ionizing photons emitted per stellar baryon over stellar lifetime

e.g. $N_i = 50{,}000$ (top-heavy IMF), $f_* = 0.2$, $f_{esc} = 0.2$ ➔ $f_\gamma = 2000$

- This yields source luminosity: $dN_\gamma/dt = f_\gamma \, M_{bary} / (\mu \, m_H \, t_*)$,

t_* = source lifetime (e.g. 2×10^7 yrs),

M_{bary} = halo baryonic mass

C^2 – Ray : A New Method for Photon-Conserving Transport of Ionizing Radiation

Mellema, Iliev, Alvarez & Shapiro (2006) *New Astronomy*, 11, 374

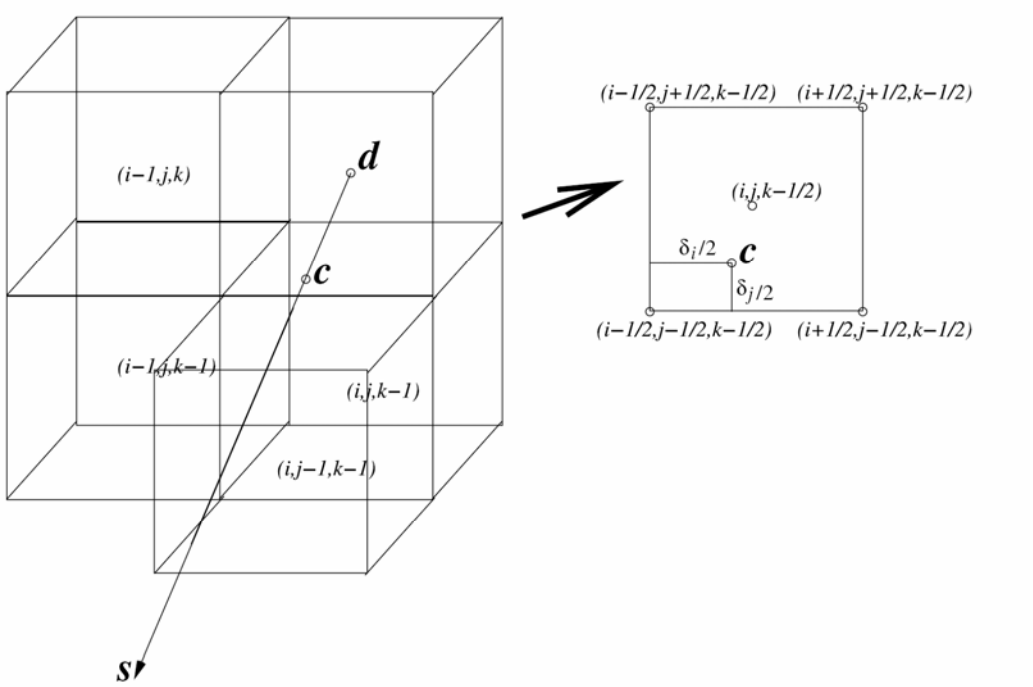

Fig. A.1. Short-characteristics ray tracing.

Cosmological Radiative Transfer Codes Comparison Project I. : The Static Density Field Tests

Iliev, Ciardi, …, Shapiro, … (2006) MNRAS, 371, 1057

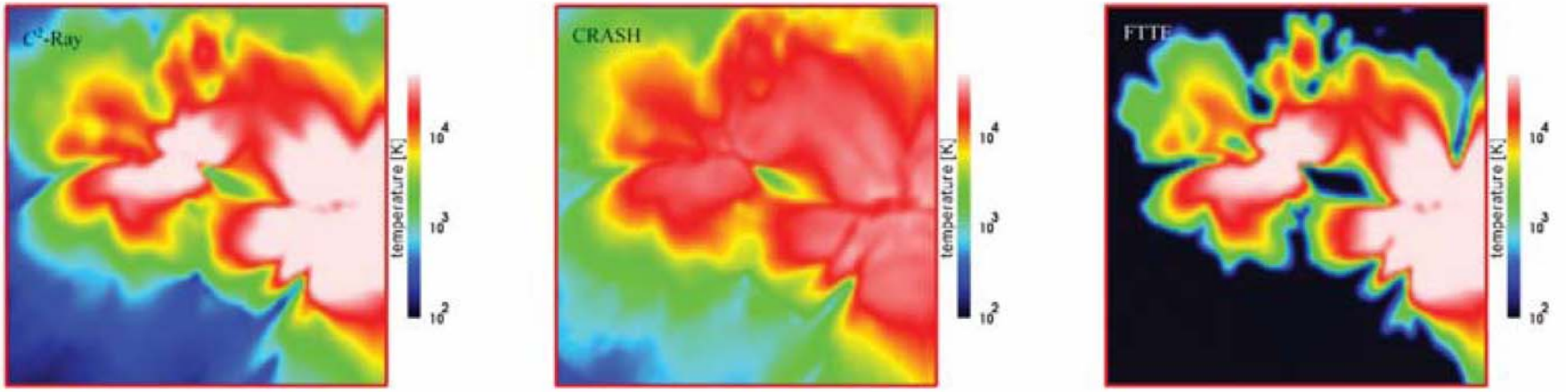

Dynamical H II Region Evolution in Turbulent Molecular Clouds

Mellema, Arthur, Henney, Iliev & Shapiro (2006) ApJ, 647, 397 (astro-ph/0512187)

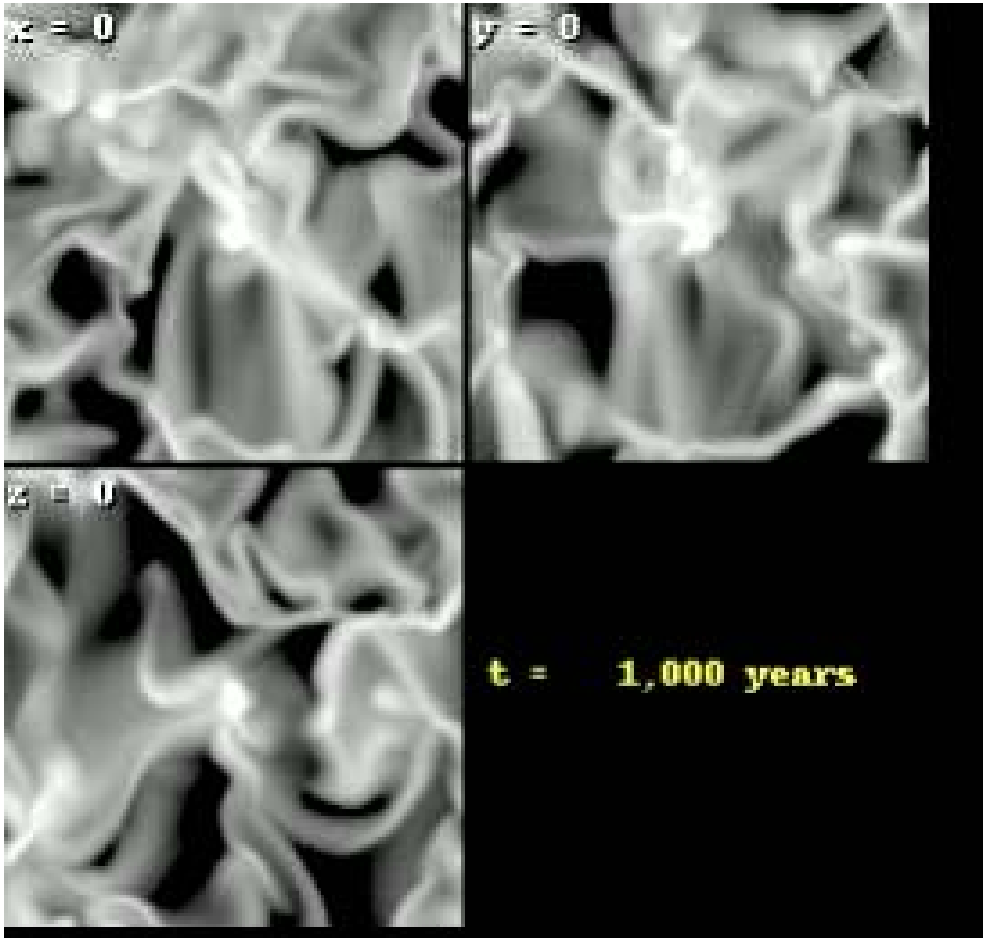

Dynamical H II Region Evolution in Turbulent Molecular Clouds

Mellema, Arthur, Henney, Iliev & Shapiro (2006) ApJ, 647, 397 (astro-ph/0512187)

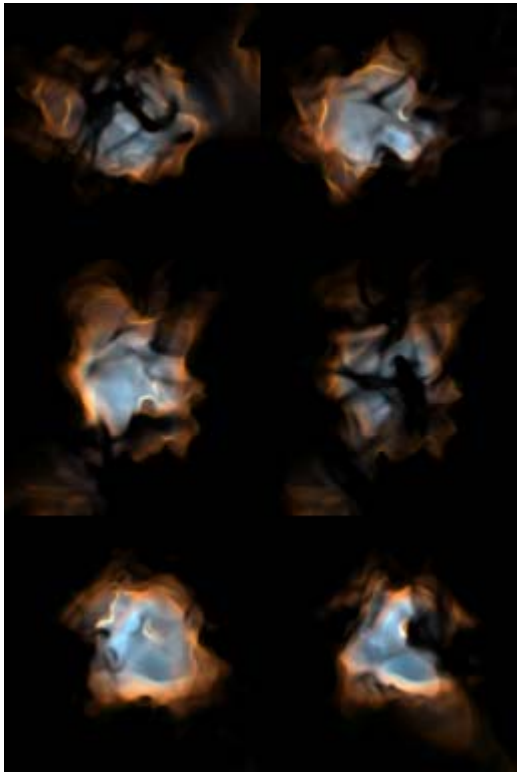

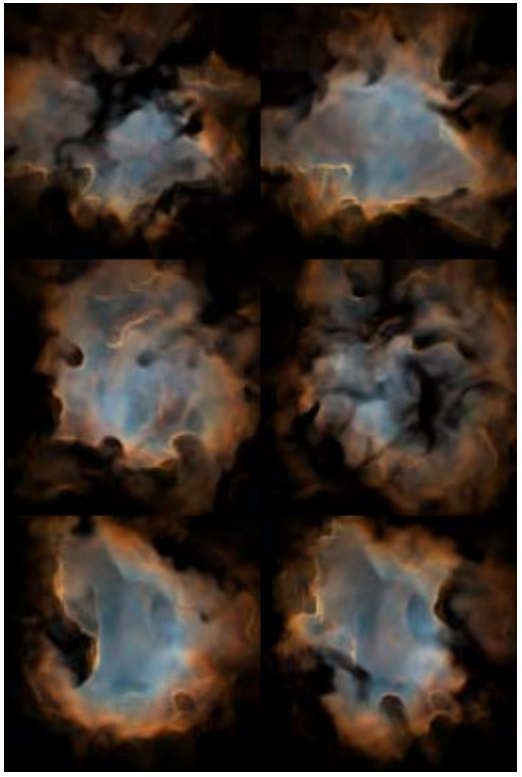

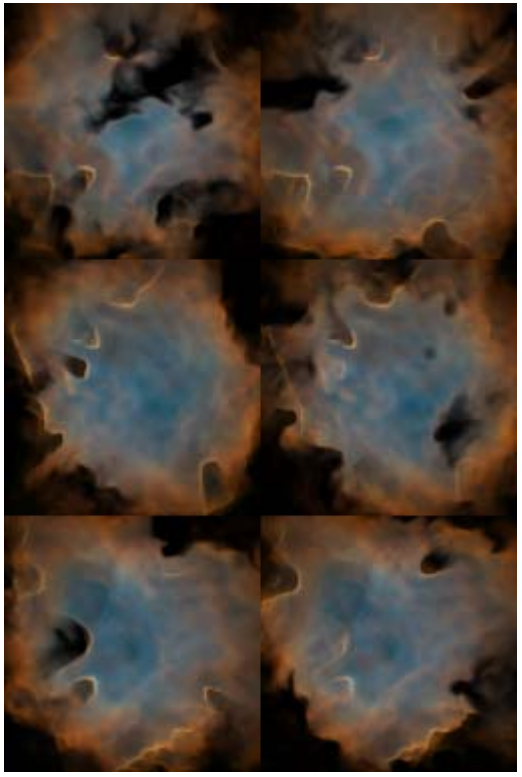

Simulating Reionization at Large Scales II : The 21-cm Emission Features and Statistical Signals

Mellema, Iliev, Pen, & Shapiro (2006), MNRAS, 372,679 (astro-ph/0603518)

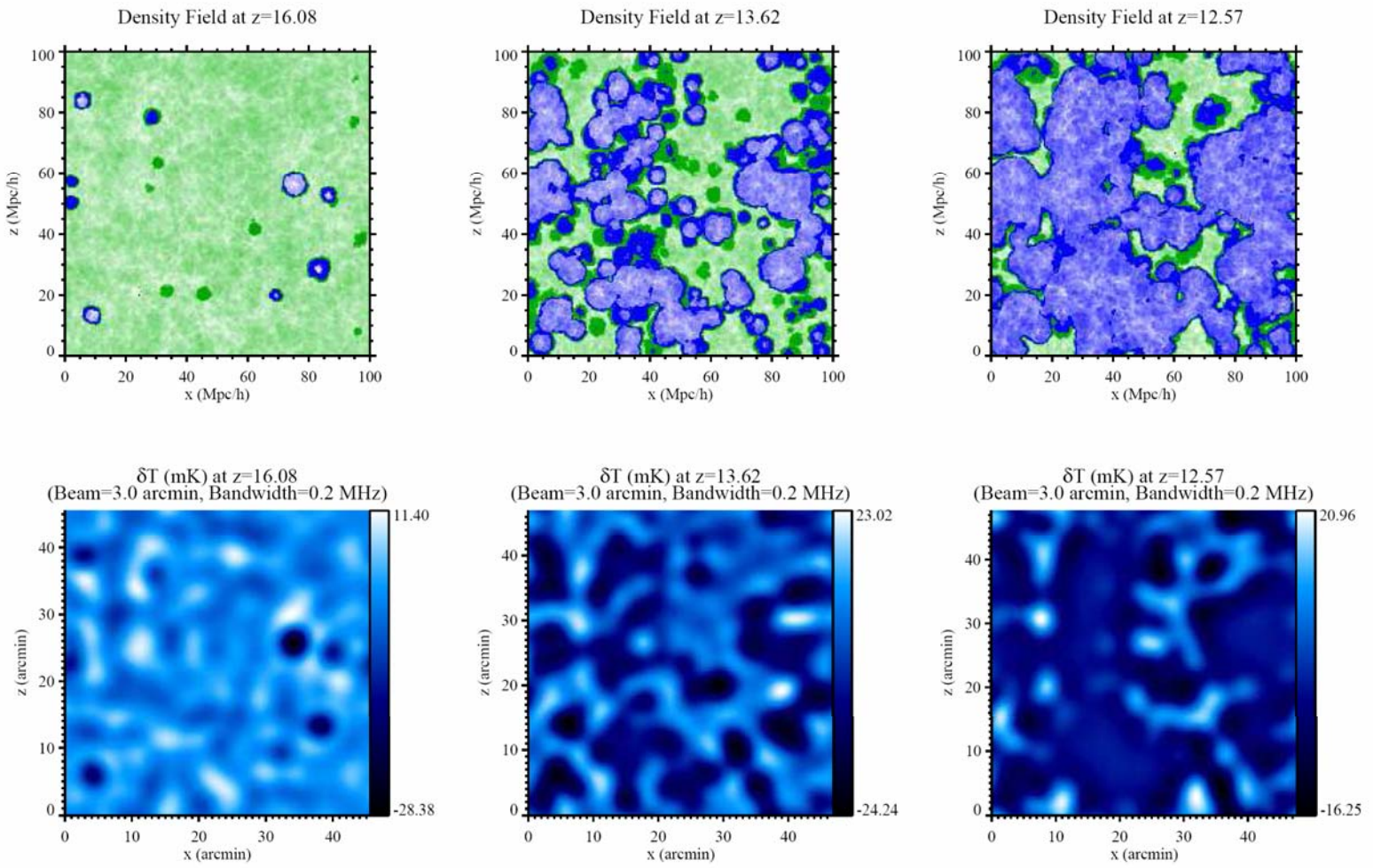

Reionization topology revealed by fluctuations in 21-cm brightness temperature, δT_b , along the line of sight

Iliev, Mellema, Pen, Bond, & Shapiro (2008), MNRAS, 384, 863 (astro-ph/0702099)

• mapping the sky along the LOS: high-resolution cuts in position-redshift space

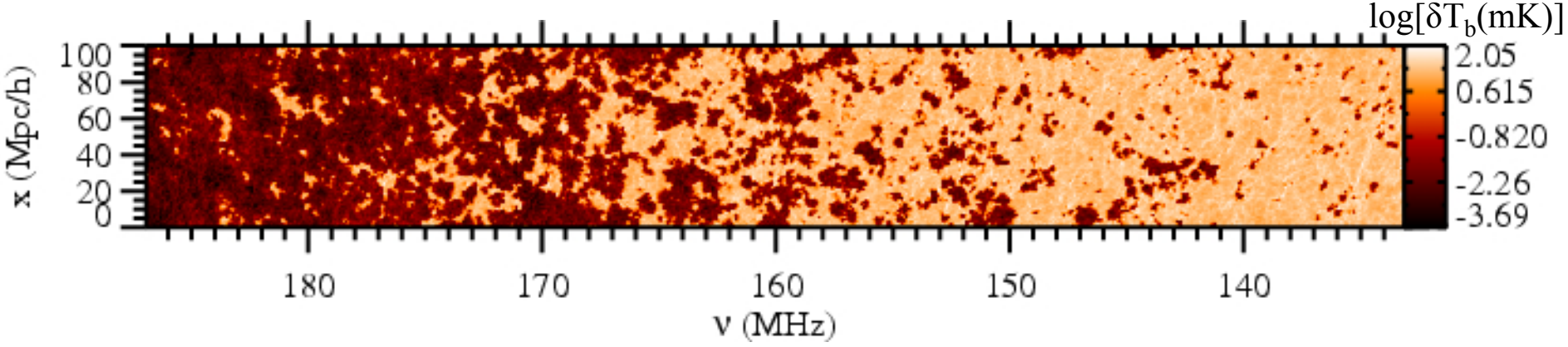

• beam- and bandwidth-smoothed : 3 arcmin, 0.2 MHz (e.g. LOFAR)

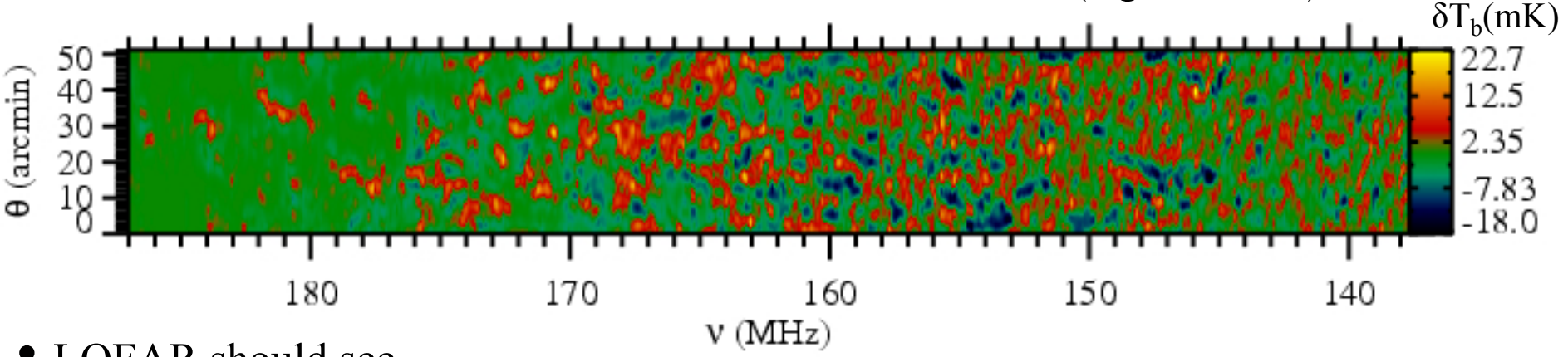

• LOFAR should see large ionized bubbles!

Case: $f_\gamma = 250$, subgrid clumping factor C(z), WMAP3

Q: How large must a reionization simulation volume be to predict 21-cm background fluctuations?

- Simulation volumes must exceed the beamsize and bandwidth of future radio arrays by a large enough factor to make 21-cm predictions meaningful.

e.g. for GMRT, MWA, LOFAR,

$\Delta\theta_{beam} \geq 3'$

$\Delta\nu_{bandwidth} > 0.1$ Mhz

- Our $(143\ \mathrm{Mpc})^3$ comoving volume simulation is the first to be large enough to predict 21-cm fluctuations.

$L_{box} = 100\ h^{-1}$ Mpc (comoving)

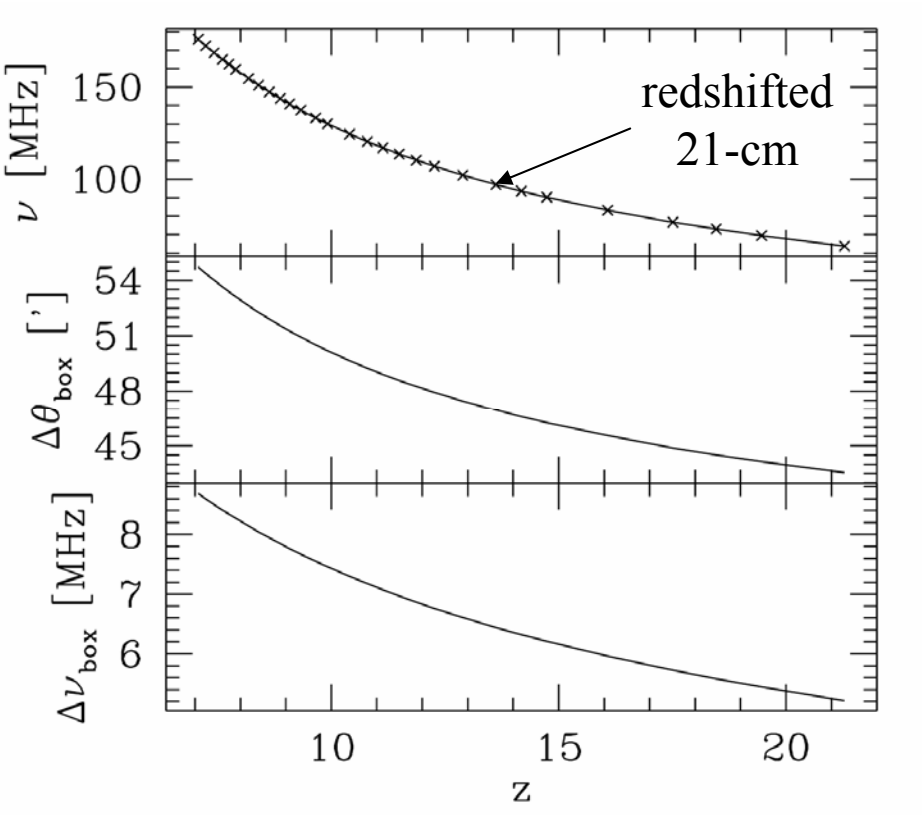

The Geometry of Reionization

for source efficiency
$f_\gamma = 2000$

from z = 20 to z = 12

a cut through the simulation volume, one cell deep

gas density (green in neutral regions, yellow in ionized regions), H II regions (red) and sources (dots)

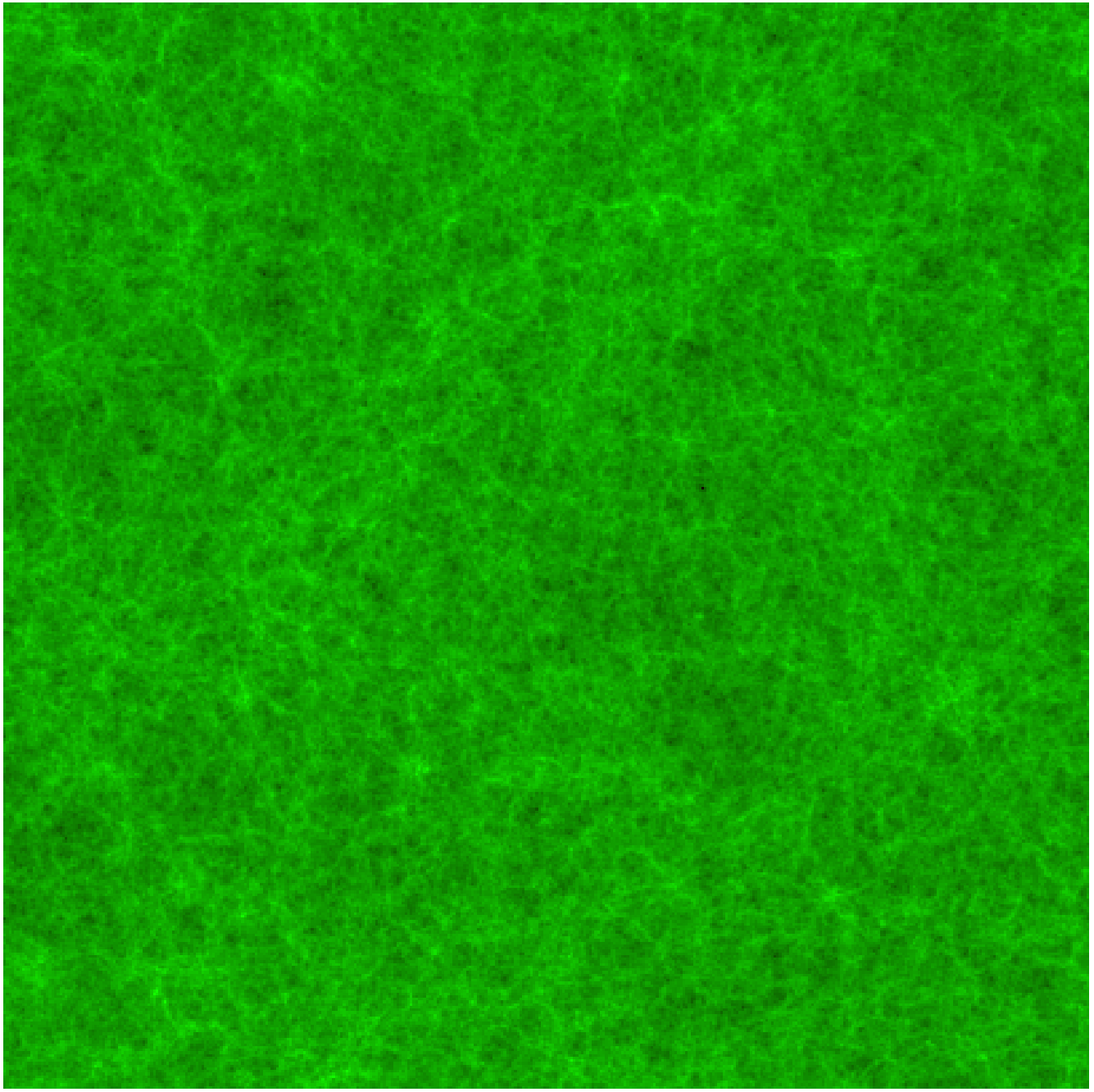

Kinetic Sunyaev-Zel'dovich Effect from Patchy Reionization

- kSZ effect is the CMB temperature anisotropy induced by electron scattering by free electrons moving along the line-of-sight:

$$\frac{\Delta T}{T_{\rm CMB}} = \int d\eta e^{-\tau_{\rm es}(\eta)} a n_e \sigma_T \mathbf{n} \cdot \mathbf{v},$$

where η is conformal time,

$$\eta = \int_0^t dt' / a(t')$$

($\delta T/T_{CMB}$) Maps of the Kinetic Sunyaev-Zel'dovich Effect from Radiative Transfer Simulations of Patchy Reionization

Iliev, Pen, Bond, Mellema & Shapiro (2007), ApJ, 660, 933; (astro-ph/0609592)
Iliev, Mellema, Pen, Bond, & Shapiro (2008), MNRAS, 384, 863; (astro-ph/0702099)

- Box size 100/h Mpc comoving
  ➔ 50' x 50'

- Even so large a box is missing large-scale power in velocity field perturbations

➔ must correct for missing large-scale velocity perturbations

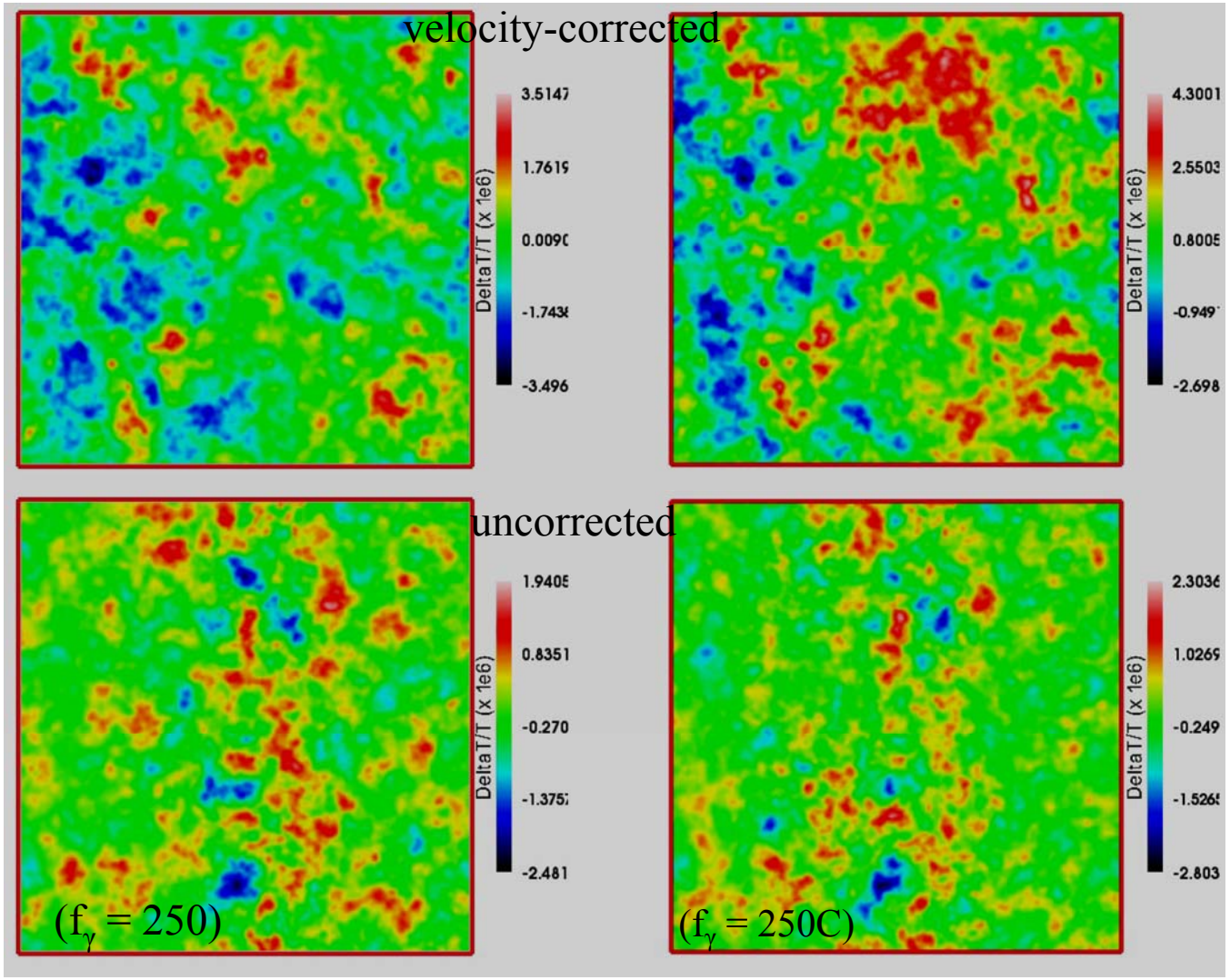

kSZ CMB Anisotropy Signal: Sky Power Spectra of $\delta T_{kSZ} / T_{CMB}$

- kSZ anisotropy from inhomogeneous reionization dominates primary CMB anisotropy for $\ell > 4000$, peaking at $\ell = 3000 - 4000$, determined by typical sizes of H II regions, 5 – 20 Mpc.

- Patchy reionization doubles *total* kSZ for $\ell = 3000 - 10{,}000$ compared to homogeneous reionization with the same total τ_{es}.

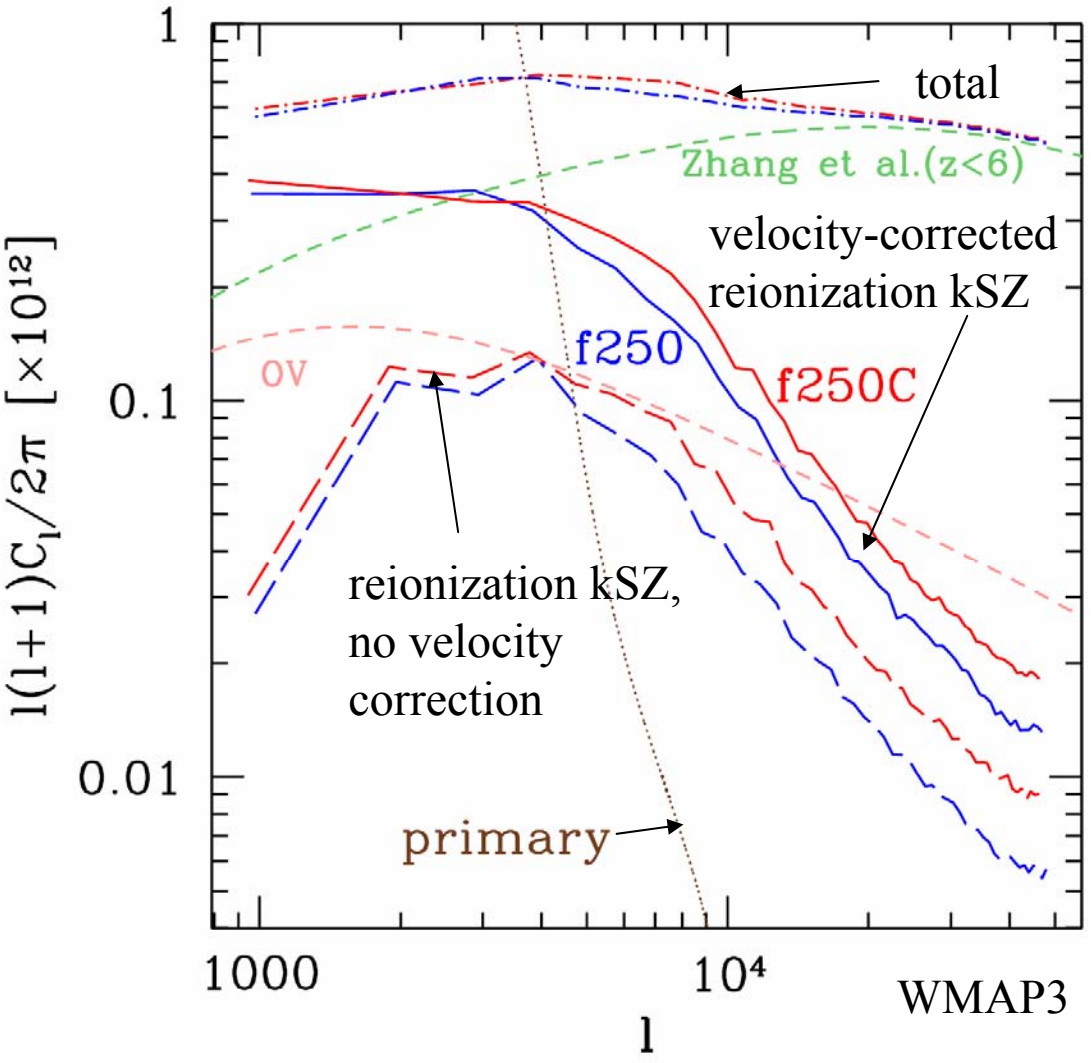

- This predicted kSZ signal at arcminute scales should be detectable by upcoming experiments. e.g. Atacama Cosmology Telescope, South Pole Telescope, (~ 1' resolution, ~ μK sensitivity)

Observability of the kSZ from reionization: sky power spectrum

- Predicted kSZ from reionization simulations and *Atacama Cosmology Telescope* (ACT) expected sensitivity;
- primary CMB and post-reionization kSZ added to noise error bars for reionization signal;
- reionization kSZ signal is comparable to that from post-reionization, so necessary to separate them to extract info on reionization, alone.
- In principle, results show that reionization signal should be observable.

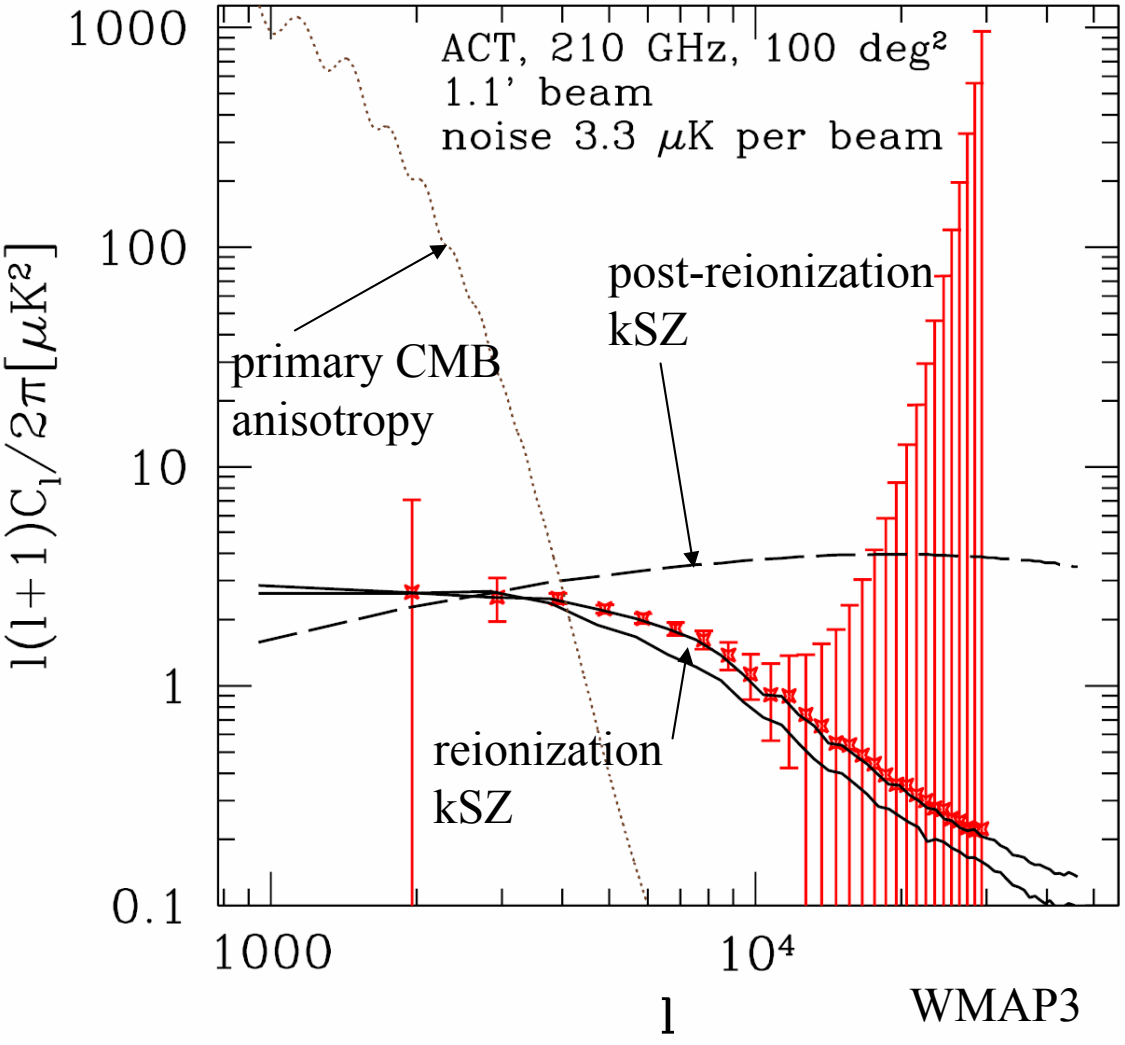

f250, f250C

Observability of the kSZ from reionization: sky power spectrum

- Predicted kSZ from reionization simulations and *South Pole Telescope* (SPT) expected sensitivity;
- primary CMB and post-reionization kSZ added to noise error bars for reionization signal;
- reionization kSZ signal is comparable to that from post-reionization, so necessary to separate them to extract info on reionization, alone.
- In principle, results show that reionization signal should be observable.

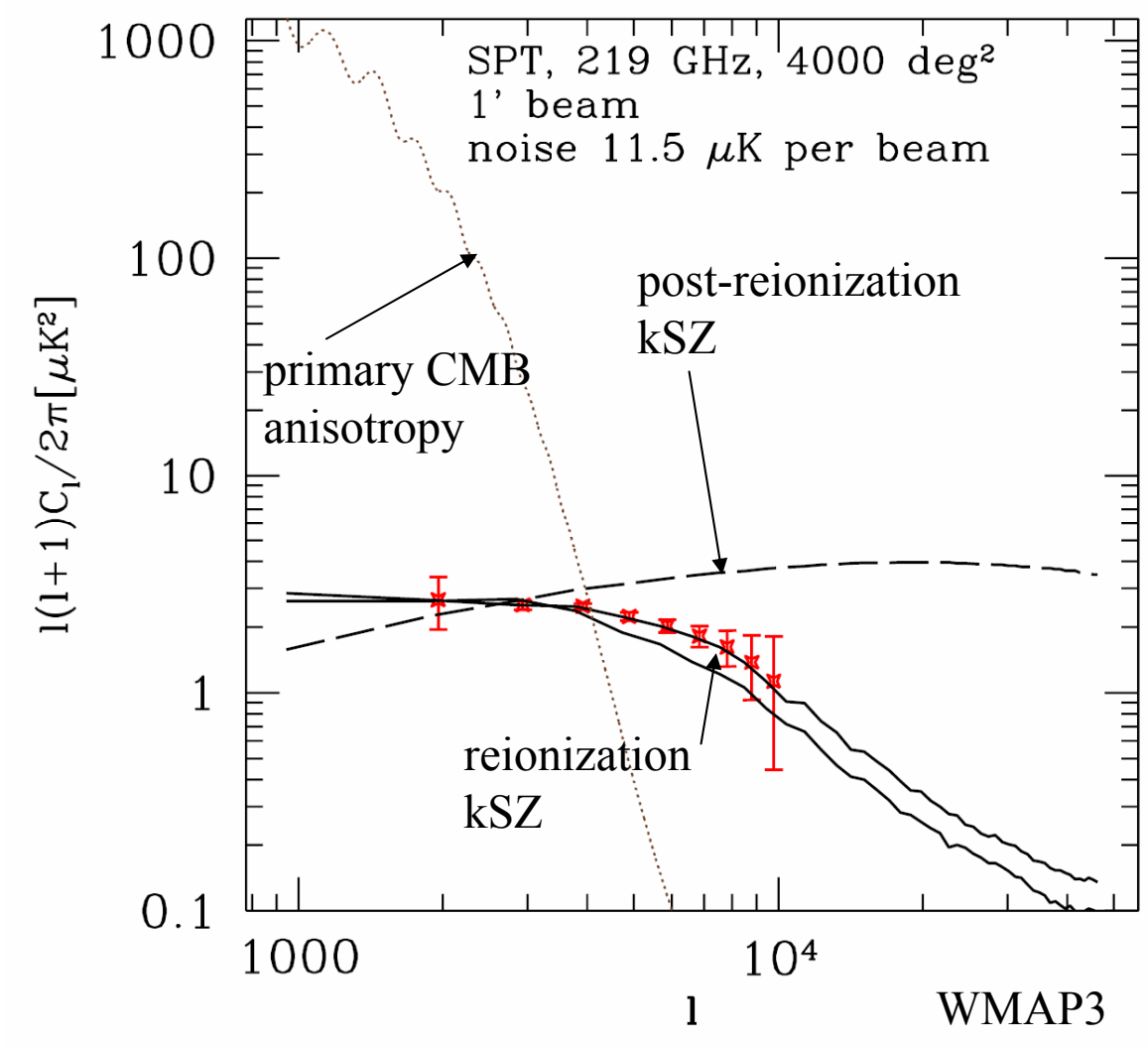

f250, f250C

Effect of IGM on Observability of Ly-α Sources During Reionization

Iliev, Shapiro, McDonald, Mellema, Pen 2007, MNRAS, submitted, astro-ph/0711.2944

•reionization, centered on most massive halo in $(100h^{-1}\ \mathrm{Mpc})^3$:

$M\ (z = 6) = 1.5 \times 10^{12}\ M_{solar}$ ➔

rare (~ 5-σ) density peak ➔

bright Ly-α emitter ;

•H II regions form first around such density peaks and grow continuously, as halos form inside, clustered around peak ➔

Ly-α emitters will be centered on large HII regions ;

(blue dots = source cells)

•Fluctuating GP optical depth inside H II regions can still affect Ly-α source detection, though;

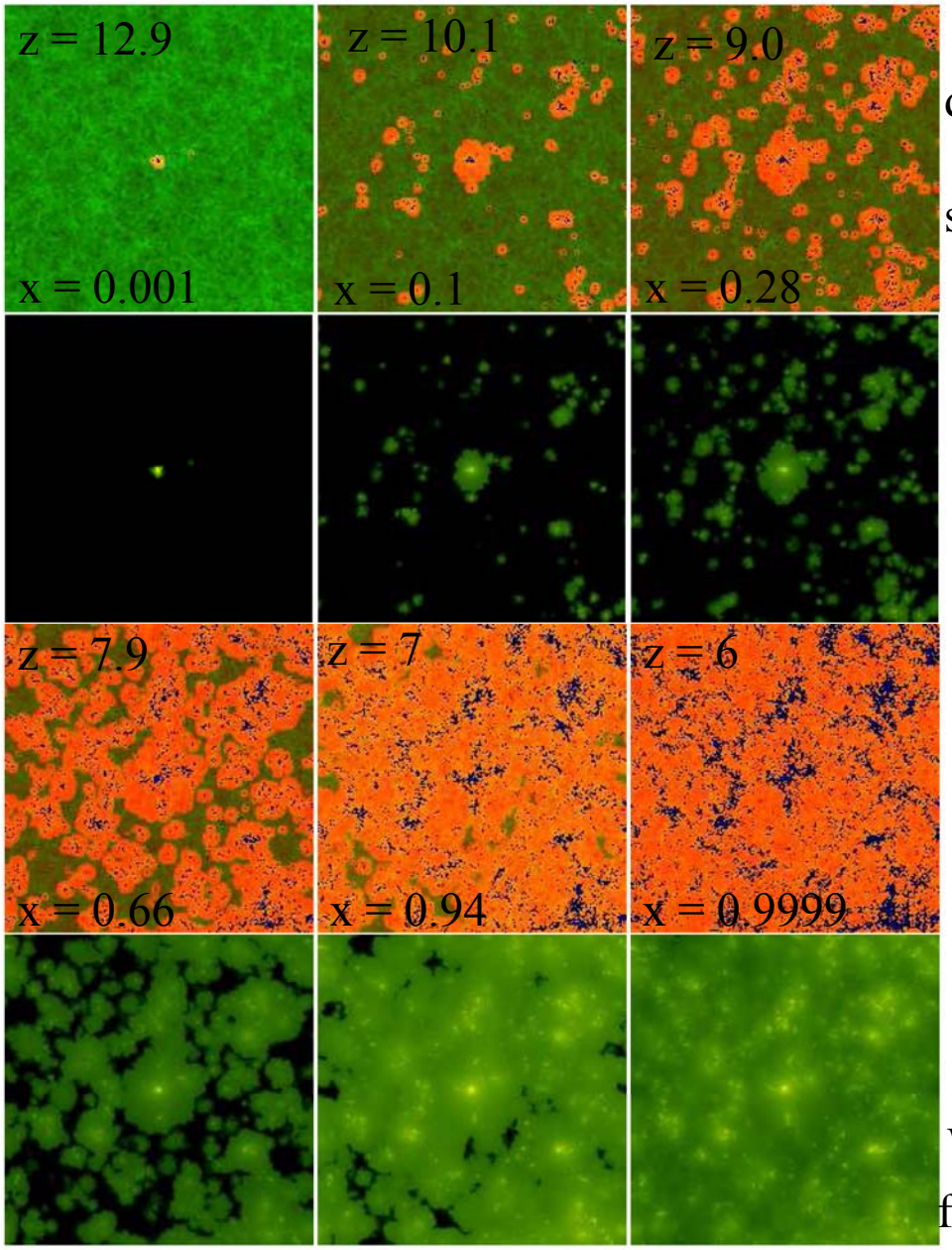

Effect of IGM on Observability of Ly-α Sources During Reionization

Iliev, Shapiro, McDonald, Mellema, Pen 2007, MNRAS, submitted, astro-ph/0711.2944

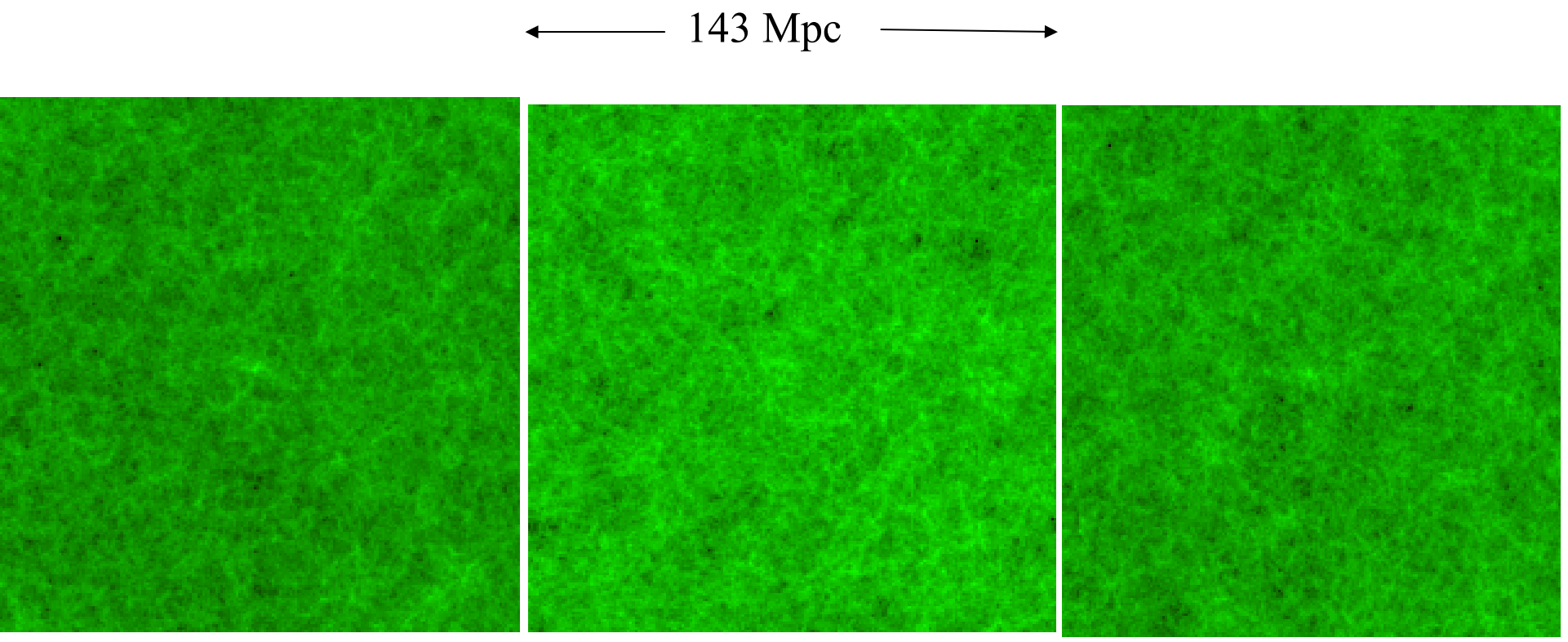

Q: Do luminous Lyman alpha emitters observed during the EOR dominate the ionization of their own H II regions?

- **A**: not really ("they get by with a little help from their friends…")
  - LAE forms at high-σ density peak, surrounded by a cluster of smaller mass halos ➔ smaller halos dominate ionization
  - e.g. most massive source contributed only

    ~50% by z = 12.9

    ~10% by z = 7

    ~1% by z = 6.25!

ionizing photons released over time by halos within a sphere of distance R from most massive object

H II region sizes @ z = 12.9, 9, 8, 7, 6.25

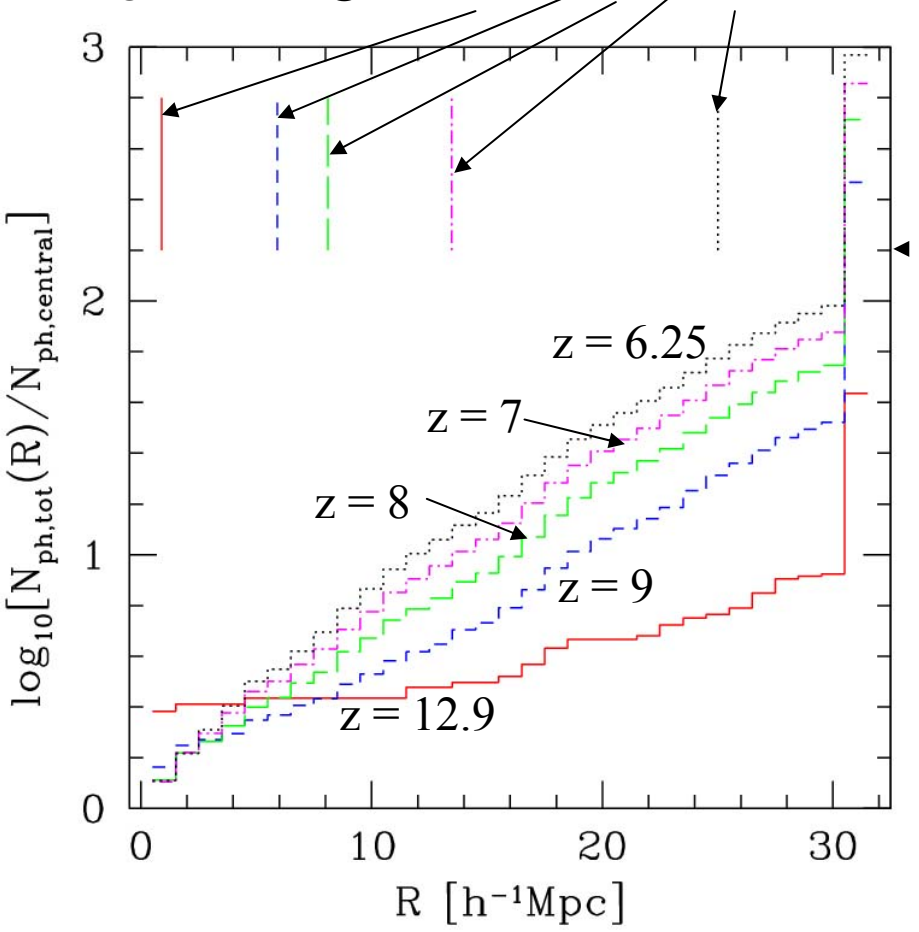

Luminous sources at the end of reionization: Ly-a spectra

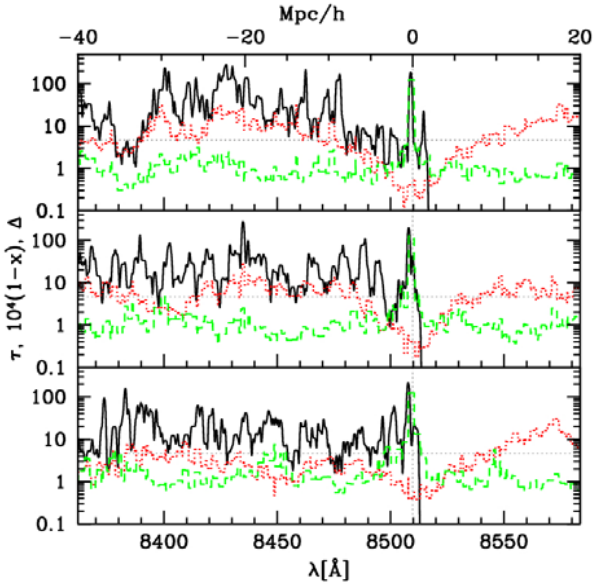

x_{HI},n,τ

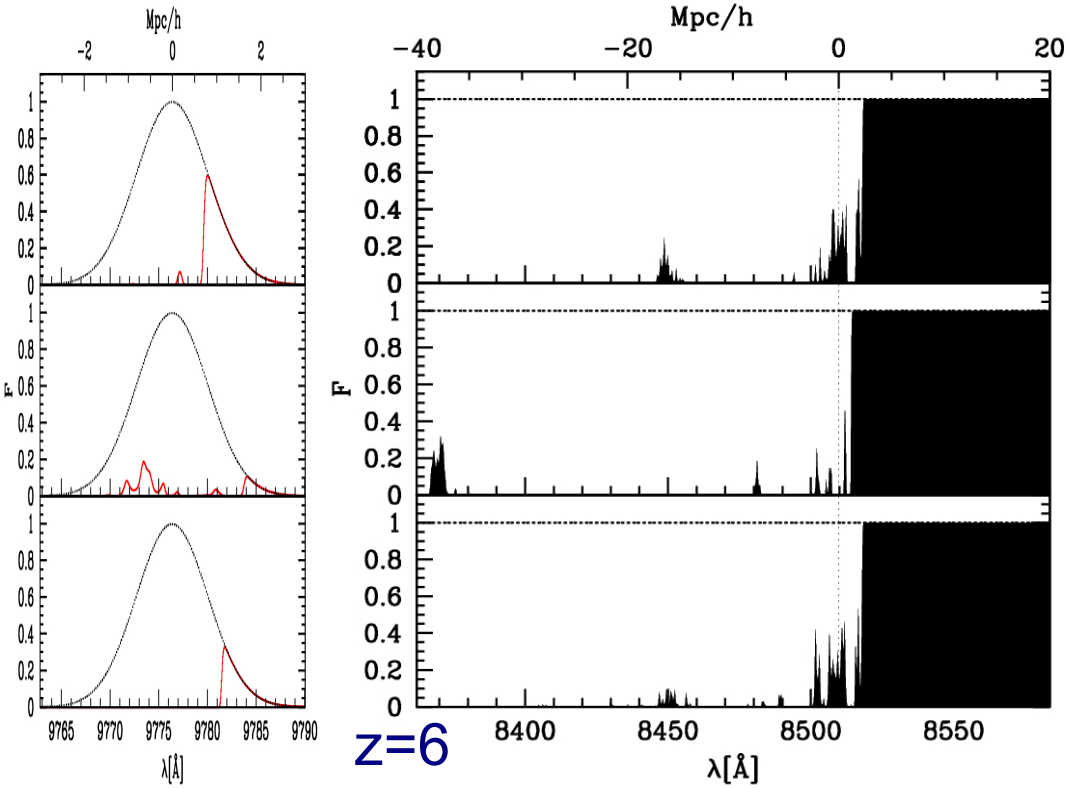

z=6

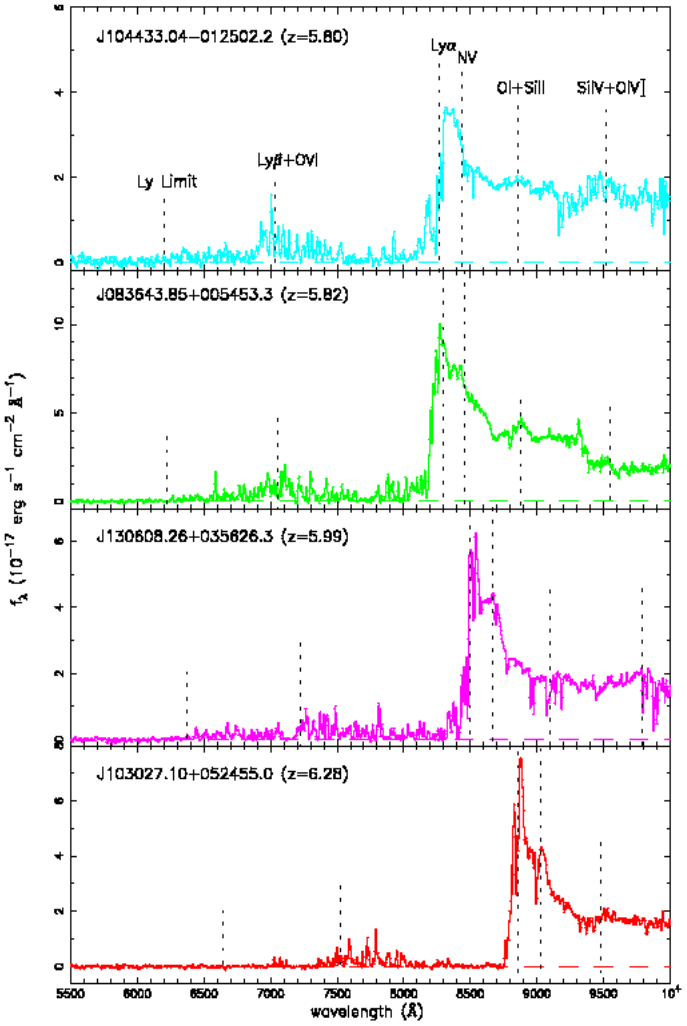

Mean Ly-α transmission vs. redshift

- Strong damping wings at z>10, only minor differences between average and luminous source.
- Some transmission on blue side of line, as IGM slowly becomes transparent; large proximity transmission region for luminous sources.

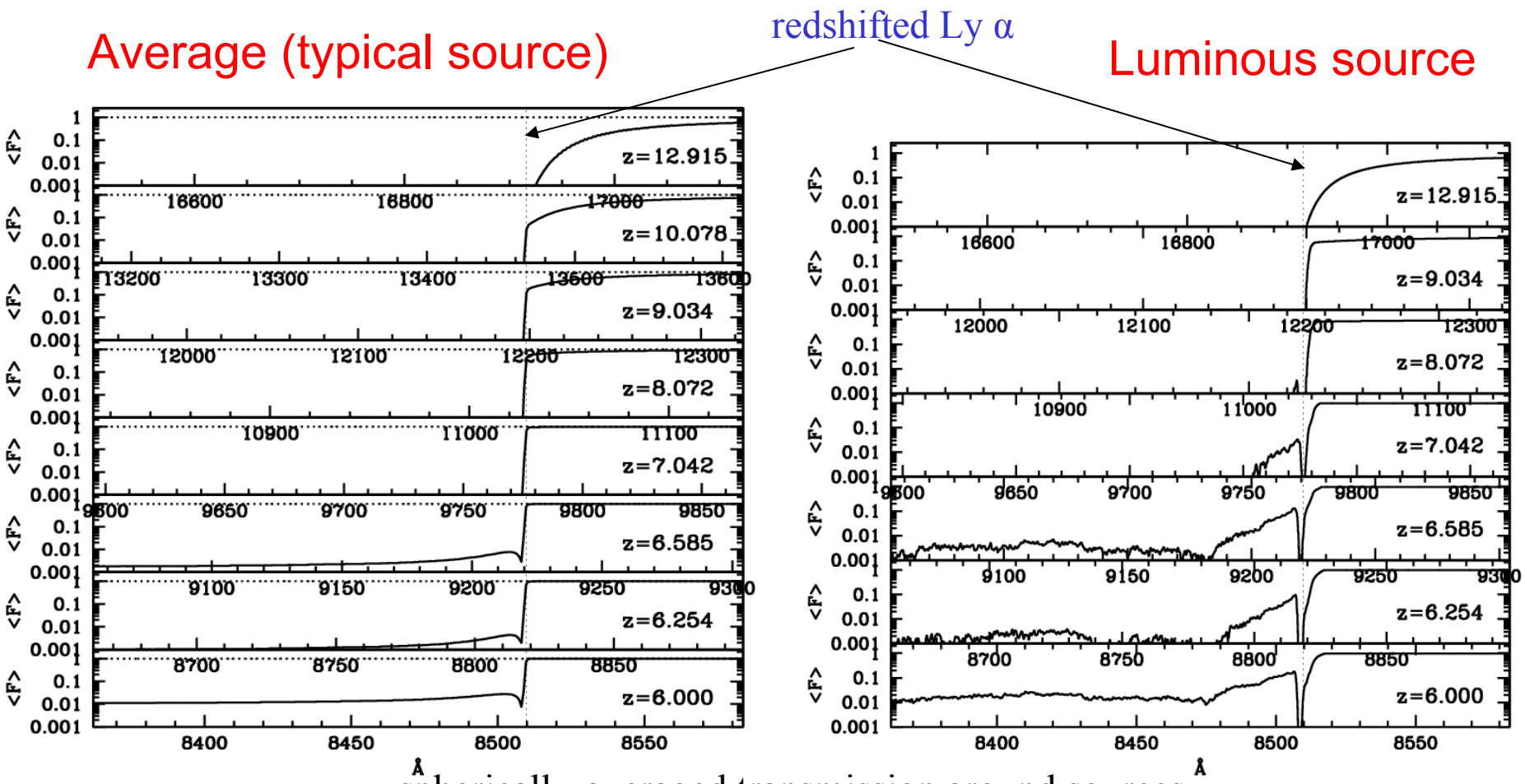

spherically-averaged transmission around sources

Mean transmitted Ly-α line profile vs. redshift

- Mostly, the red wing comes through (but damped at z>10).
- Infall more important for luminous sources, changes the line shape.

Average (typical source)

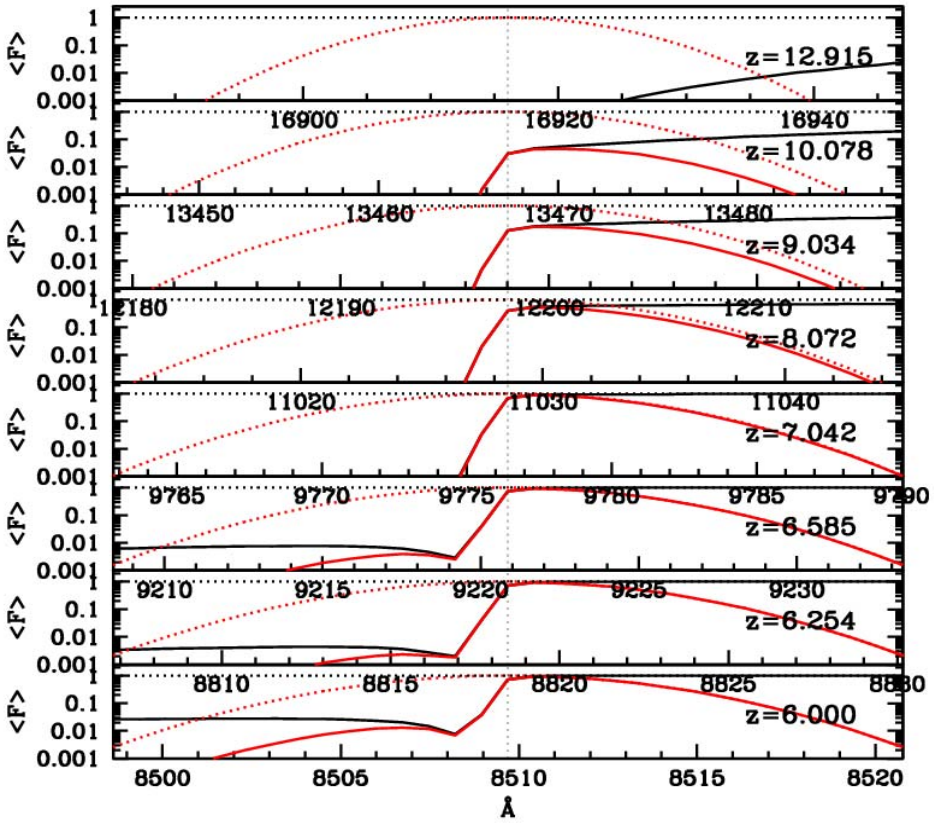

Luminous source

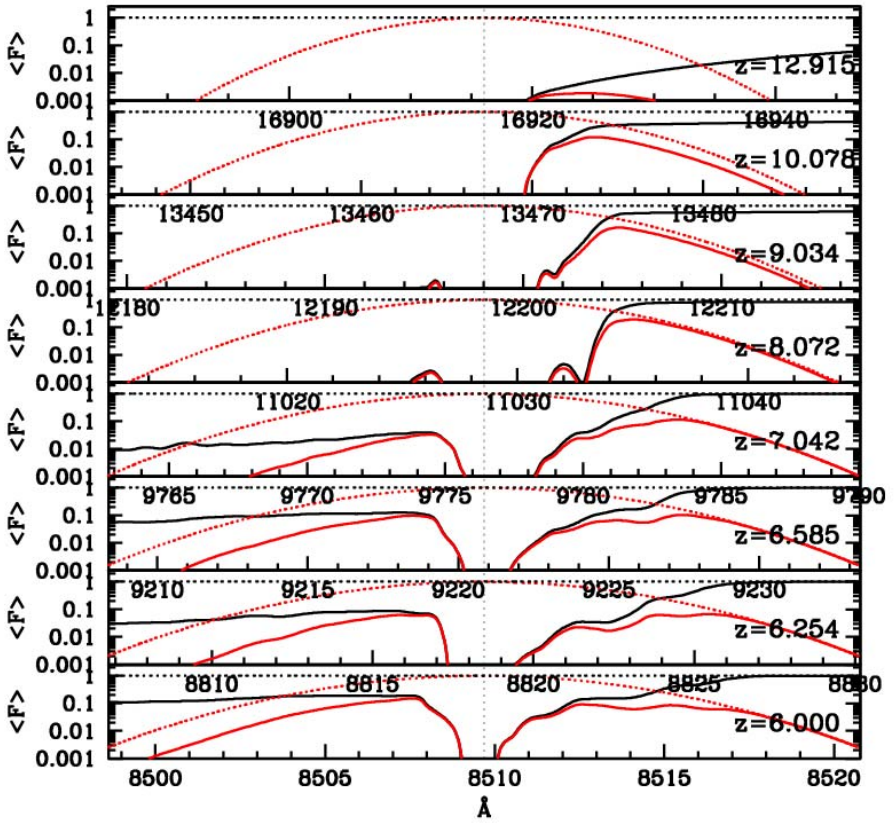

spherically-averaged transmitted line profiles

The Intergalactic Medium Surrounding the Most Massive Galaxy at the End of Reionization : $\langle x_{H\,II} \rangle = 99\%$

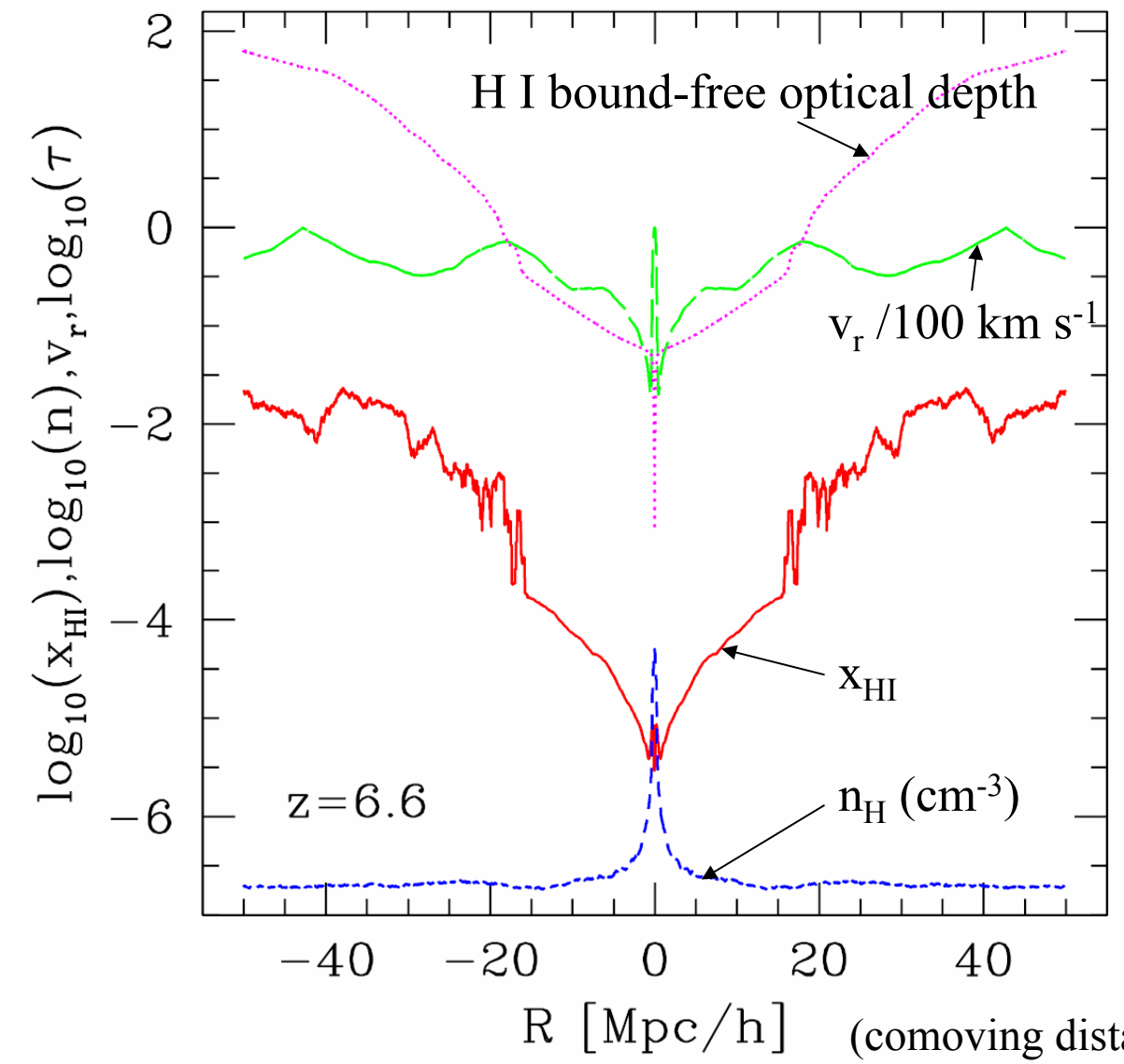

spherically-averaged profiles

(comoving distance from galaxy)

Luminosity Function of High-Redshift Ly-α Sources is Filtered By the Partially Ionized IGM

- Assuming all halos are Ly-α emitters with M/L = constant and 160 km/s Gaussian line profile;
- At z = 9, observed luminosity function is reduced by 0.01 -0.1 from intrinsic luminosity function;
- Attenuation exceeds 50% (i.e. blue-half absorbed, red-half not), since damping wings reduce the red-half, as well..

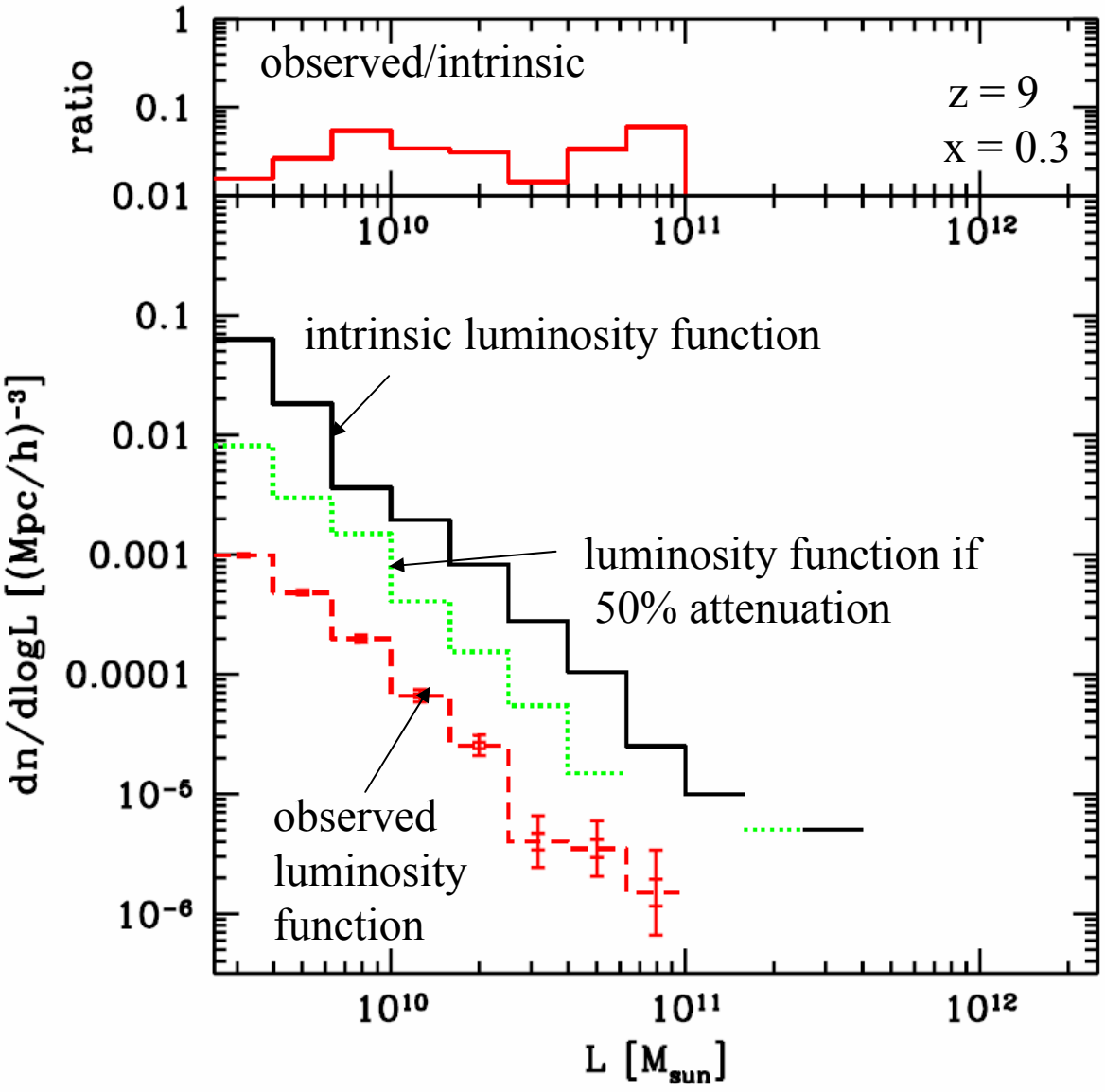

Luminosity Function of High-Redshift Ly-α Sources is Filtered By the Partially Ionized IGM

- Assuming all halos are Ly-α emitters with M/L = constant and 160 km/s Gaussian line profile;
- At z = 7, observed luminosity function is reduced by 0.5 from intrinsic luminosity function, except at bright end where factor is 0.1 or below;
- Attenuation exceeds 50% (i.e. blue-half absorbed, red-half not), now, only at bright end.

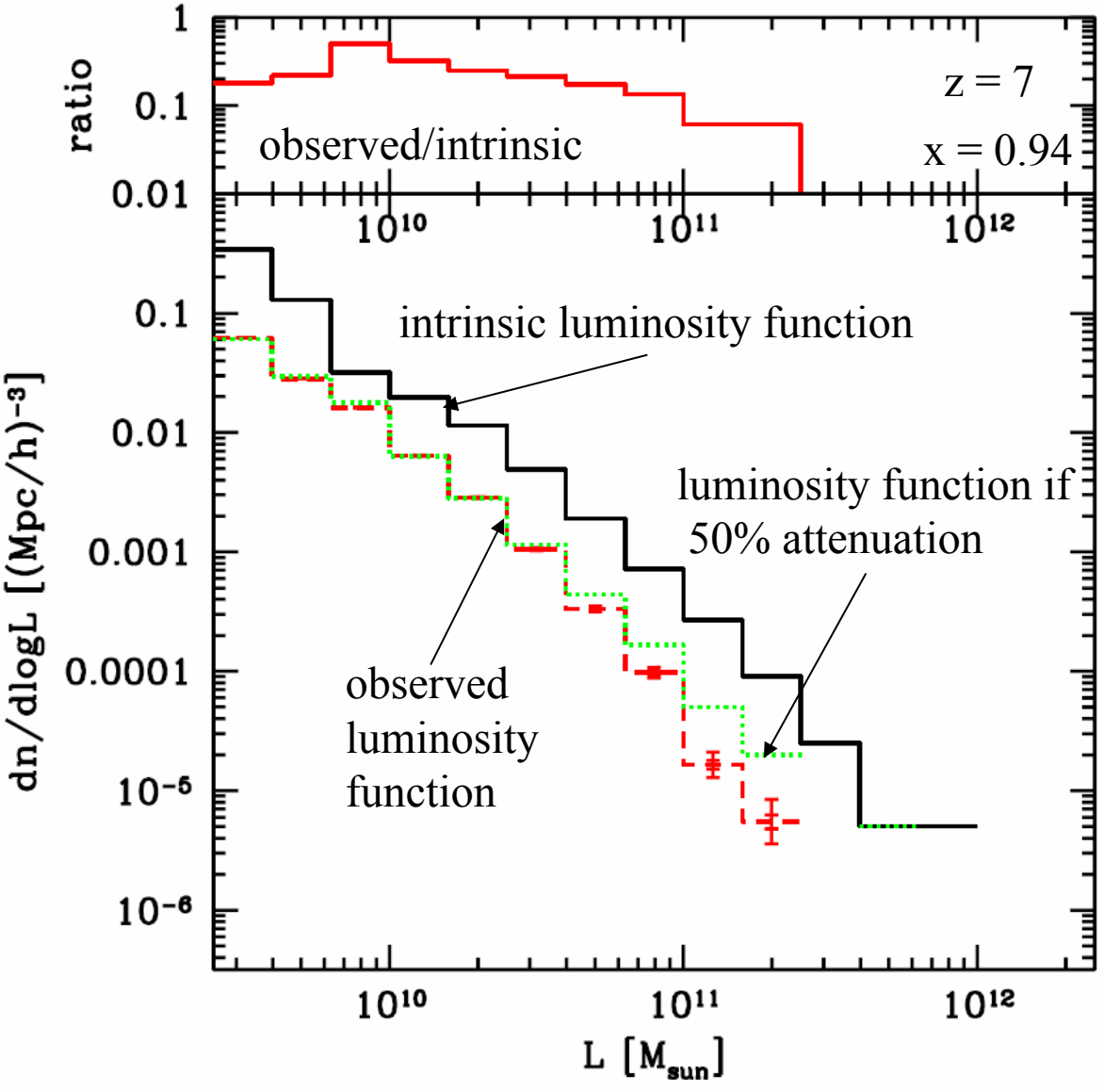

Luminosity Function of High-Redshift Ly-α Sources is Filtered By the Partially Ionized IGM

- Assuming all halos are Ly-α emitters with M/L = constant and 160 km/s Gaussian line profile;
- Even at z = 6, observed luminosity function is reduced by 0.5 from intrinsic luminosity function, except at bright end where factor is 0.1 or below;
- Attenuation exceeds 50% (i.e. blue-half absorbed, red-half not), now, but only at bright end.

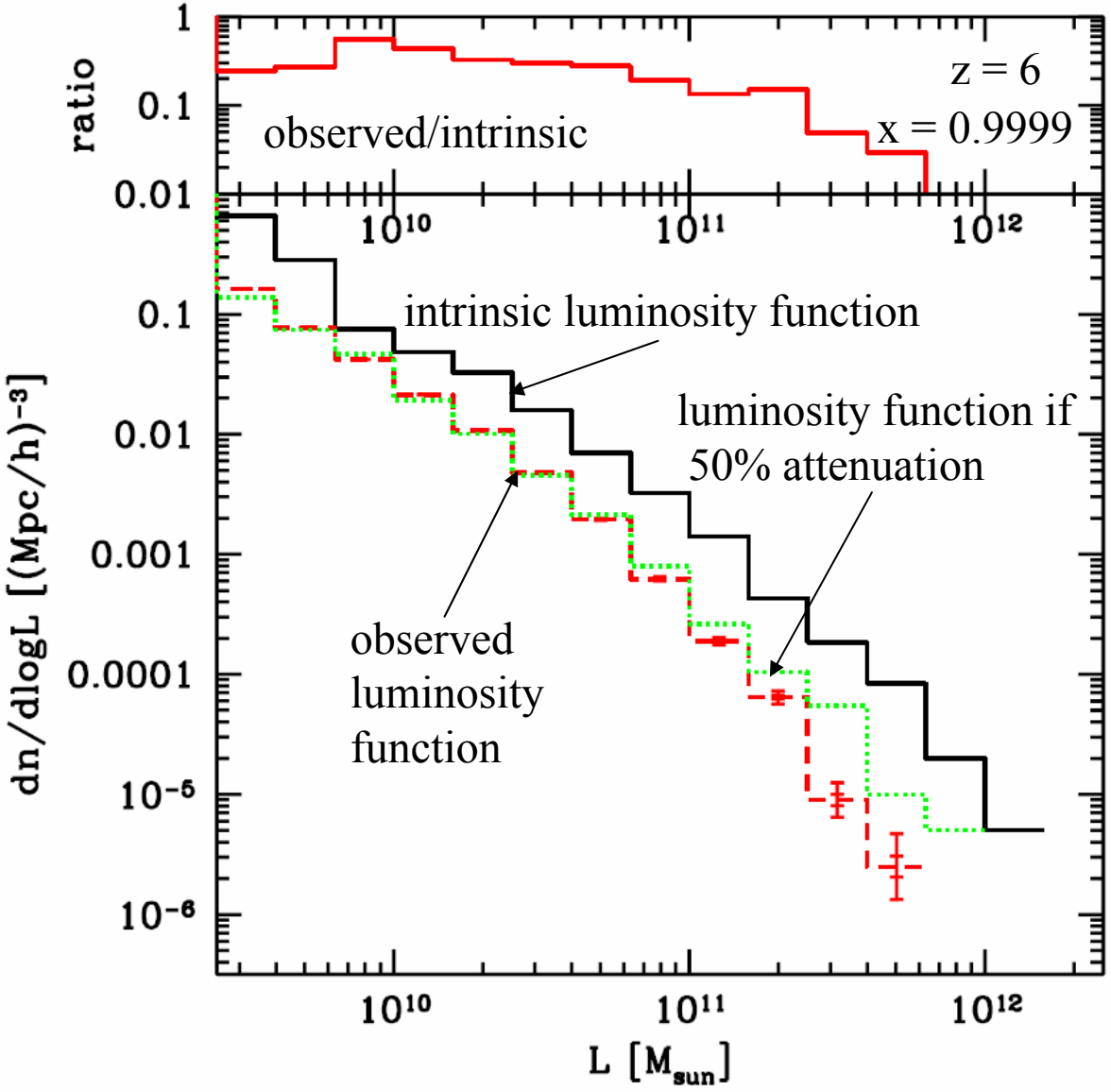

Predicting the observed luminosity function of Ly-α sources at the end of the EOR : simulations vs. observations

- To use our simulations to predict the observed LF, we "tune" the assumed M/L per halo to match the number density of sources in our simulations to the observed one reported by Kashikawa et al. (2006)
- ➔ simulated LF is an excellent match of the shape, for an assumed faint-end slope of -1.5 for the fit to the observations.
- ➔ the majority of sources responsible for reionization are too faint to be observed at present.

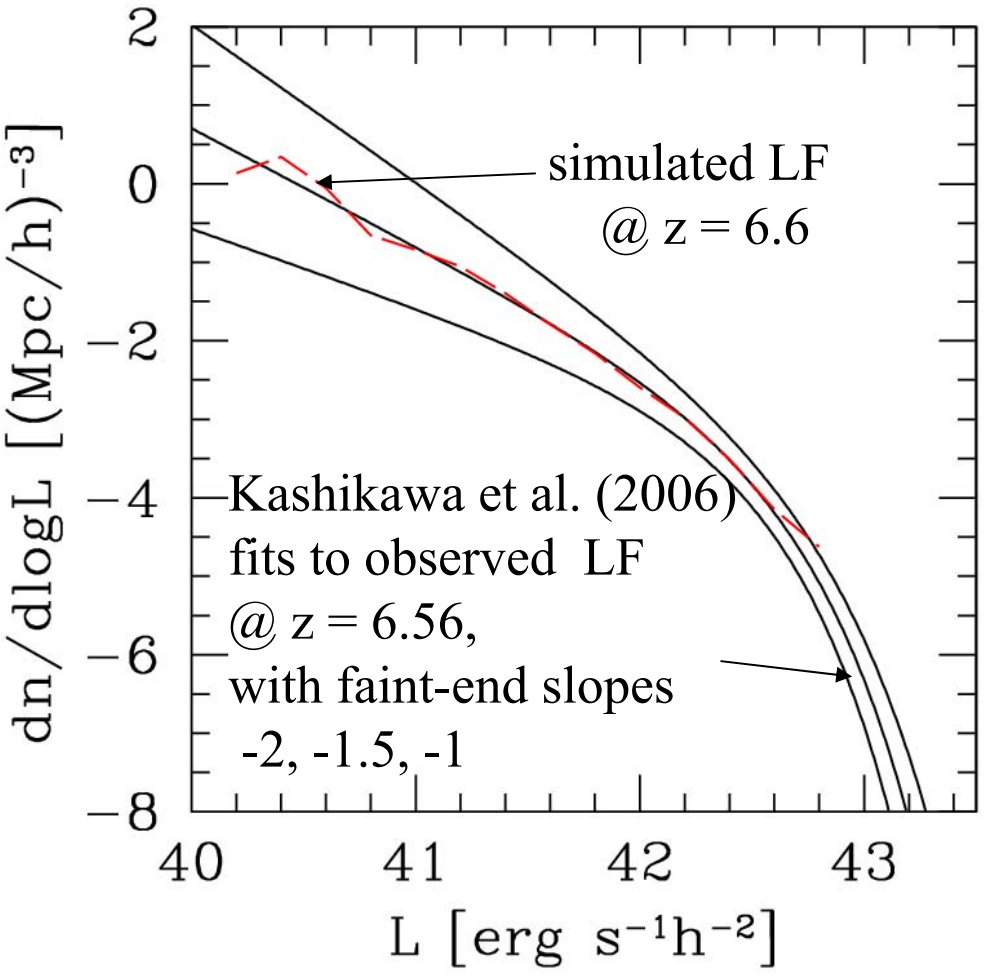

Mean IGM transmission due to Lyman-line resonance scattering at the end of the EOR : the Gunn-Peterson Effect at z > 6

- Simulations predict the Ly-α, Ly-β, and Ly-γ opacity of the IGM and its evolution during the EOR ➔ compare with the absorption spectra of observed high-redshift quasars to test the theory and the efficiencies assumed for the release of ionizing photons by early galaxies.

- e.g. for this illustrative simulation, EOR ended a bit too early to match the data from Fan et al. (2006) ➔ predicts somewhat higher transmission than observed, but captures the observed trend with redshift well ➔ lower source efficiencies are required for a better fit.

- Higher-z data can constrain reionization parameters better.

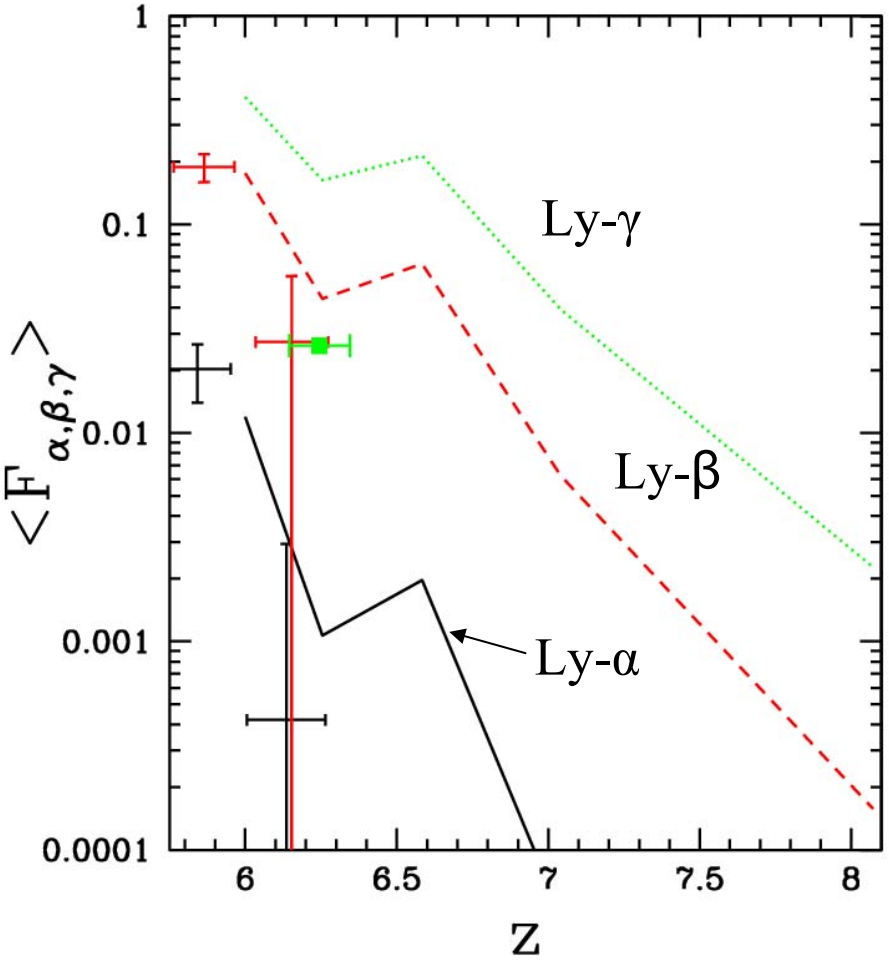

The inhomogeneous intergalactic photoionization rate during the EOR

z=8

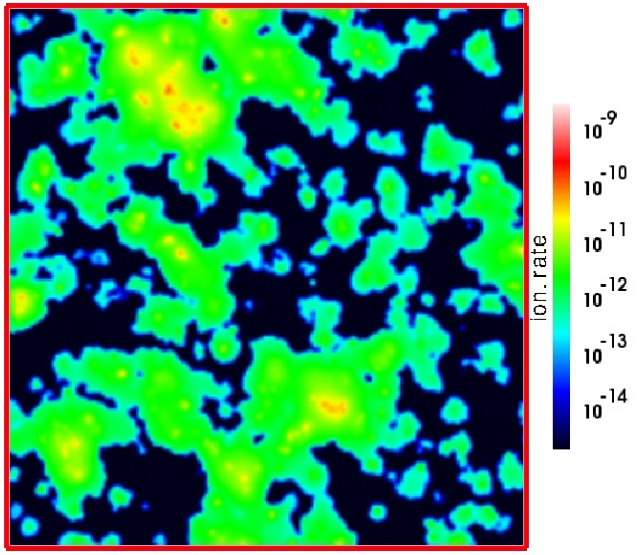

z=7

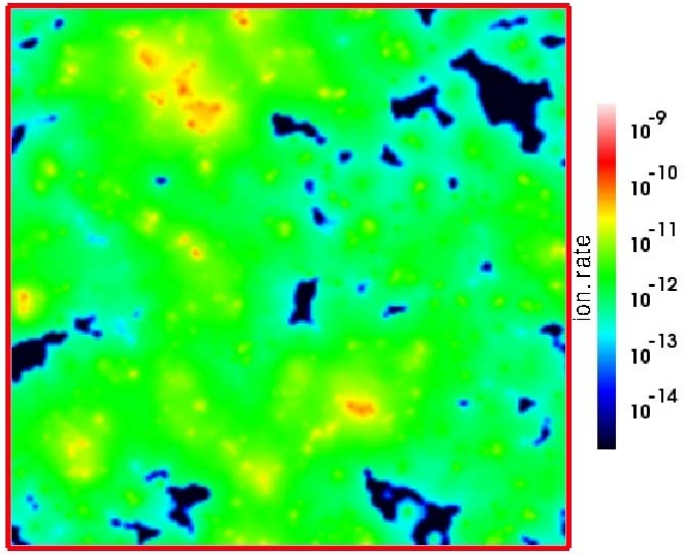

- Photoionization rates highly inhomogeneous
- Ionization is non-equilibrium behind I-fronts
- Average rate peaks at $\Gamma_{-12} \sim 1$ @ $z = 6$ (post-overlap)

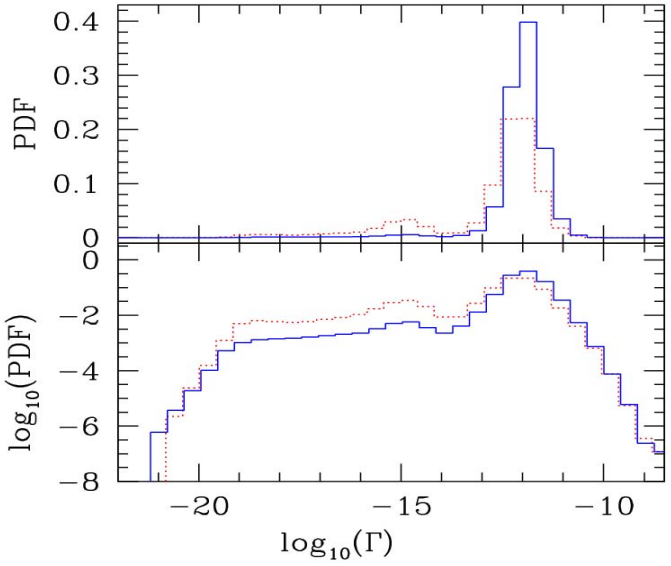

Self-Regulated Reionization

Iliev, Mellema, Shapiro, & Pen (2007), MNRAS, 376, 534; (astro-ph/0607517)

•Jeans-mass filtering ➔ low-mass source halos ($M < 10^9 M_{solar}$) cannot form inside H II regions ;

•35/h Mpc box, 406^3 radiative transfer simulation, WMAP3, $f_\gamma = 250$;

•resolved all halos with $M > 10^8 M_{solar}$ (i.e. all atomically-cooling halos), (blue dots = source cells);

• Evolution: z=21 to $z_{ov} = 7.5$.

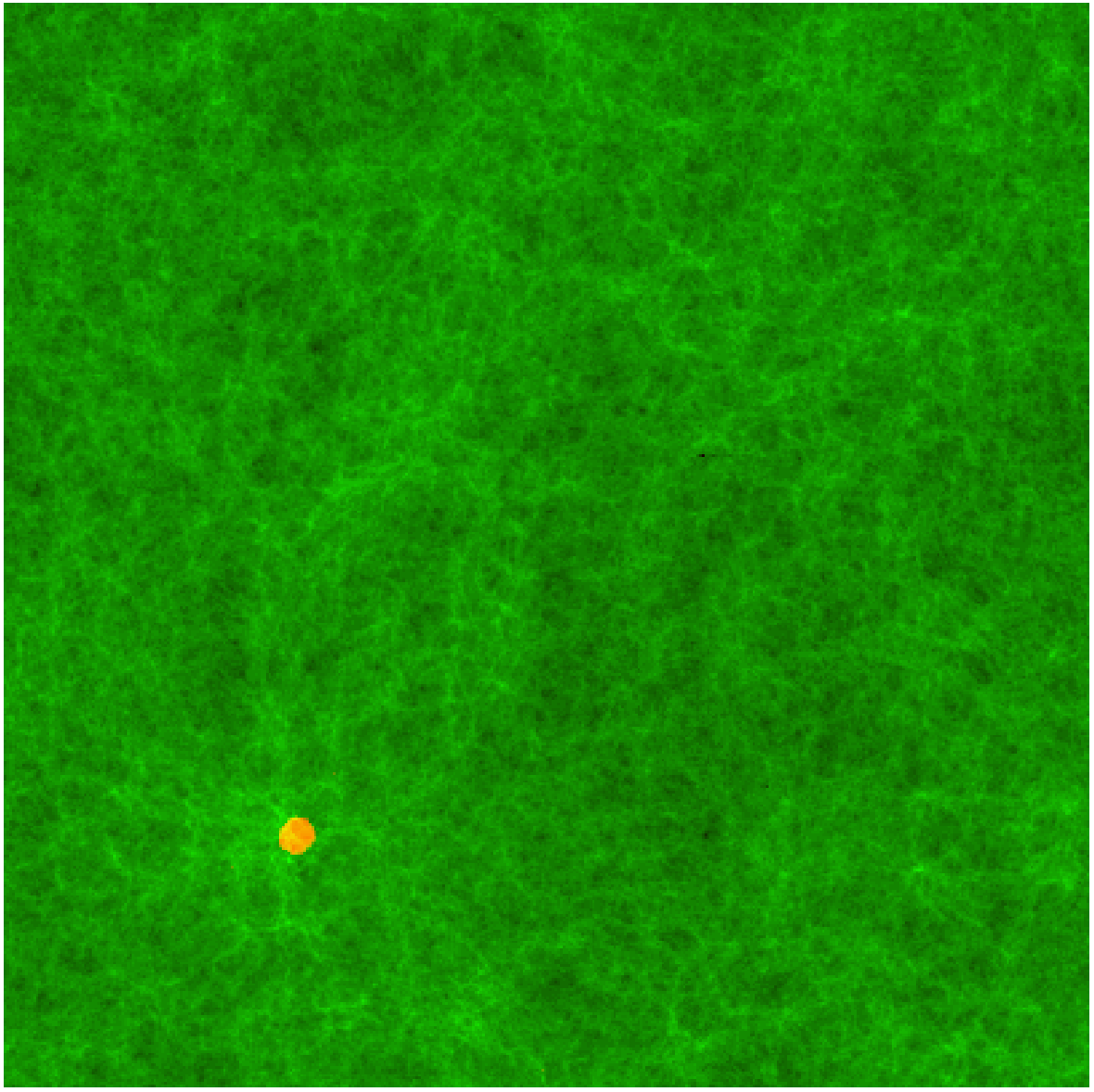

Extended reionization: Jeans-mass filtering, halo-mass-dependent emissivity

Cases

1. Halo masses $M_{solar} > 10^9$
   $f_\gamma = 2000$ (e.g. Pop III);

2. Halo masses $M_{solar} > 10^9$
   $f_\gamma = 250$ (e.g. Pop II);

3. Halo masses $M_{solar} > 10^8$
   $f_\gamma = 250$ (e.g. Pop II),
   lower-mass halos
suppressed inside H II regions
(Jeans-mass filtering) ;

4. Same as 3., but
   $f_\gamma = 2000$ ($M_{solar} < 10^9$)
   $f_\gamma = 250$ ($M_{solar} > 10^9$)

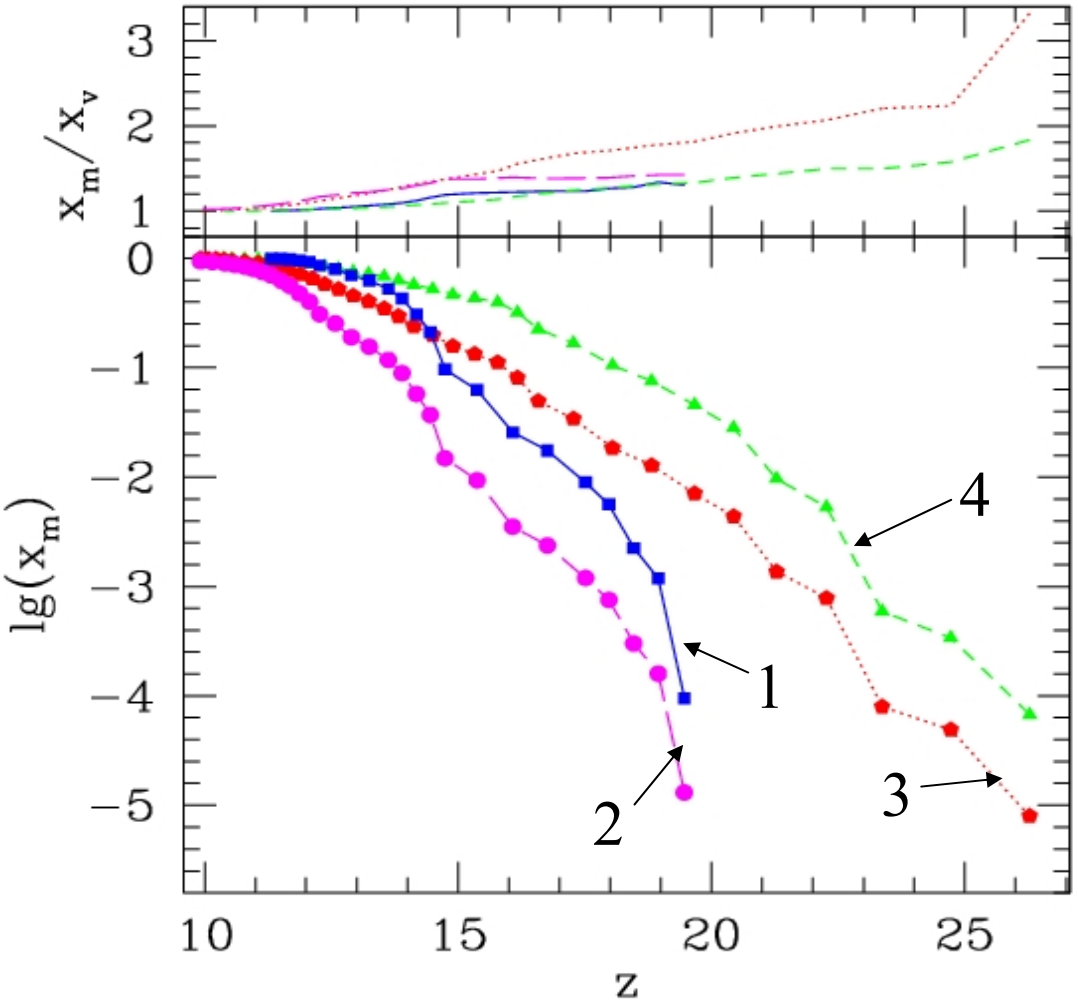

New, Large-Scale Simulations of Self-Regulated Reionization

Iliev, Mellema, Pen, Shapiro, and Merz (2008), in press (astro-ph/0806.2887);

Shapiro, Iliev, Mellema, Pen, & Merz (2008), in press (astro-ph/0806.3091)

CubeP^{3}M N-body ΛCDM sim with
3072^3 (29 billion) particles,
6144^3 cells,
box size = 160 Mpc;
particle mass =
5 million solar masses

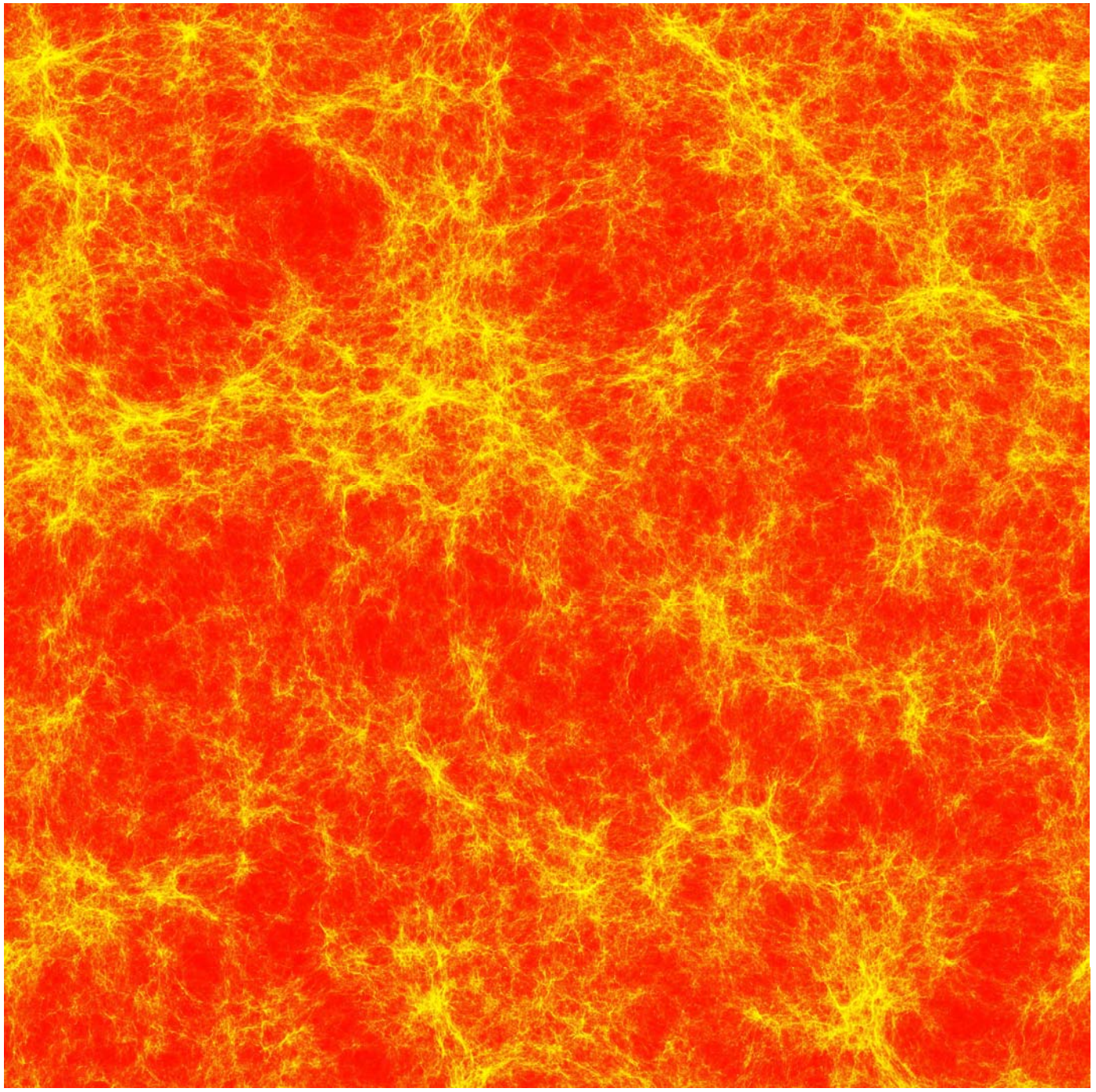

New, Large-Scale Simulations of Self-Regulated Reionization

Iliev, Mellema, Pen, Shapiro, and Merz (2008), in press (astro-ph/0806.2887);

Shapiro, Iliev, Mellema, Pen, & Merz (2008), in press (astro-ph/0806.3091)

CubeP^{3}M N-body ΛCDM sim with 3072^3 (29 billion) particles, resolves halos above 10^8 solar masses

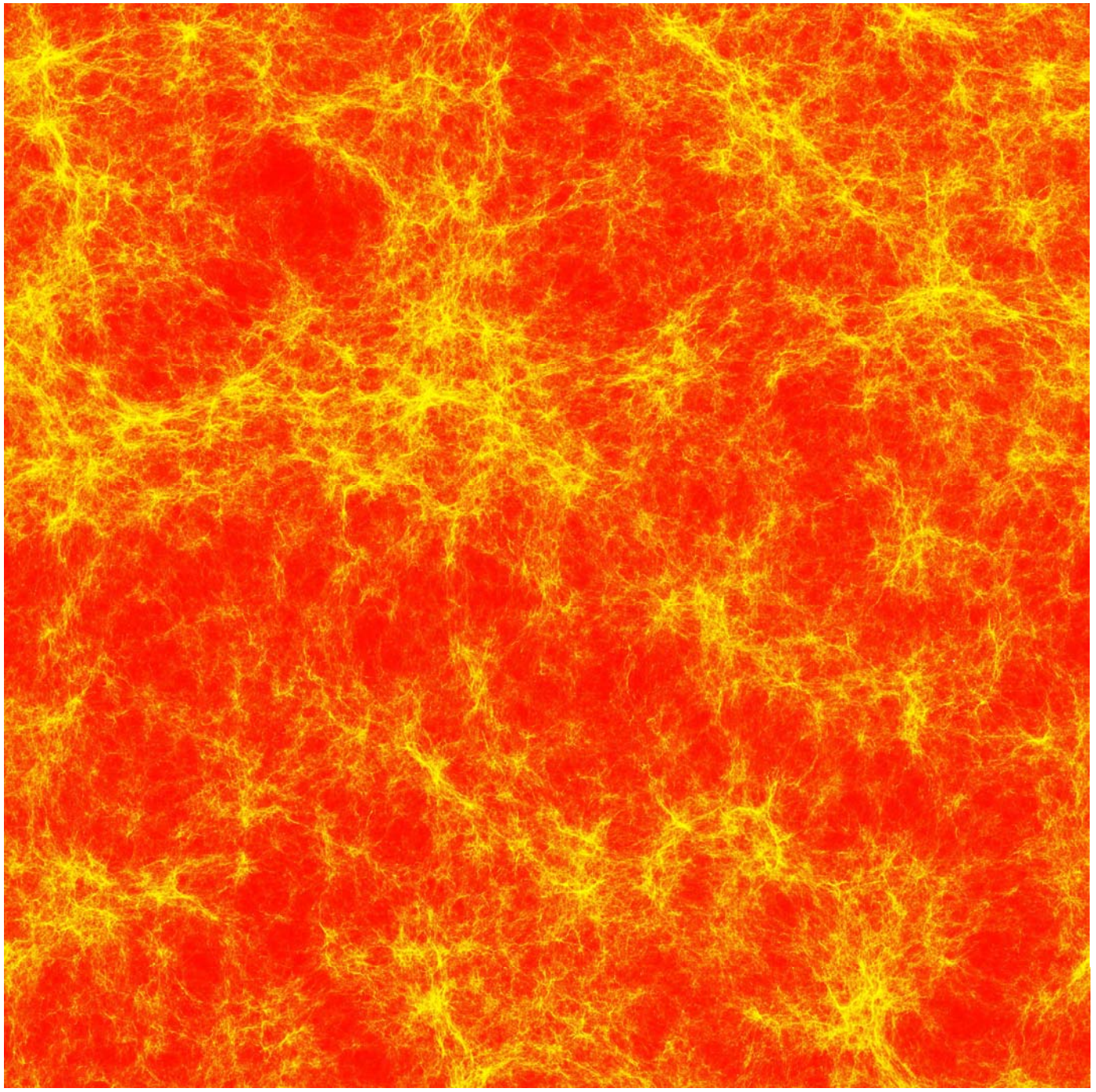

New, Large-Scale Simulations of Self-Regulated Reionization

Iliev, Mellema, Pen, Shapiro, and Merz (2008), in press (astro-ph/0806.2887);

Shapiro, Iliev, Mellema, Pen, & Merz (2008), in press (astro-ph/0806.3091)

CubeP^{3}M N-body

- new Texas Sun Constellation Linux Cluster, *Ranger*, 2048 cores, 159,000 SUs (cores x hours)

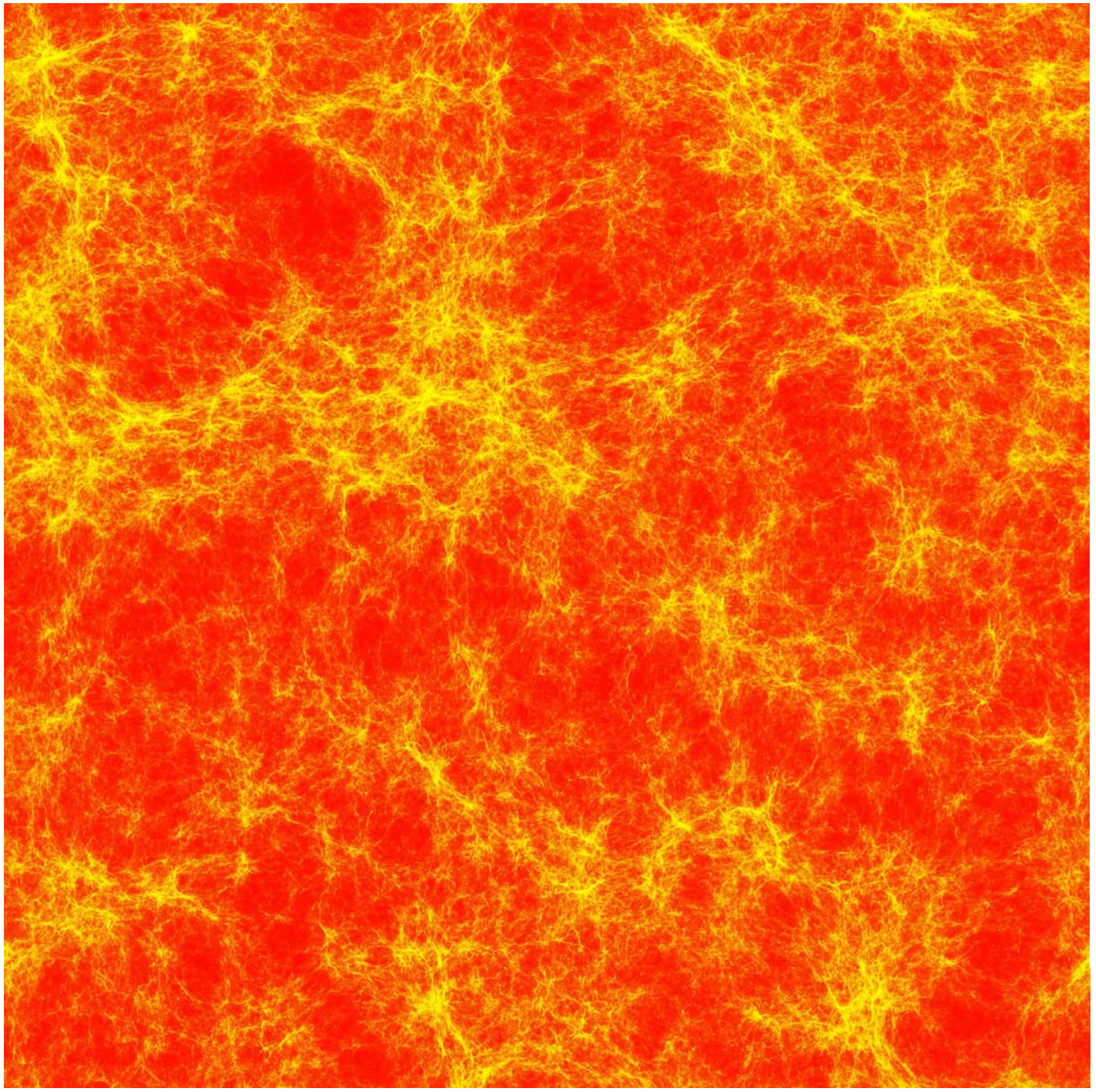

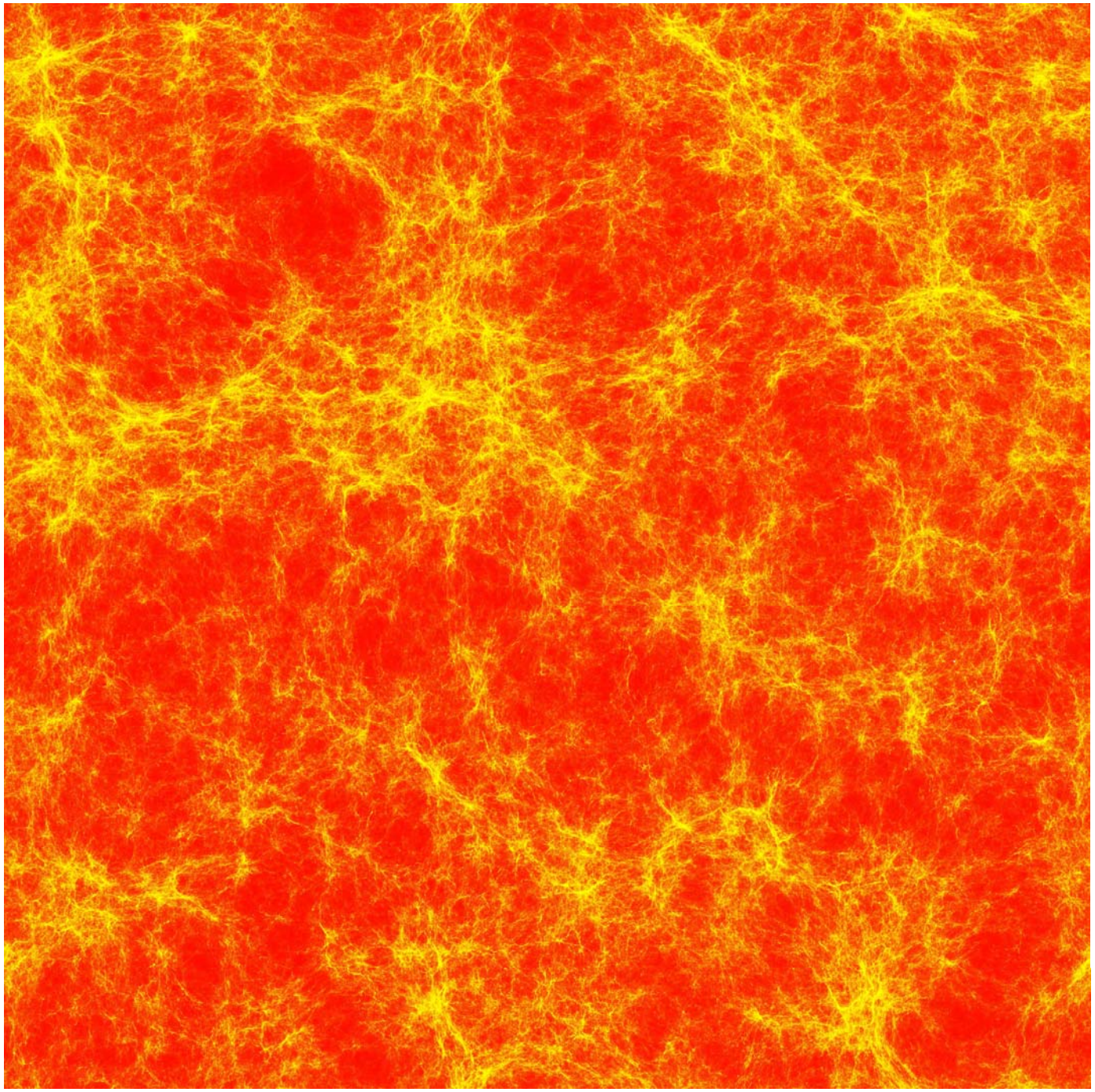

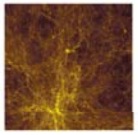

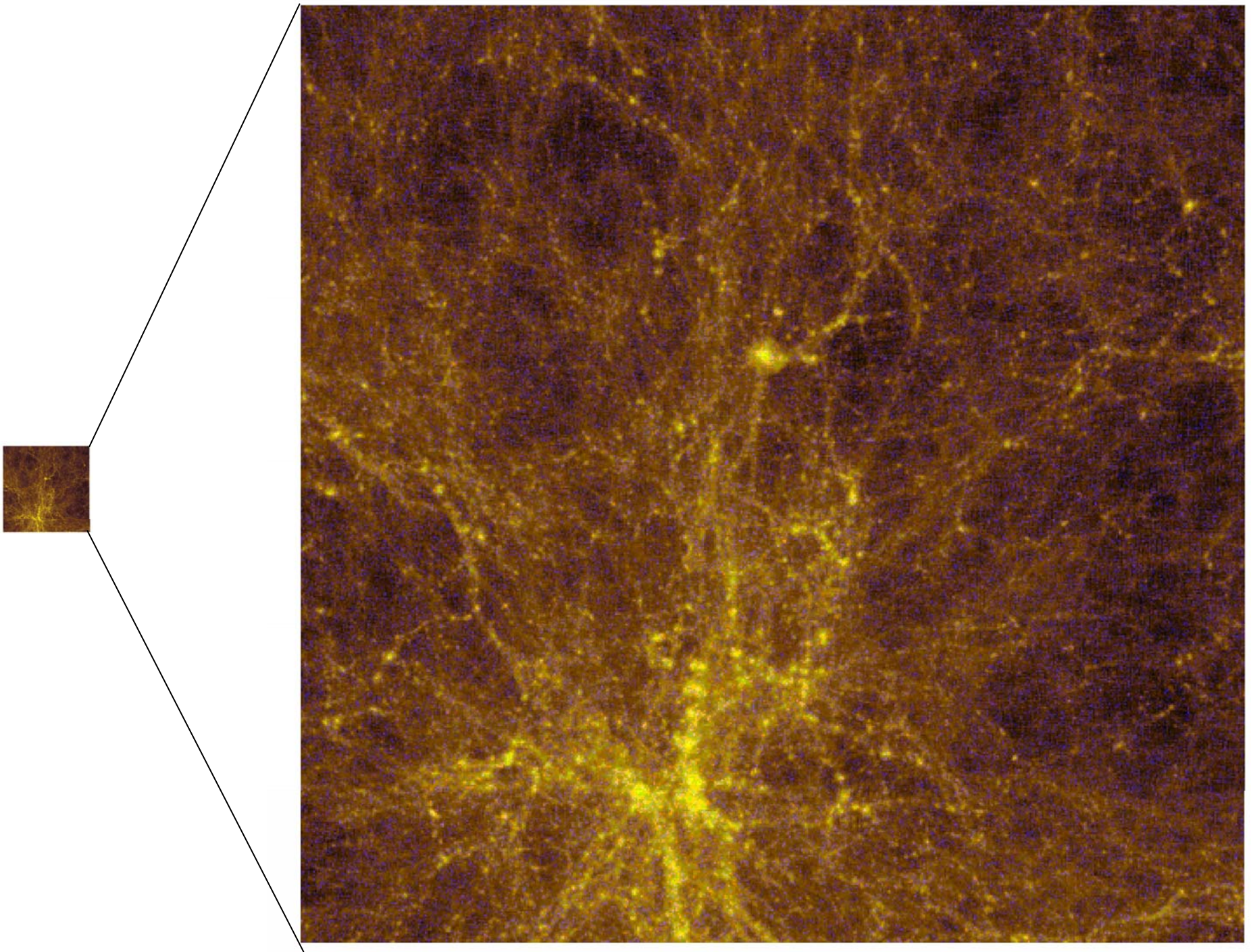

ΛCDM Halo Mass Function ($M > 10^8$ Solar Masses)

from CubeP^{3}M N-body Simulations

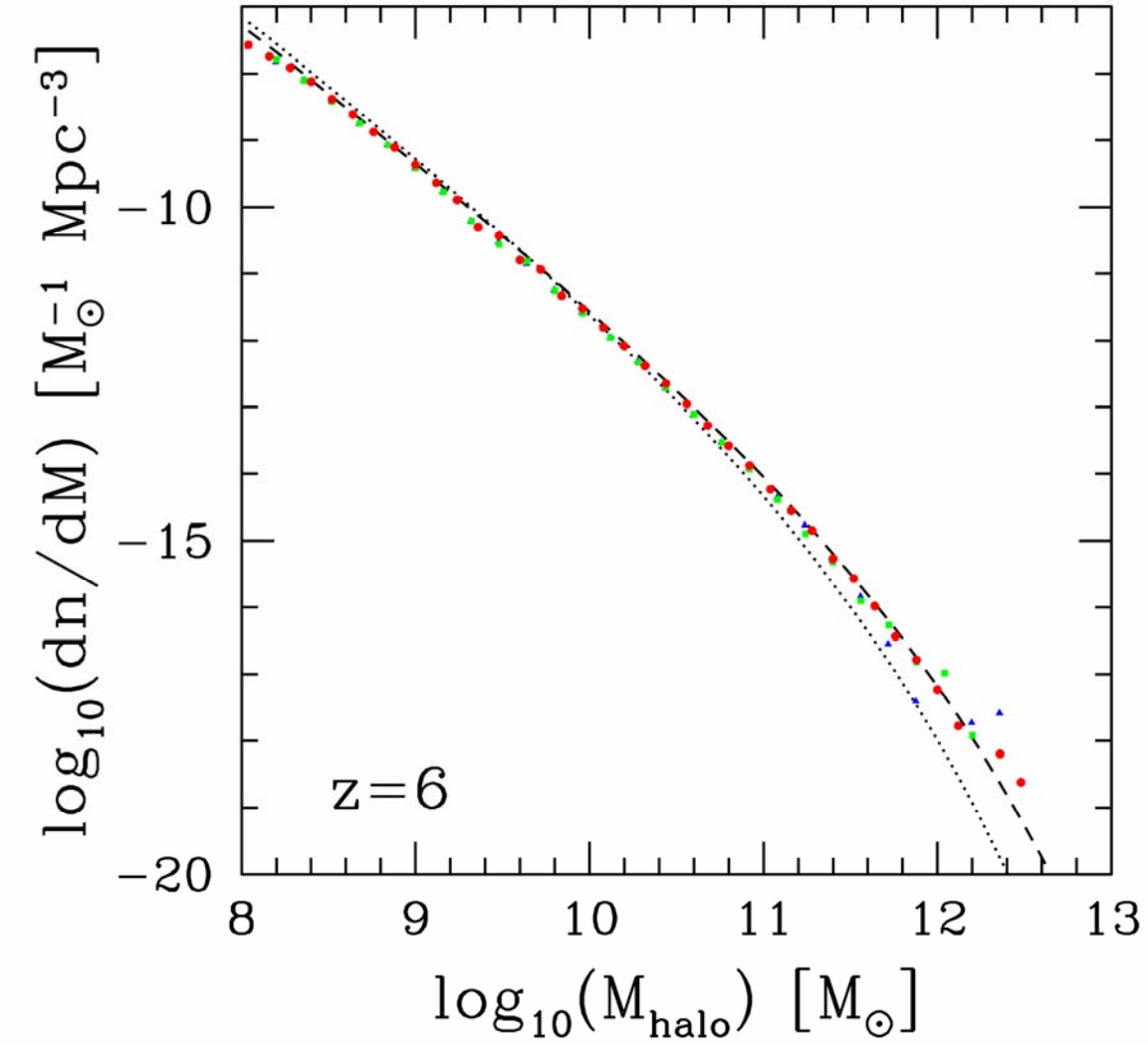

simulation box sizes 91 Mpc, 103 Mpc, 163 Mpc

C^2Ray radiative transfer

- RT grid 432^3 cells
- box size = 90 Mpc

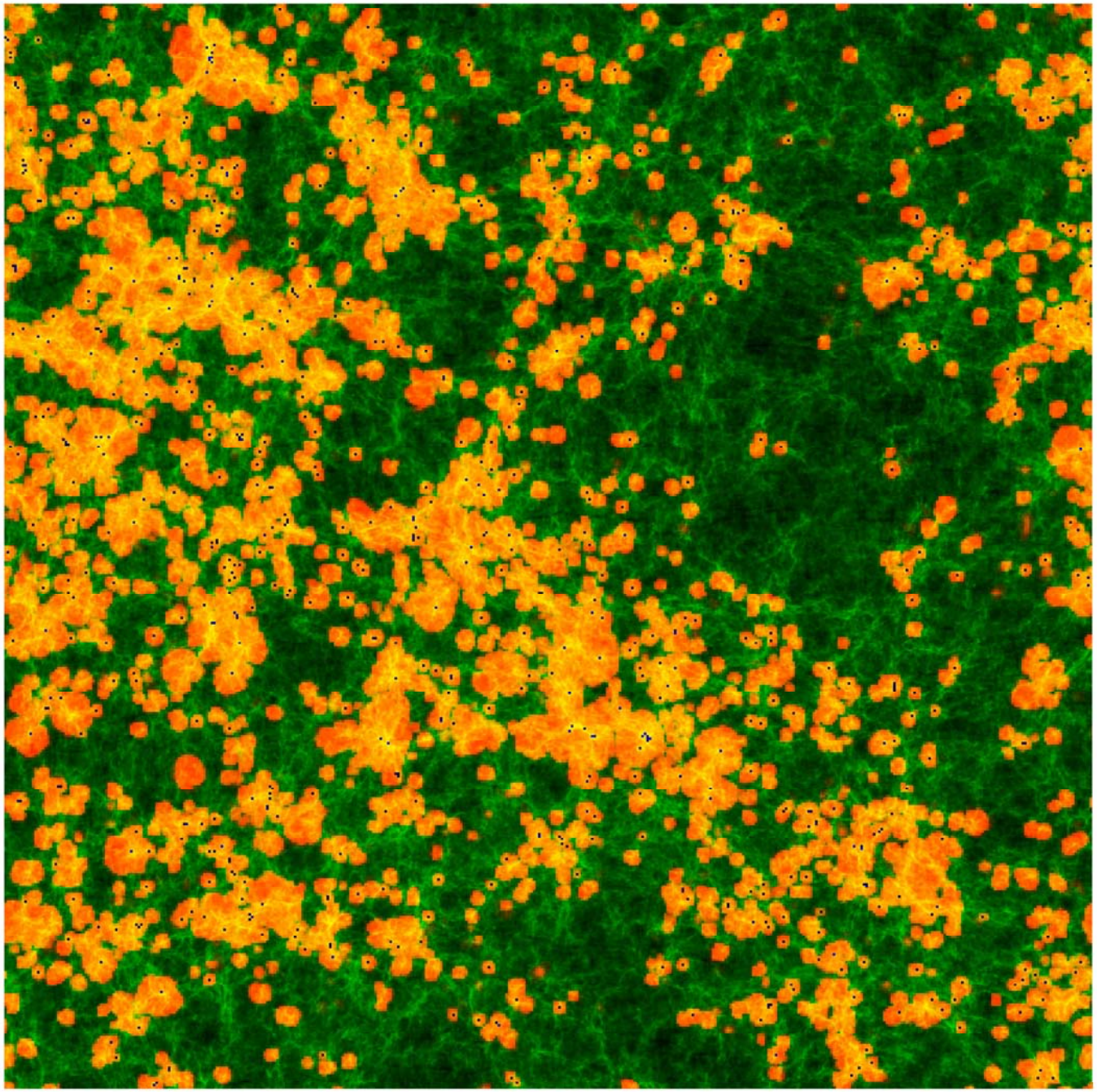

C^2Ray radiative transfer

- RT grid 432^3 cells
- box size = 90 Mpc
- *Ranger*, Texas Sun Constellation Linux Cluster, 700,000 SUs (cores x hours), up to 10,000 cores

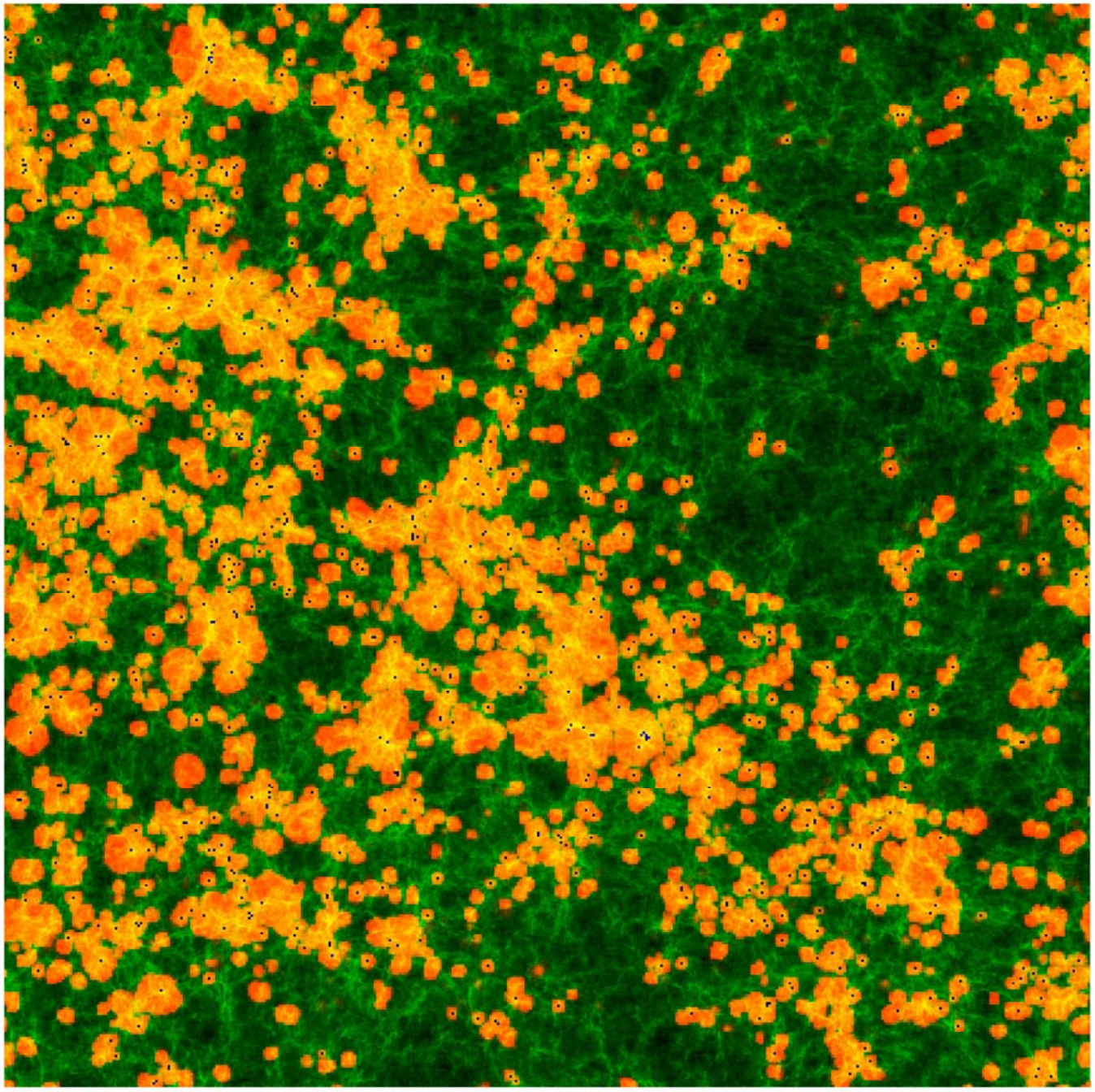

Self-Regulated Reionization in ΛCDM

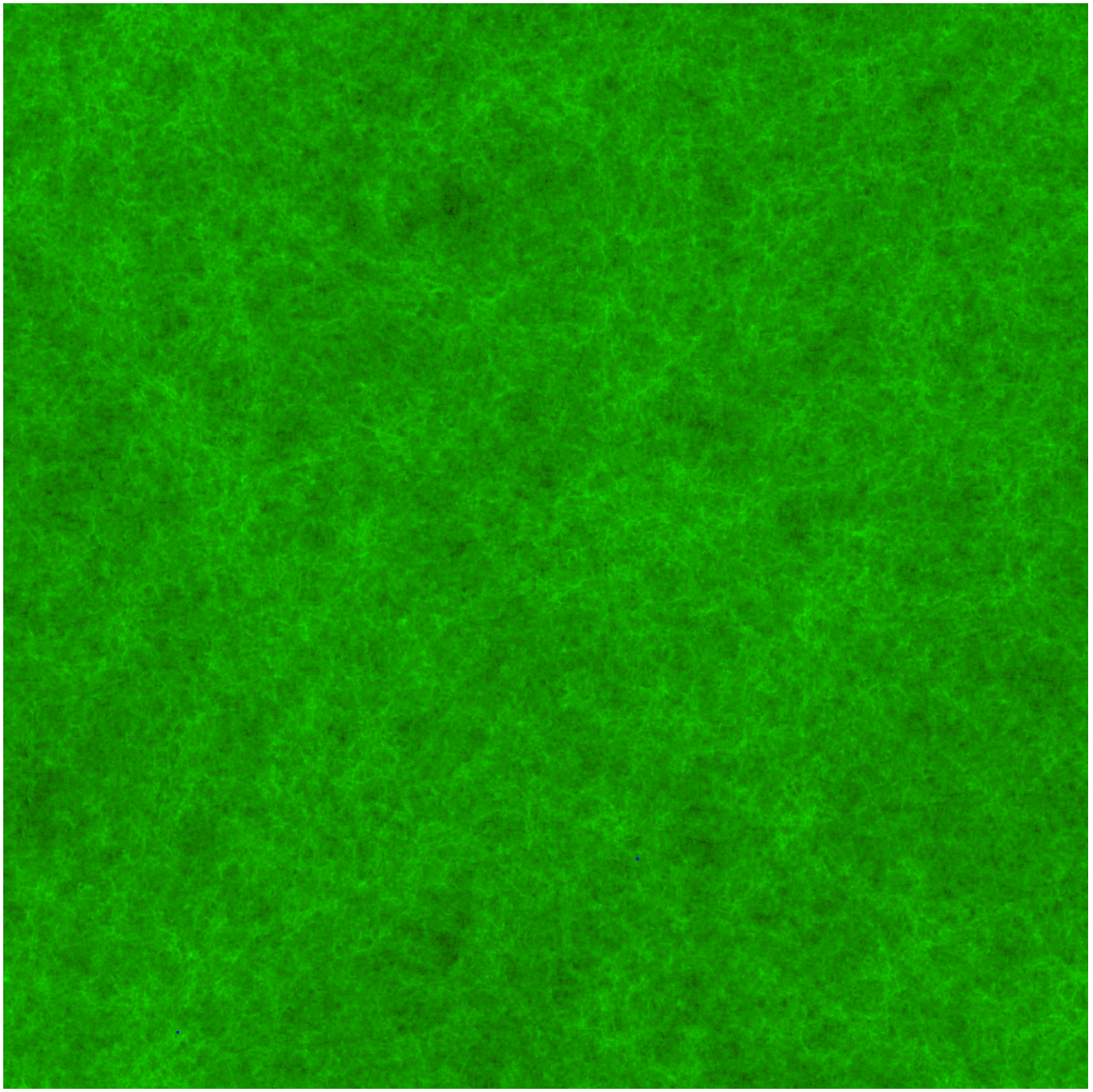

- 90 Mpc box

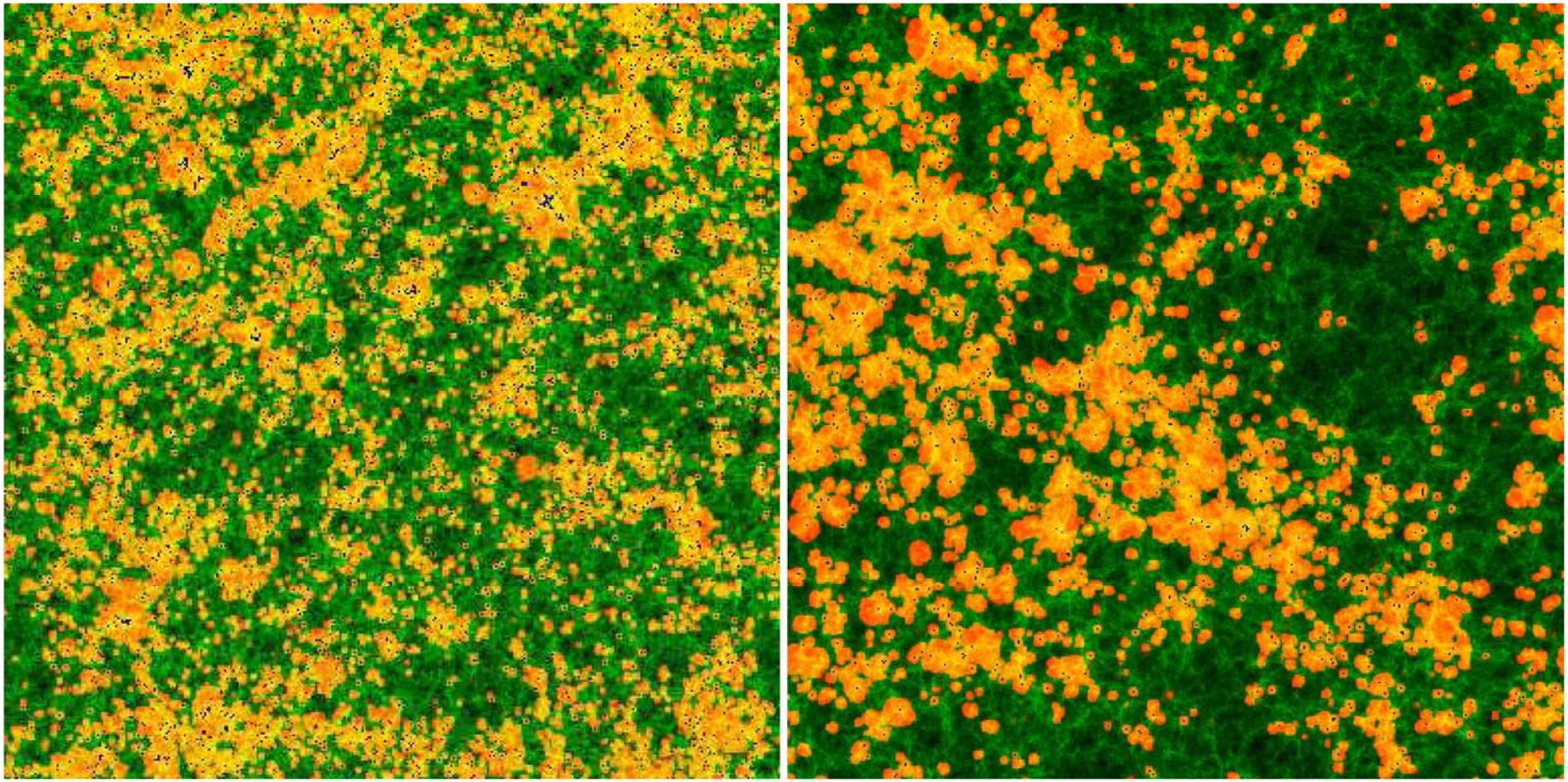

160 Mpc box

z = 11.6

90 Mpc box

z = 11.9

when mass-weighted mean ionized fraction of universe $x_m = 0.3$

Self-regulated halo mass function

- Jeans-mass filtering suppresses formation of sources in small-mass halos which form inside H II regions
- clustering of small-mass halos around density peaks enhances this effect ➔ suppression is strongly biased

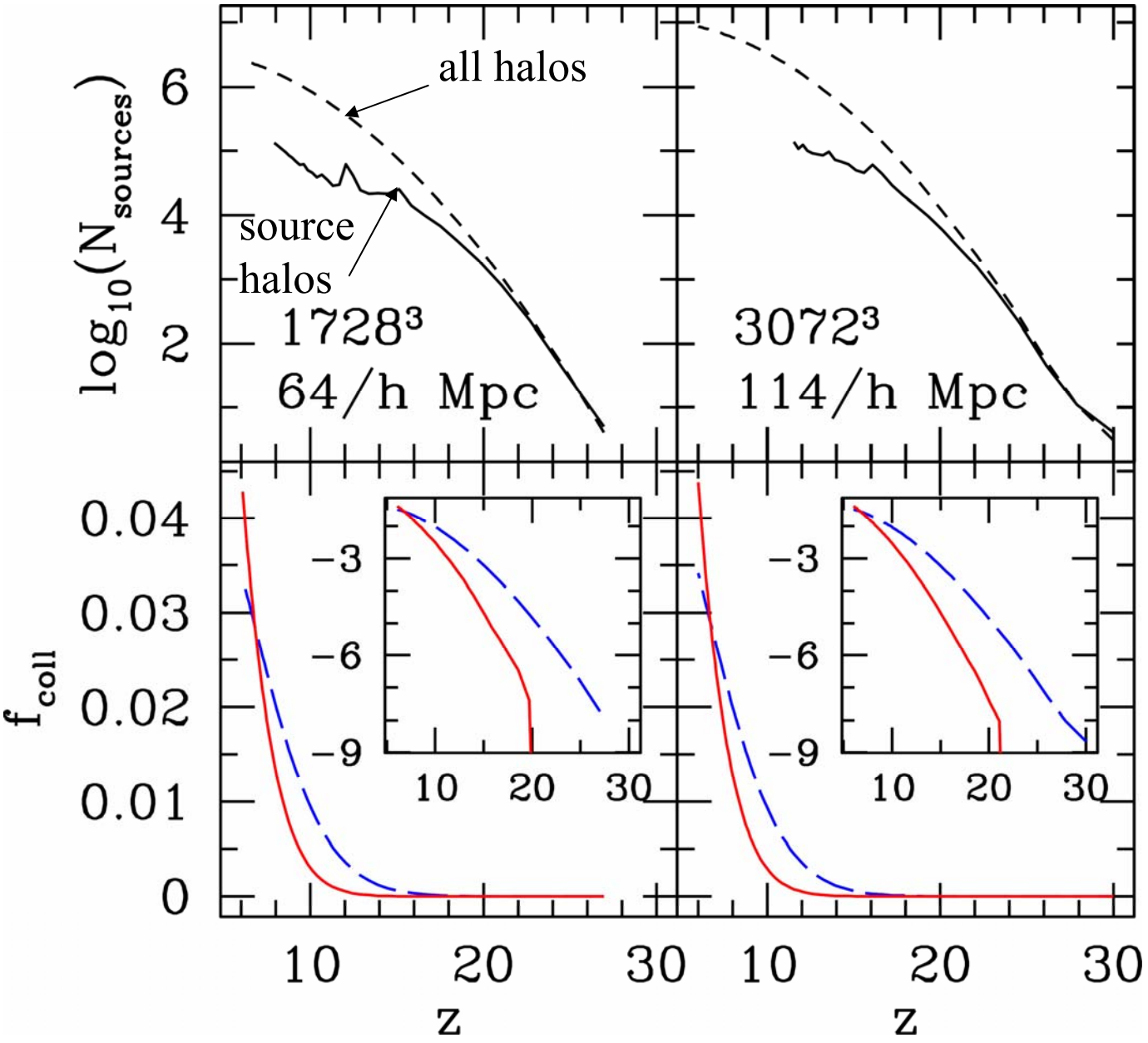

Evolution of the Mean Ionized Fraction of the Universe

- self-regulated reion.
  (i.e. small-mass halos resolved) starts earlier, but ends about the same time ➔
- high-mass halos dominate the end of EOR

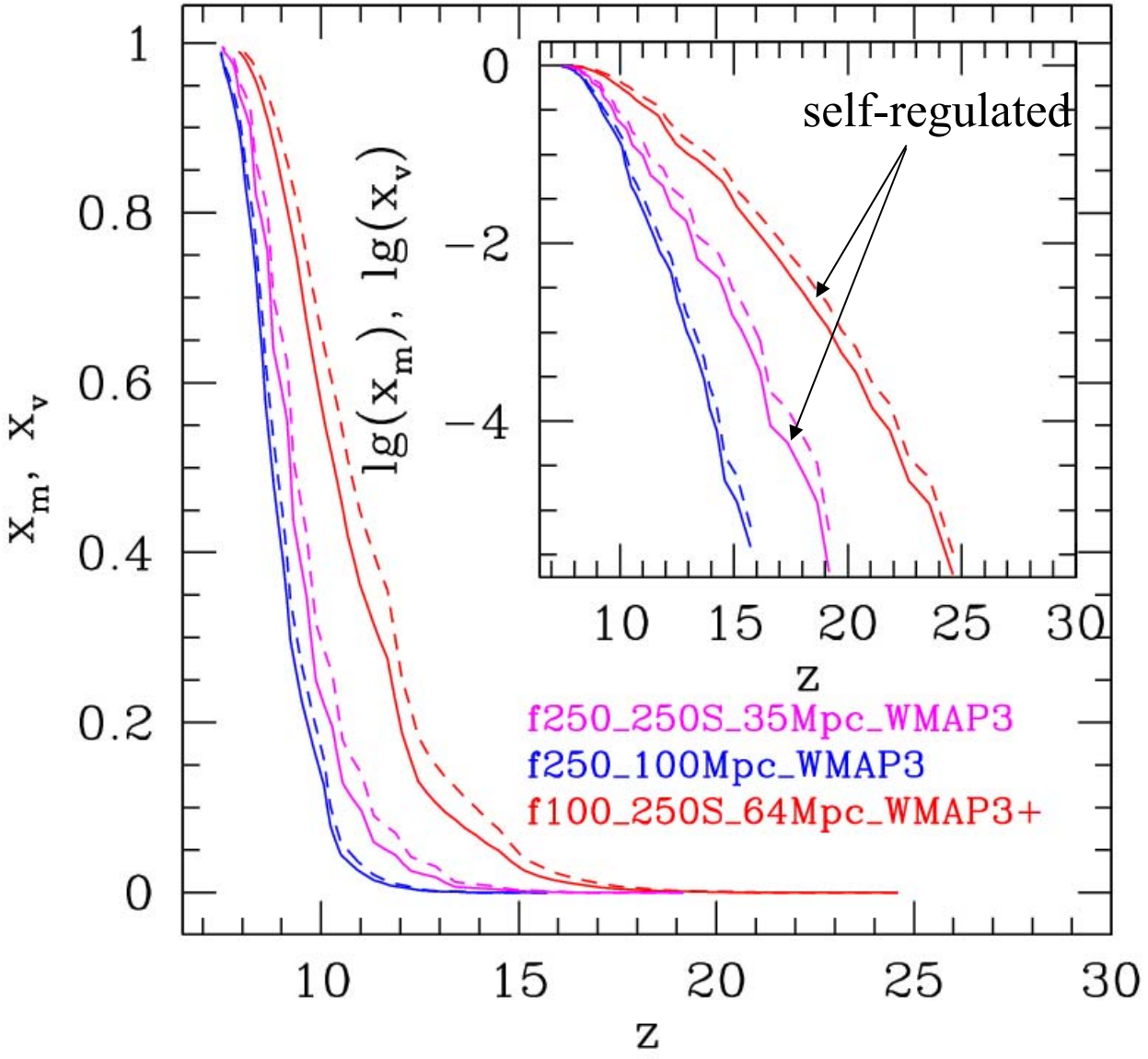

Seeing Invisible Light From the Dark Ages and the Epoch of Reionization that Ended Them

- Hydrogen atoms in the early universe can be detected in absorption or emission against the Cosmic Microwave Background (CMB) at redshifted radio wavelength 21 cm.
- Halos formed during the dark ages are dense and hot enough to appear in emission.
- The intergalactic medium, too, can appear in either emission or absorption.
- Future radio astronomy antenna arrays are being designed and built to detect this 21 cm emission.

Low Frequency Array (LOFAR)

Murchison Widefield Array (MWA)

PrimevAl Structure Telescope (PAST/21CMA)

Prototype Tests, Ulastai, Xin Jiang, China

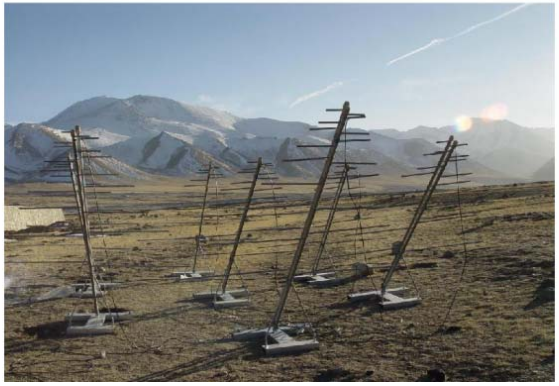

Giant Meterwave Radio Telescope (GMRT)

Square Kilometer Array (SKA)

21-cm Level Population of Atomic Hydrogen

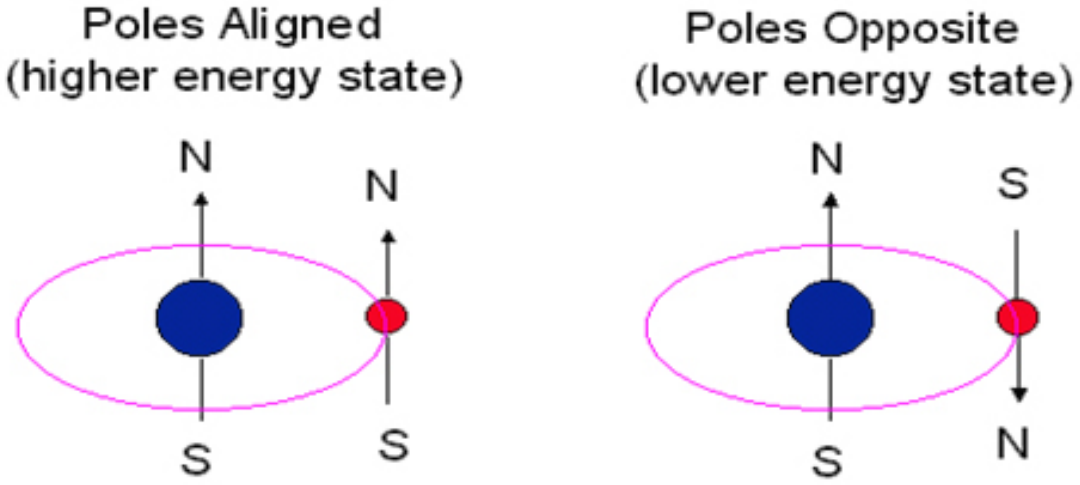

$$\frac{n_2}{n_1} = 3\exp\left(-\frac{h\upsilon_0}{kT_{spin}}\right)$$

21-cm Radiation Background

- Foreground emission or absorption by H atoms at redshift z seen against CMB at redshifted wavelength 21(1+z) cm.

Emission $\leftrightarrow$ $T_{spin} > T_{CMB}$

Absorption $\leftrightarrow$ $T_{spin} < T_{CMB}$

Transparent $\leftrightarrow$ $T_{spin} = T_{CMB}$

3 Ways to Change the 21-cm Level Population

- An H atom can:
  - Absorb a 21-cm photon from the CMB

    (CMB Pumping)
  - Collide with another atom (or an electron or ion)

    (Collisional Pumping)
  - Absorb a UV photon at 1215 Angstrom to make Lyman alpha transition of H atom, then decay to one of 21-cm levels

    (Lyman Alpha Pumping)

3 Ways to Change the 21-cm Level Population

- An H atom can:
  - Absorb a 21-cm photon from the CMB

    (CMB Pumping)
  - Collide with another atom

    (Collisional Pumping)
  - **Absorb a UV photon at 1215 Angstrom to make Lyman alpha transition of H atom, then decay to one of 21-cm levels**

    (Lyman Alpha Pumping)

Stages of 21-cm Background

- Dark Ages
  - $z \geq 150$, $T_{spin}=T_{CMB}$ → nothing
  - $20 \leq z \leq 150$, $T_{spin}<T_{CMB}$ → absorption
  - $z \leq 20$, $T_{spin}>T_{CMB}$ in minihalos → emission
- Epoch of Reionization ($6 \leq z \leq 20$)
  - $T_{spin}>T_{CMB}$ in minihalos → emission
  - After sources turn on, Lyman alpha pumping →
    - Without heating, $T_{spin}<T_{CMB}$ → IGM in absorption
    - With heating, $T_{spin}>T_{CMB}$ → IGM in emission

Stages of 21-cm Background

- Dark Ages
  - $z \geq 150$, $T_{spin}=T_{CMB}$ → nothing
  - **$20 \leq z \leq 150$, $T_{spin}<T_{CMB}$ → absorption**
  - **$z \leq 20$, $T_{spin}>T_{CMB}$ in minihalos → emission**
- Epoch of Reionization ($6 \leq z \leq 20$)
  - $T_{spin}>T_{CMB}$ in minihalos → emission
  - After sources turn on, Lyman alpha pumping →
    - Without heating, $T_{spin}<T_{CMB}$ → IGM in absorption
    - With heating, $T_{spin}>T_{CMB}$ → IGM in emission

The 21-cm Background from the Cosmic Dark Ages: Minihalos and the Intergalactic Medium Before Reionization : Collisionally Pumped Spin Temperature

- Iliev, Shapiro, Ferrara & Martel 2002, ApJL, 572, L123
- Iliev, Scannapieco, Shapiro, & Martel 2003, MNRAS, 341, 81
- Shapiro, Ahn, Alvarez, Iliev, Martel & Ryu (2006), ApJ, 646, 681; (astro-ph/0512516)

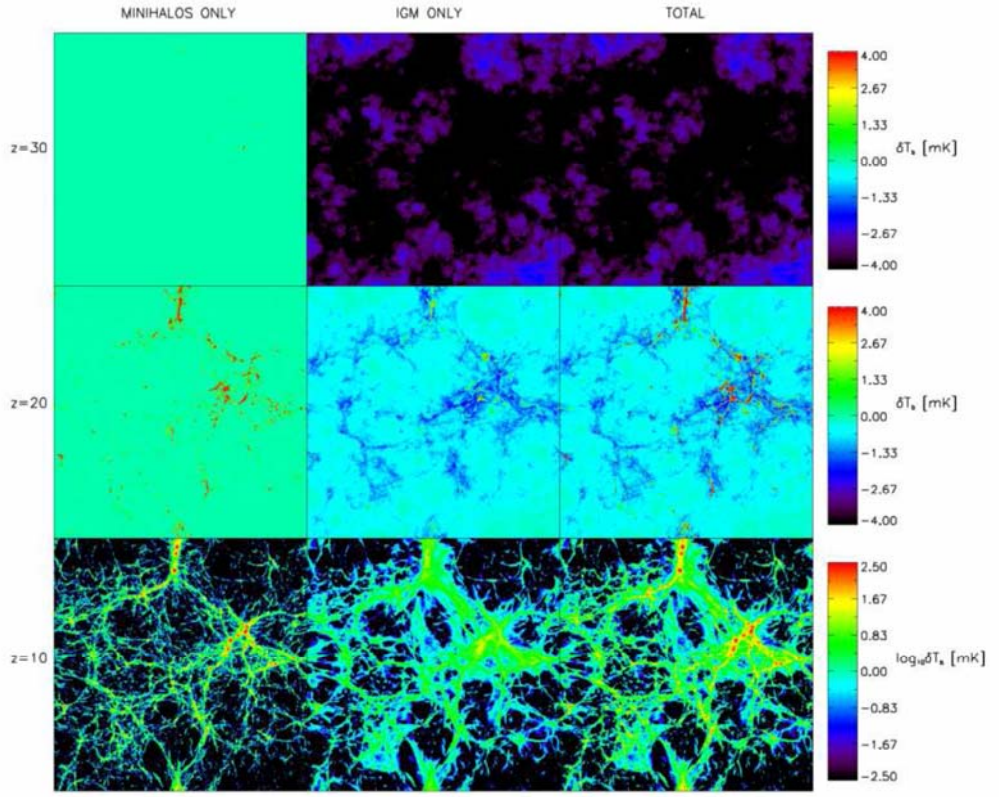

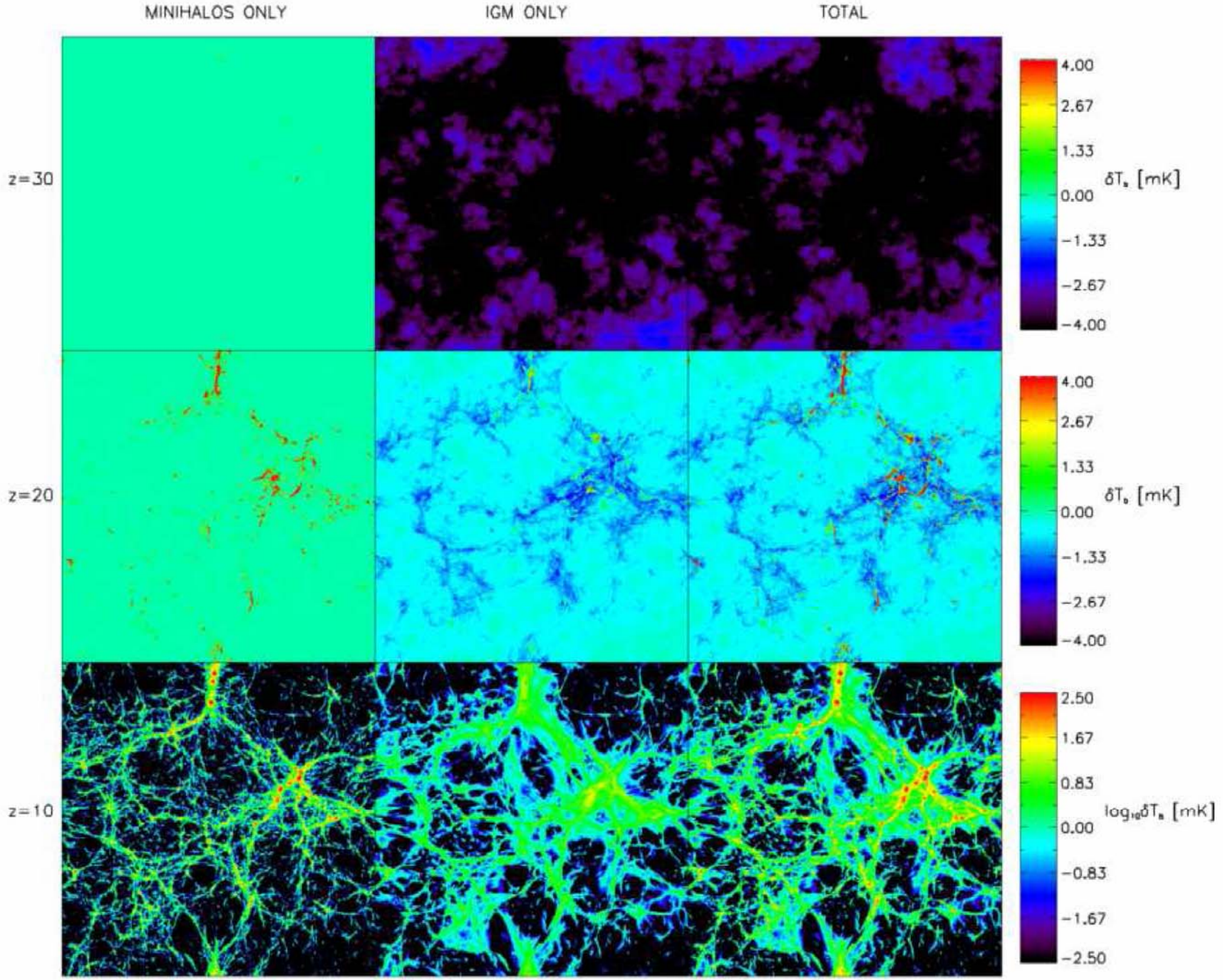
MINIHALOS ONLY
IGM ONLY
TOTAL
z=30
z=20
z=10
4.00
2.67
1.33
0.00
−1.33
−2.67
−4.00
δT_b [mK]
4.00
2.67
1.33
0.00
−1.33
−2.67
−4.00
δT_b [mK]
2.50
1.67
0.83
0.00
−0.83
−1.67
−2.50
log10δT_b [mK]

Stages of 21-cm Background

- Dark Ages
  - $z \geq 150$, $T_{spin}=T_{CMB}$ → nothing
  - $20 \leq z \leq 150$, $T_{spin}<T_{CMB}$ → absorption
  - $z \leq 20$, $T_{spin}>T_{CMB}$ in minihalos → emission
- **Epoch of Reionization ($6 \leq z \leq 20$)**
  - $T_{spin}>T_{CMB}$ in minihalos → emission
  - **After sources turn on, Lyman alpha pumping →**
    - Without heating, $T_{spin}<T_{CMB}$ → IGM in absorption
    - With heating, $T_{spin}>T_{CMB}$ → IGM in emission

Stages of 21-cm Background

- Dark Ages
  - $z \geq 150$, $T_{spin}=T_{CMB}$ → nothing
  - $20 \leq z \leq 150$, $T_{spin}<T_{CMB}$ → absorption
  - $z \leq 20$, $T_{spin}>T_{CMB}$ in minihalos → emission
- **Epoch of Reionization ($6 \leq z \leq 20$)**
  - $T_{spin}>T_{CMB}$ in minihalos → emission
  - **After sources turn on, Lyman alpha pumping →**
    - **Without heating, $T_{spin}<T_{CMB}$ → IGM in absorption**
    - With heating, $T_{spin}>T_{CMB}$ → IGM in emission

Decoupling the spin temperature of the 21-cm transition of H I from the CMB

(Chuzhoy and Shapiro 2006, ApJ, 651, 1; astro-ph/0512206)

- Spin temperature

$$T_{\rm s} = \frac{T_{\rm CMB} + y_\alpha T_\alpha + y_{\rm c} T_{\rm k}}{1 + y_\alpha + y_{\rm c}},$$

where $y_\alpha = (P_{10}\, T_*)/(A_{10}\, T_\alpha)$

$P_{10} \propto J_\alpha$ = mean intensity at Ly α

(Field 1958, 1959)

- <u>Standard assumption</u>:

scattering ➔ atomic recoil ➔ $T_\alpha = T_k$

and

$J_\alpha = J_{\alpha,0}$ = background level

- But there is a backreaction of the Ly α scattering :

hyperfine splitting + atomic recoil
===>

(1) $T_\alpha \neq T_k$
(T_α between T_k and T_{CMB})

(2) $J_\alpha \neq J_{\alpha,o}$
(Chen and Miralda-Escude 2004; without hyperfine splitting)

(3) T_α , J_α both depend on local departure from Hubble flow
===> small-scale structure affects mean 21-cm signal

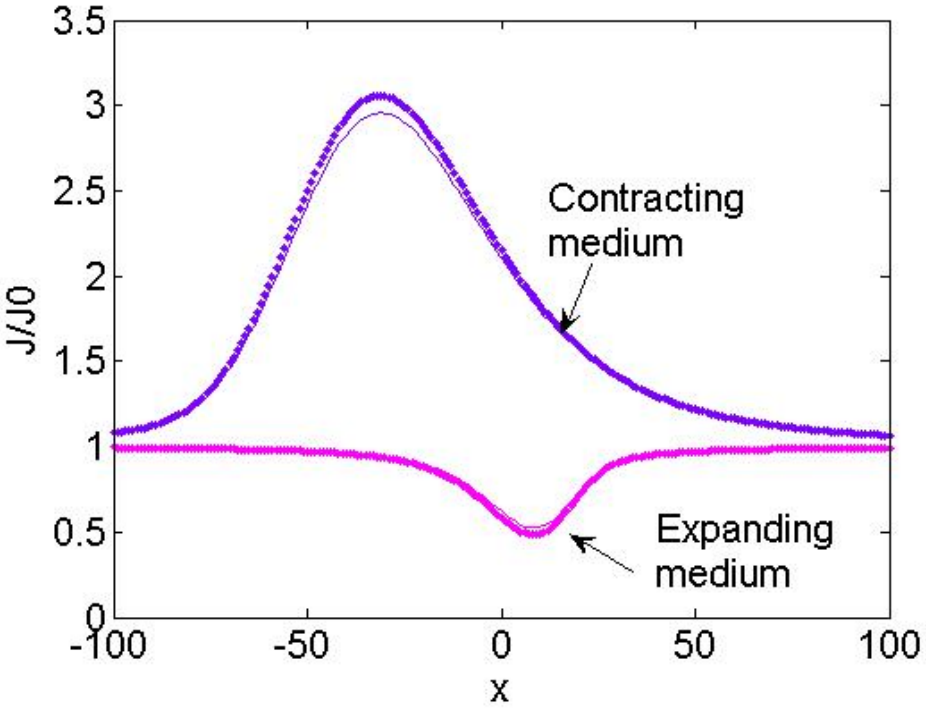

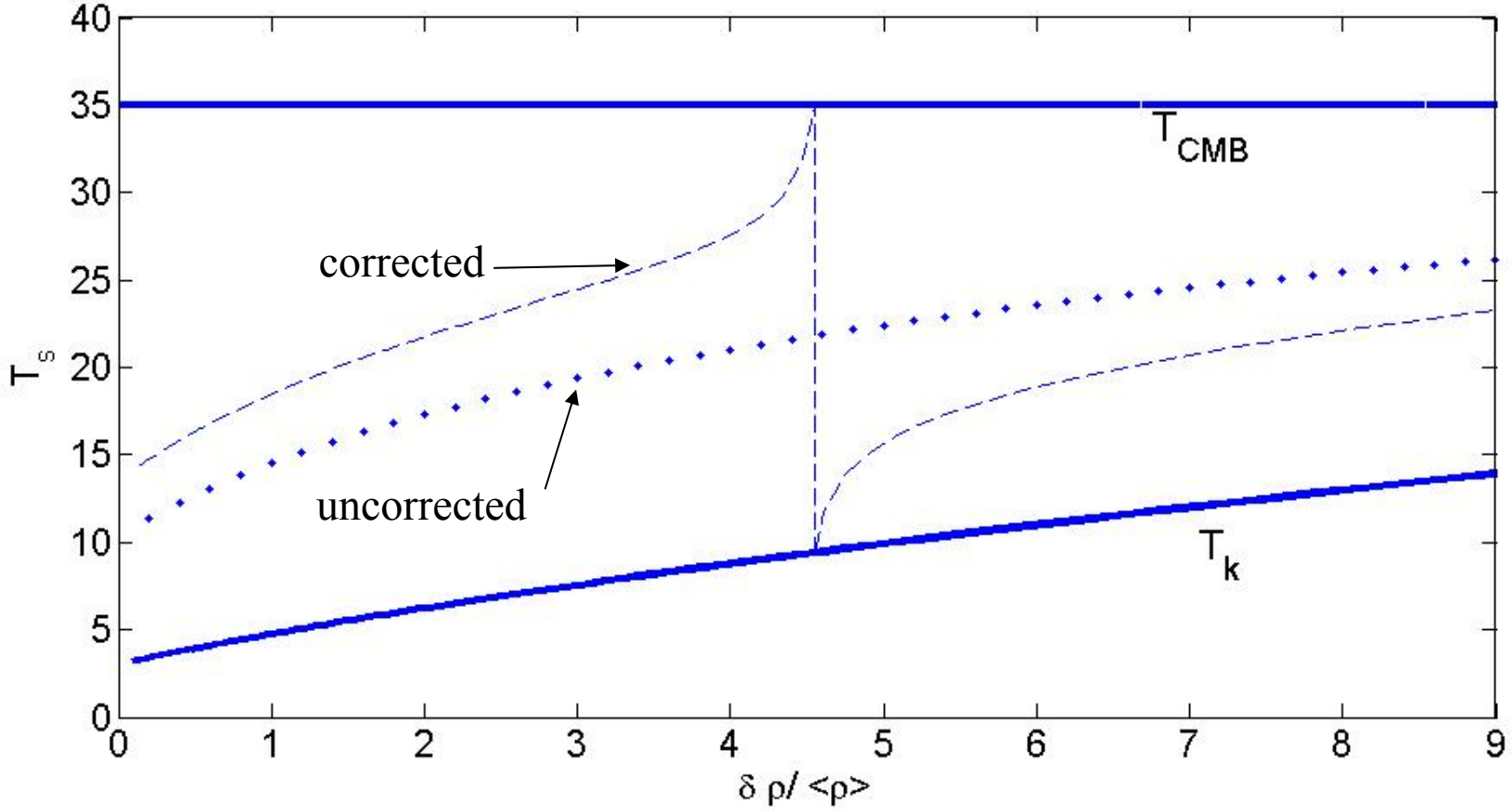

Hydrogen spin temperature at z ~ 12 for an illustrative radiation intensity, for different overdensities

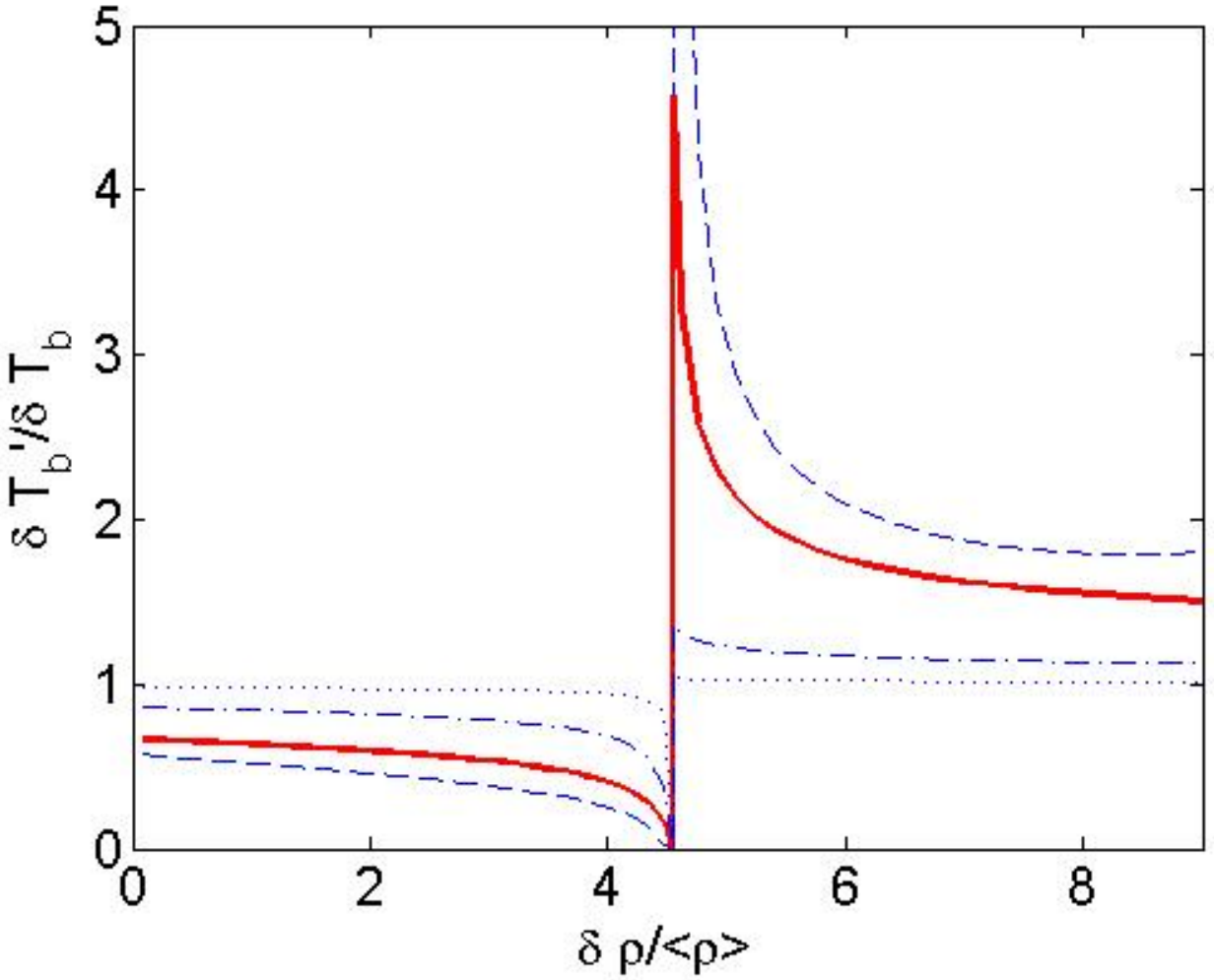

The correction factor to the differential brightness temperature (the 21-cm absorption signal) for different radiation intensities, for different overdensities

Recognizing the First Radiation Sources Through Their 21-cm Signature :

Brightness temperature vs. comoving radius around a radiation source at z =20

a. X-ray source,
L = 5e40 erg/s,
@ t (Myrs) ,
10 (solid),
20 (dash-dot),
40 (dotted);

b. UV source,
L (Ly α to LL)
in erg/s =
5e41 (dashed),
5e42 (dash-dot),
5e43 (solid);

c. Galactic wind,
Lα (erg/s) =
1e41 (solid),
1e40 (dashed),
1e39 (dash-dot).

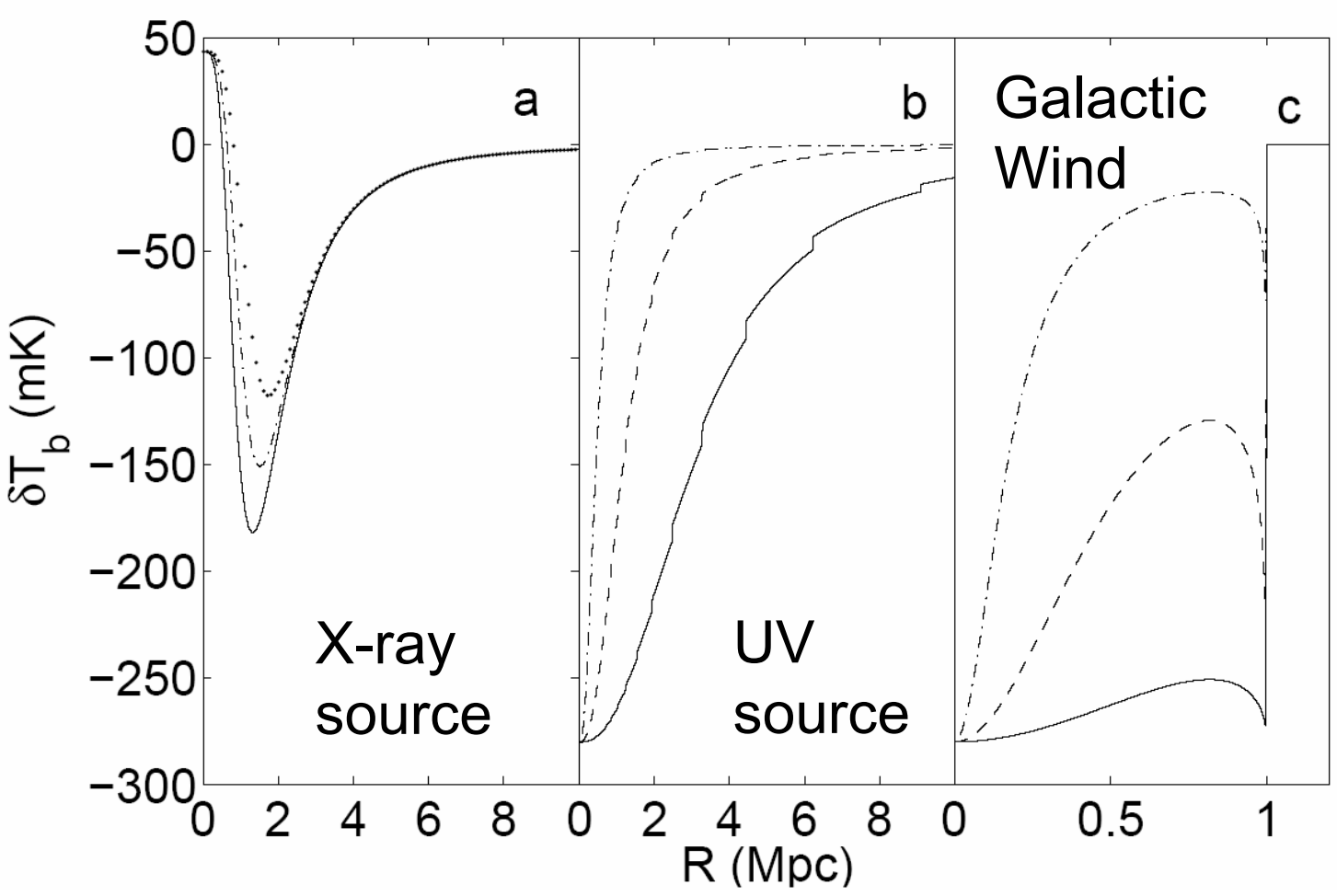

(Chuzhoy, Alvarez & Shapiro 2006, ApJL, 648, L1; astro-ph/0605511)

Recognizing the First Radiation Sources Through Their 21-cm Signature

(Chuzhoy, Alvarez & Shapiro 2006, ApJL, 648, L1; astro-ph/0605511)

Power spectrum of fluctuating 21-cm signal at z = 20

- Ly α pumping is by halo sources clustered in space
- Assume each halo is either an X-ray source or a UV source from Pop III stars
- X-ray sources influence smaller regions than Pop III stellar sources, typically, so they yield greater fluctuations on small scales
- Future radio arrays plan to detect the 21-cm background and may be able to distinguish this.

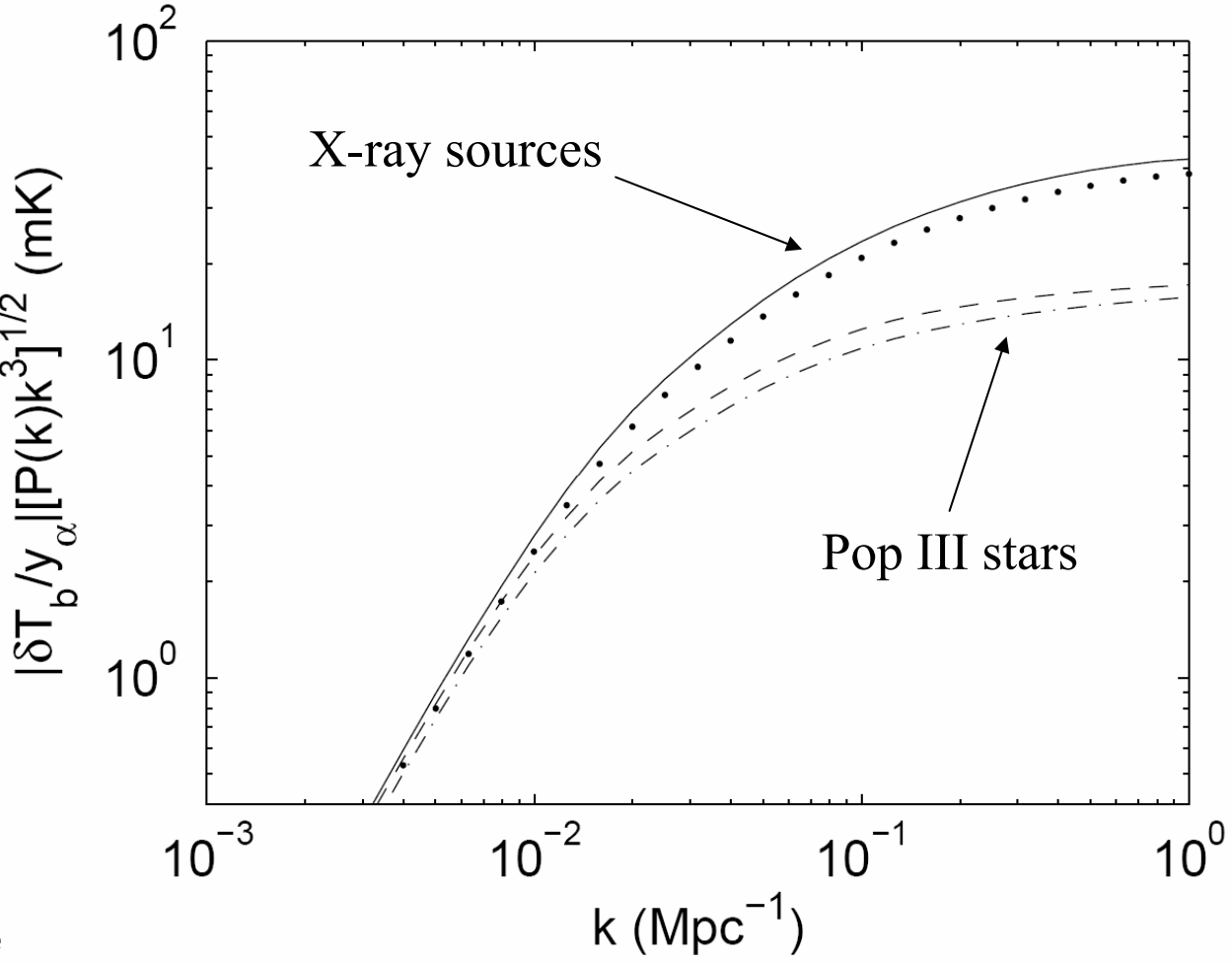

Stages of 21-cm Background

- Dark Ages
  - $z \geq 150$, $T_{spin}=T_{CMB}$ → nothing
  - $20 \leq z \leq 150$, $T_{spin}<T_{CMB}$ → absorption
  - $z \leq 20$, $T_{spin}>T_{CMB}$ in minihalos → emission
- **Epoch of Reionization ($6 \leq z \leq 20$)**
  - $T_{spin}>T_{CMB}$ in minihalos → emission
  - **After sources turn on, Lyman alpha pumping →**
    - Without heating, $T_{spin}<T_{CMB}$ → IGM in absorption
    - **With heating, $T_{spin}>T_{CMB}$ → IGM in emission**

The Redshifted 21cm Signal From the EoR

- The measured radio signal is the differential brightness temperature
- $\delta T_b = T_b - T_{CMB}$:
  $\delta T_b(z) \approx 27 \mathbf{x_{HI}} (1+\delta)(1-T_{CMB}/\mathbf{T_s})[(1+z)/10]^{1/2}$ mK

  (for WMAP3 cosmological parameters).
- Depends on:
  - x_{HI}: neutral fraction
  - δ: overdensity
  - T_s: spin temperature
- For $T_s \gg T_{CMB}$, the dependence on T_s drops out
- The signal is a spectral *line*: carries spatial, temporal, and velocity information.

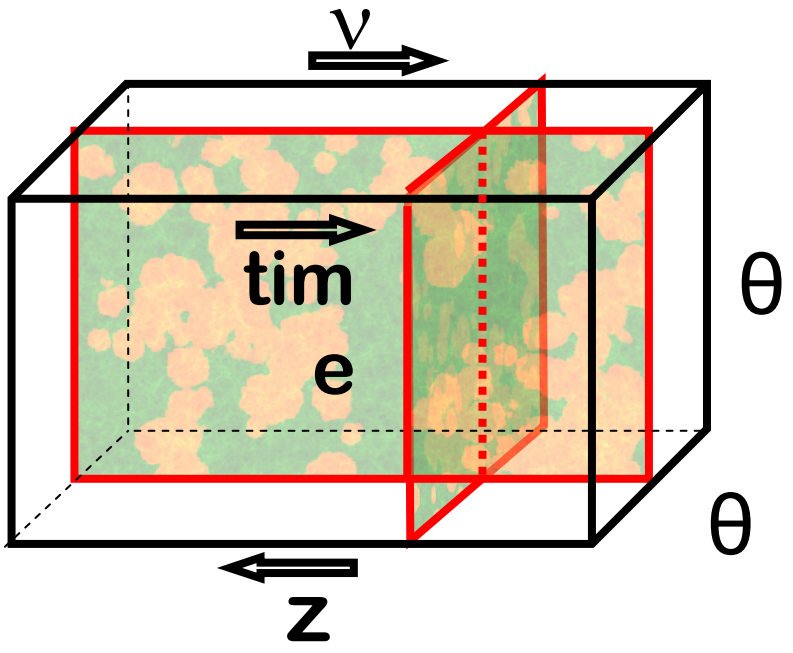

The image cube: images stacked in frequency space

Reionization topology revealed by fluctuations in 21-cm brightness temperature, δT_b , along the line of sight

(Shapiro, Iliev, Mellema, Pen, and Merz 2008, in press; astro-ph/0806.3091)

• mapping the sky along the LOS: high-resolution cuts in position-redshift space

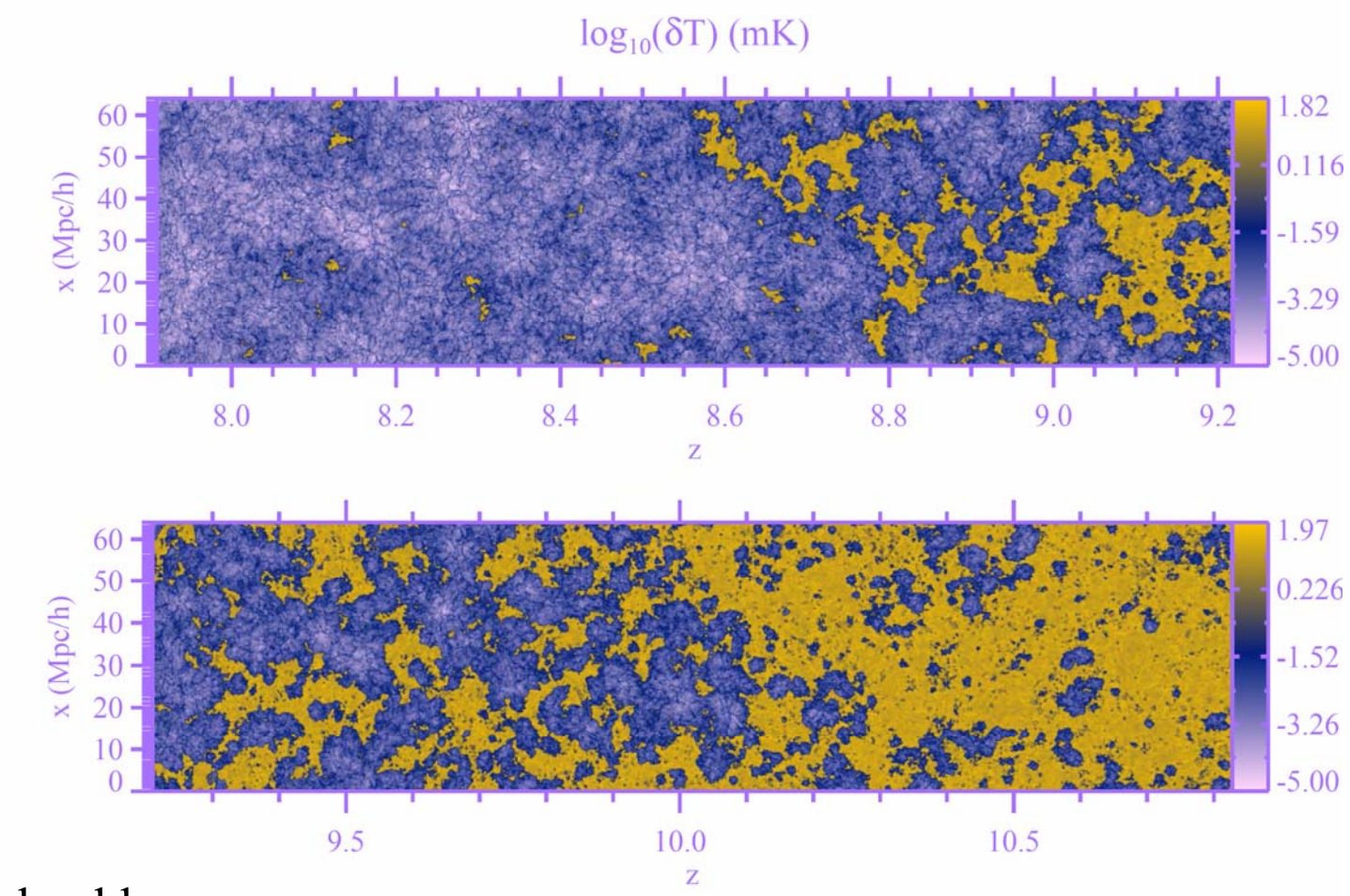

• LOFAR should see large ionized bubbles!

90 Mpc box, WMAP3+

Sky Maps of 21cm Background Brightness Temperature Fluctuations During Epoch of Reionization : Travel through Time

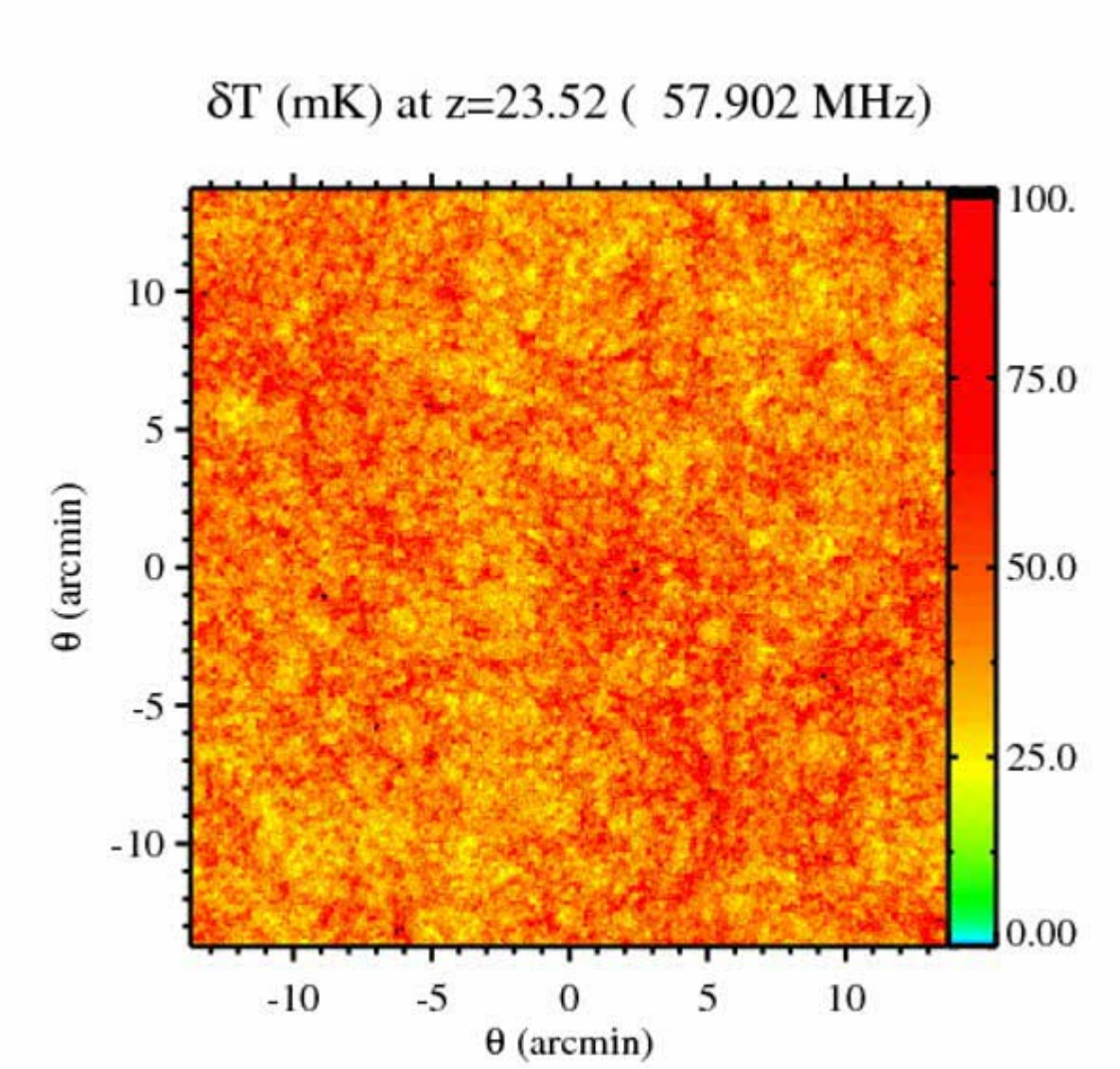

Notation

- Our simulations are characterized by

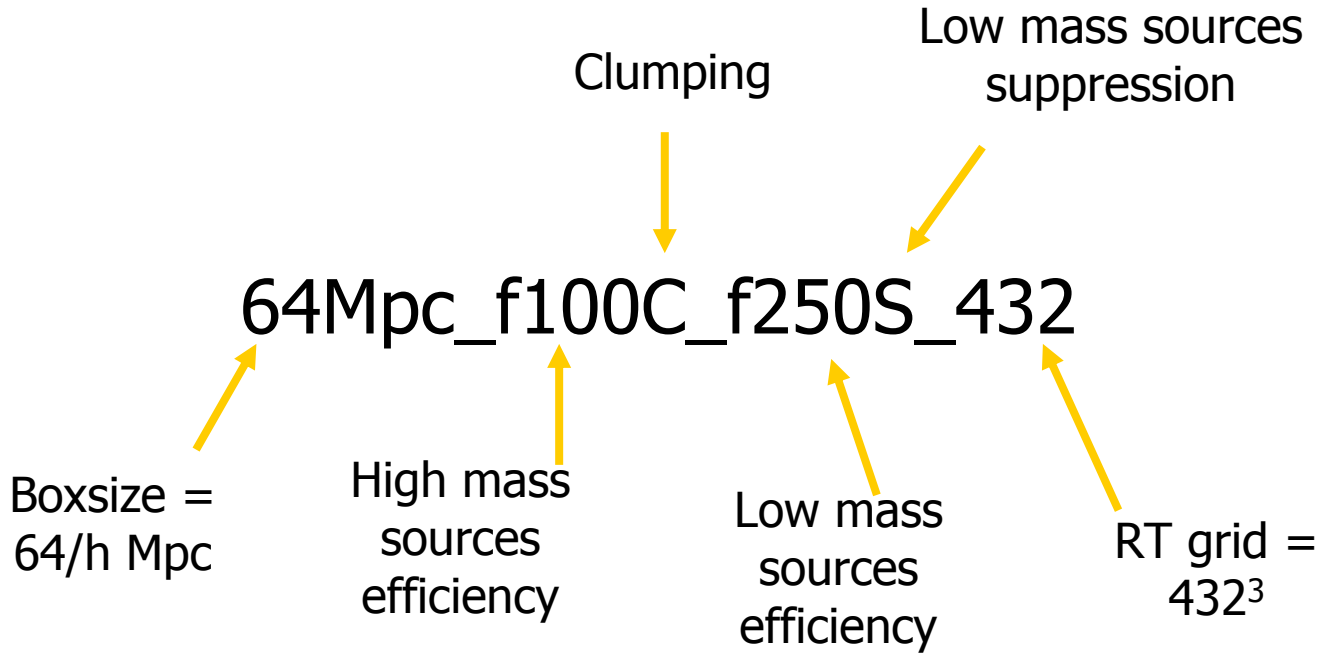

Statistical Measurements of the 21cm Background During the EoR

- The sensitivity of the upcoming EoR experiments will be too low to image 21cm from reionization pixel by pixel: Statistical measurements needed.
  - **First goal**: to reliably detect signatures from reionization (and separate them from foreground and instrumental effects).
  - **Second goal**: to interpret them in terms of astrophysics (source population and properties).
- Luckily, the 21cm line signal is rich in properties:
  1. Global signals: mean signal, fluctuations.
  2. Angular properties: power spectra
  3. Frequency properties: correlation length, Kaiser effect
  4. Non-Gaussianity.

EDGES (Mileura Station, Western Australia)
Bowman, Rogers, and Hewitt (2008)

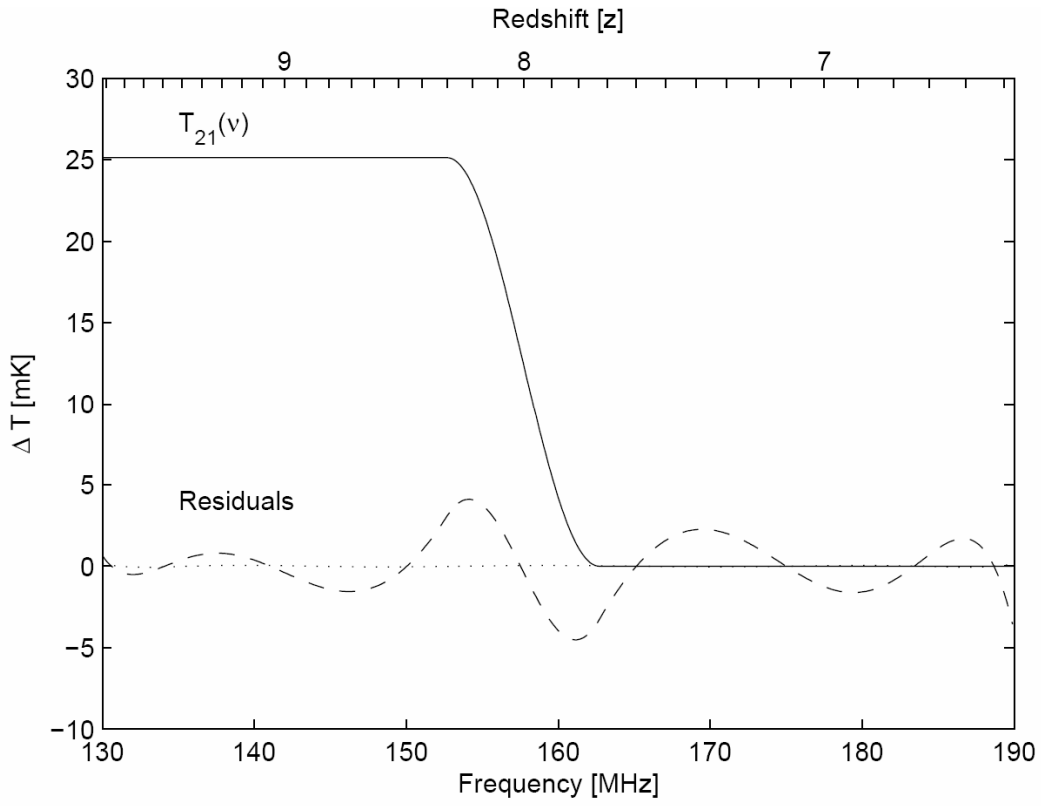

- Search for a “jump” in the global mean brightness temperature when reionization ends

EDGES (Mileura Station, Western Australia)
Bowman, Rogers, and Hewitt (2008)

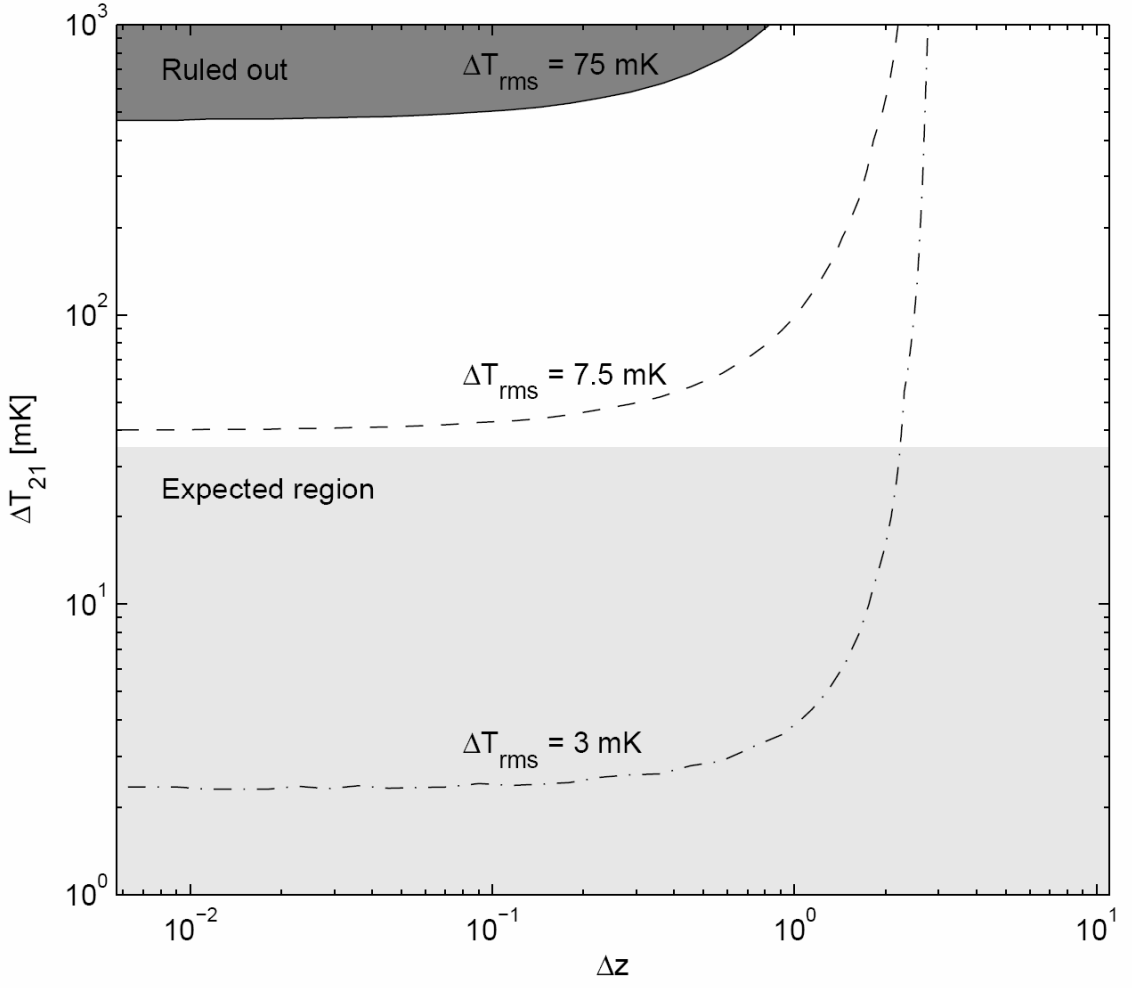

- First results only rule out extreme cases.

Global Signals

- In principle, a single dish telescope could measure the change of the global signal with frequency: contrary to early expectations, however, simulations do not show a sharp transition.
- The corresponding measurement by an interferometer would be the change of the 21cm (rms) fluctuations.
- Simulations: 64Mpc_f100_f250S_432 and 64Mpc_f100_f250S_216

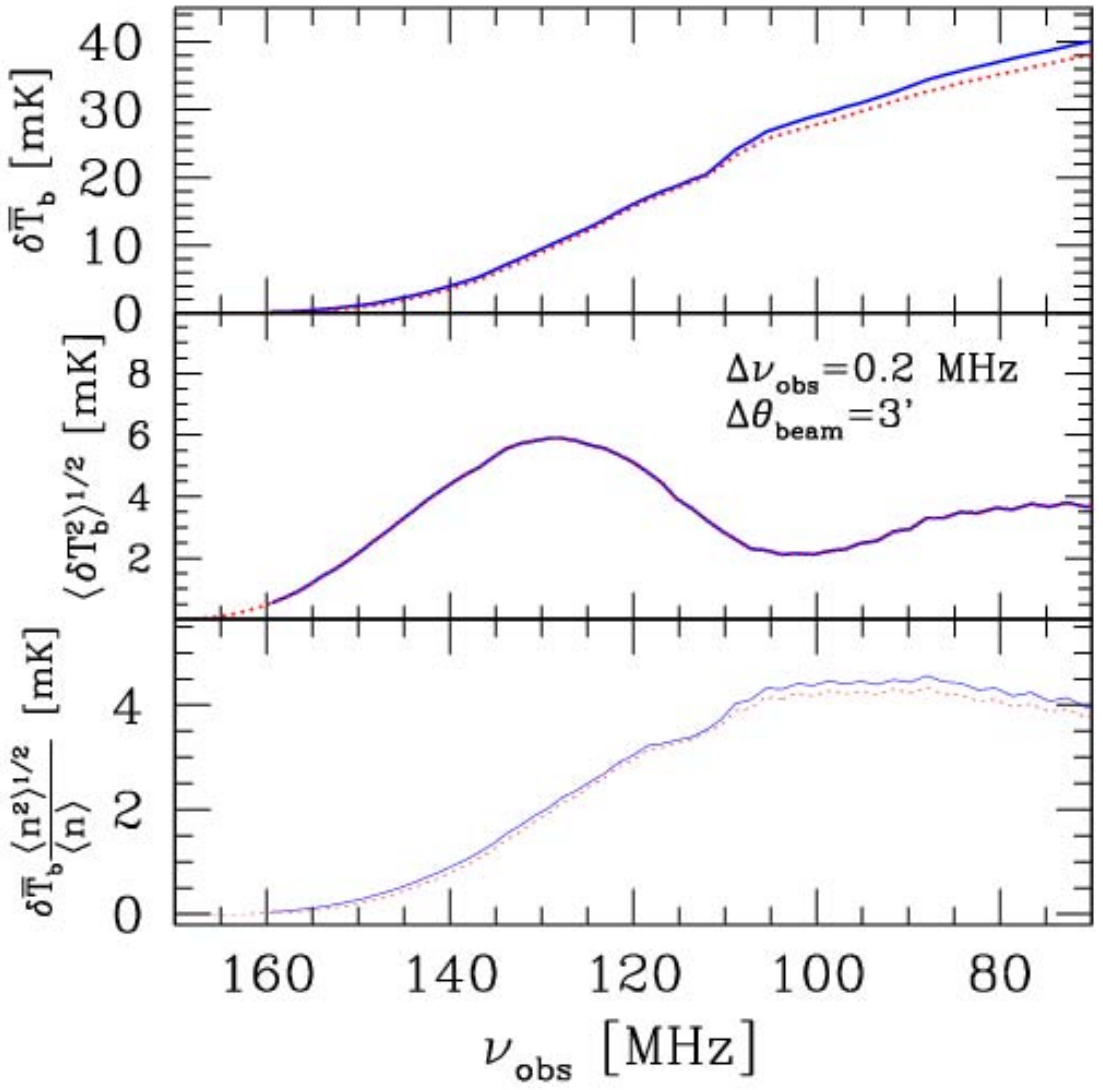

Evolution of 21cm Brightness Temperature Fluctuations

- When plotted against the mean mass-weighted ionization fraction x_m(H II), the evolution of fluctuations shows roughly similar behaviour for different (simulation) resolution and source parameters, but the amplitude differs.
- Peak around x_m(HII)~0.6-0.7 (shifts to lower values for higher angular resolution).

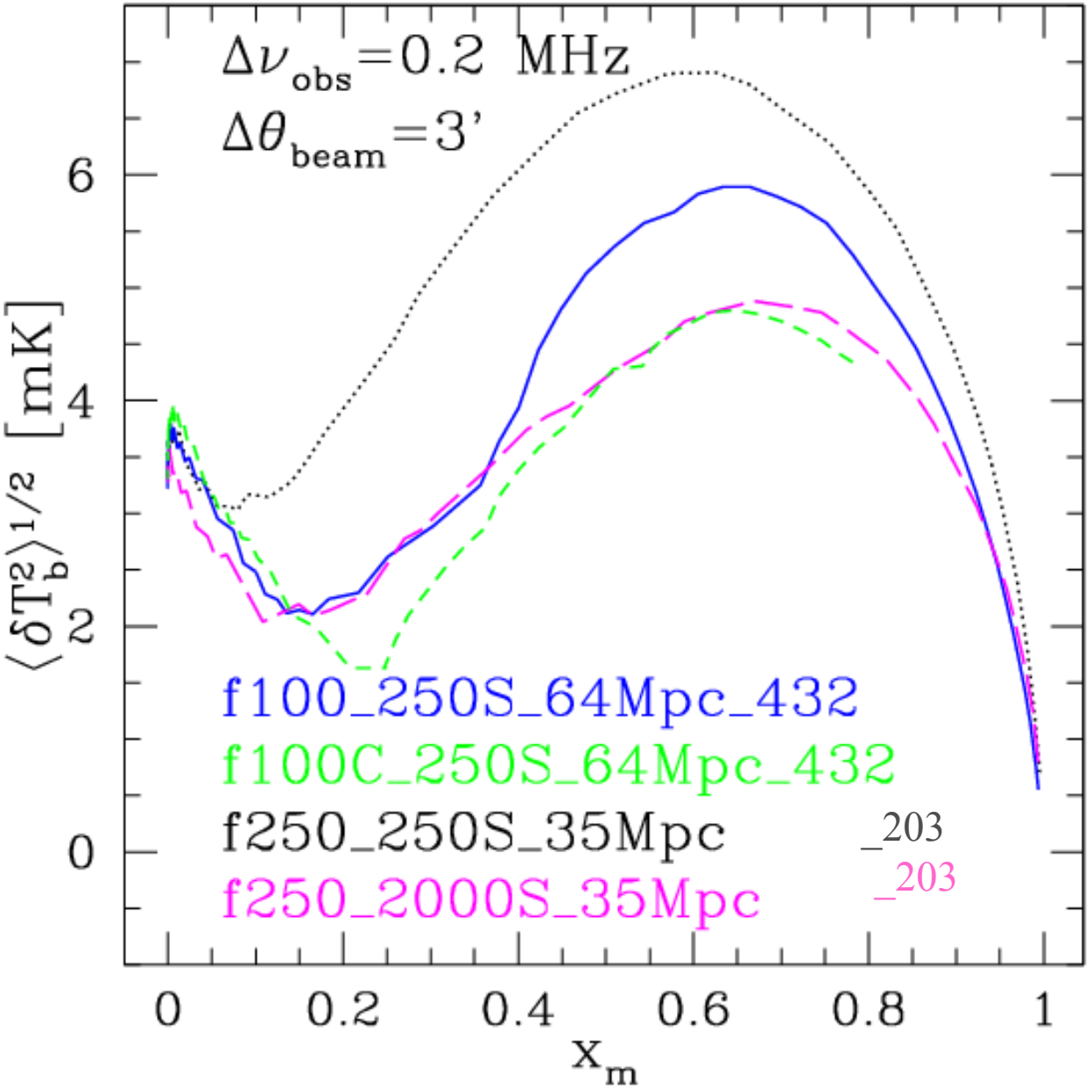

21cm Brightness Temperature Fluctuation Power Spectra

- Information about the length scales can be obtained from the power spectra.
- Power shifts to larger scales as reionization progresses, and the power spectrum flattens.
- Note that the angular power spectrum is measured directly by an interferometer, the multipole l is equivalent to $\sqrt{(u^2+v^2)}$ in a visibility map.

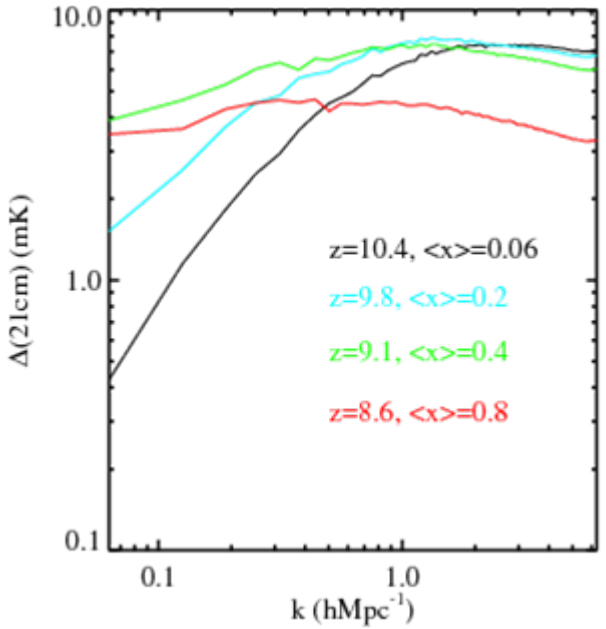

100Mpc_f250C_f0_203

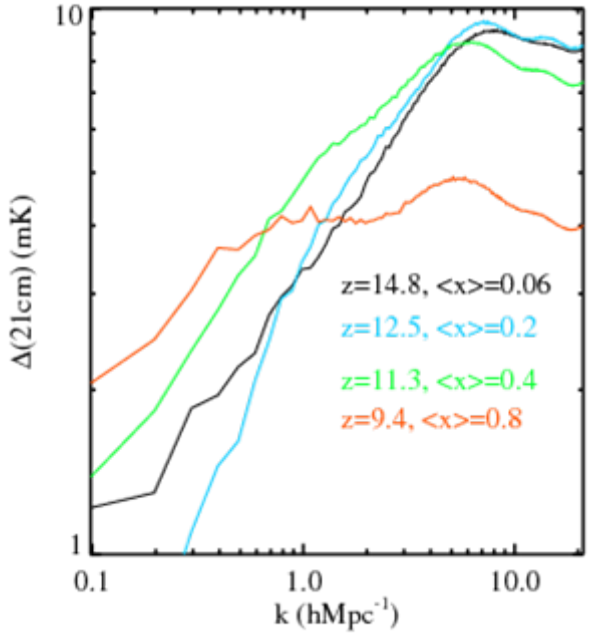

64Mpc_f100_f250S_432

Observability of the 21-cm signal : 3D power spectrum of the neutral hydrogen density

- We show our predicted 21-cm signal at z = 8.6 (x ~ 0.5) for case with z_{ov} = 6.6, with GMRT sensitivity, for 100 hrs integration, 15 MHz bandwidth and T_{sys} = 480 K, pointing at zenith.

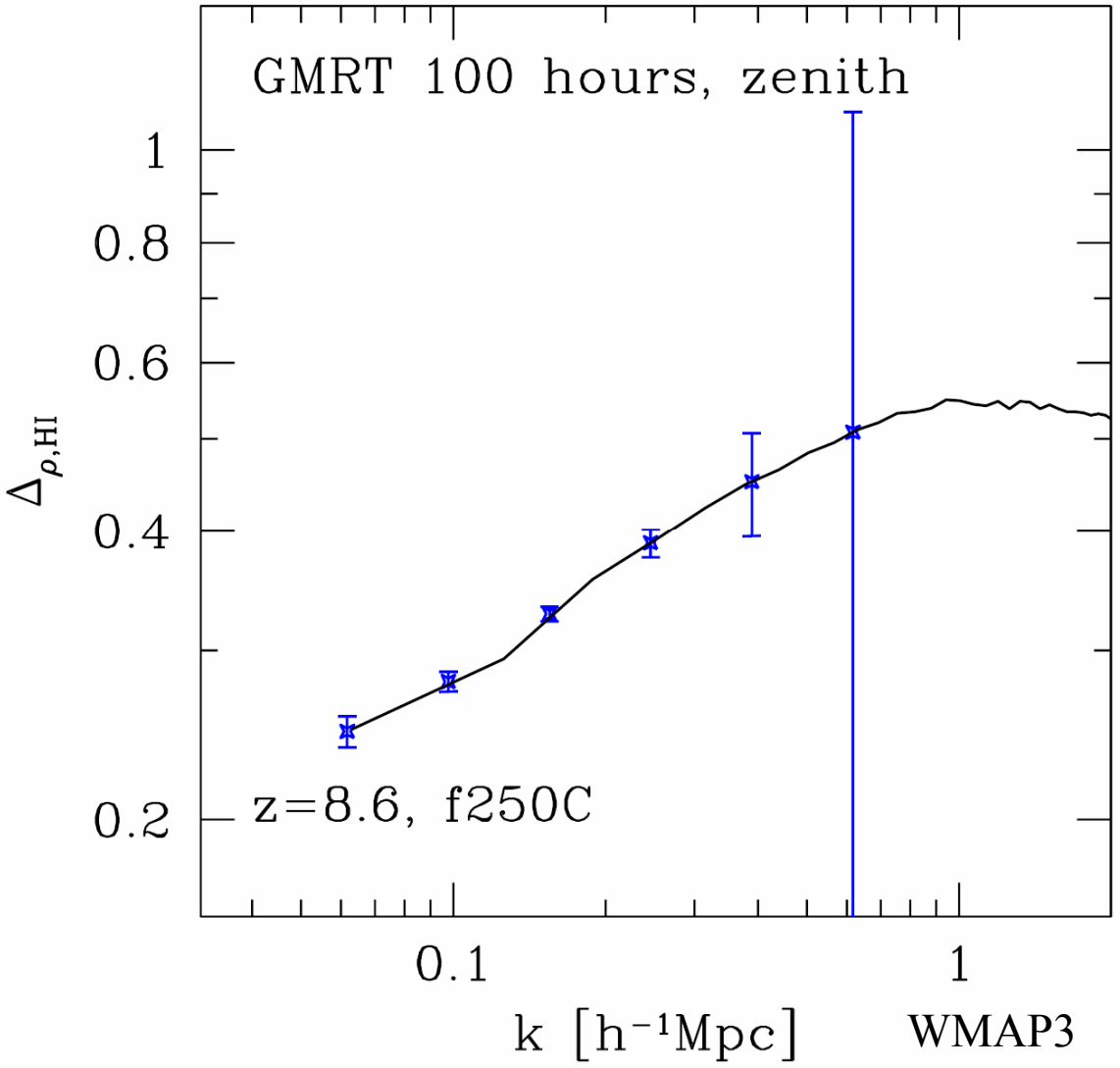

Peculiar Velocities Cause Redshift Distortions

- Due to the peculiar velocity field, the signal can be displaced from its cosmological redshift.
- `Kaiser effect´ or `velocity compression´: due to infall, signal concentrates at the high density peaks.
- This is clearly seen in the simulations and gives ~30% increase in fluctuations (and up to a factor of 2).

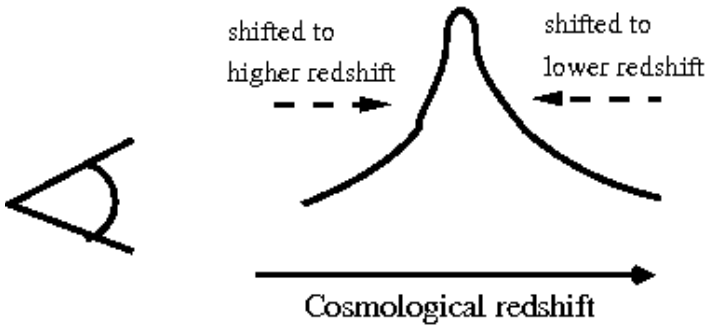

Effect of the Peculiar Velocity Field : Redshift Distortion

- Adding the velocity distortions visibly increases the fluctuations in the neutral medium.
- Maximum value also larger.
- The effect remains noticeable even at LOFAR-like resolution (3′, 200 kHz).
- Simulation: 100Mpc_f250C_f0_203.

no velocity correction

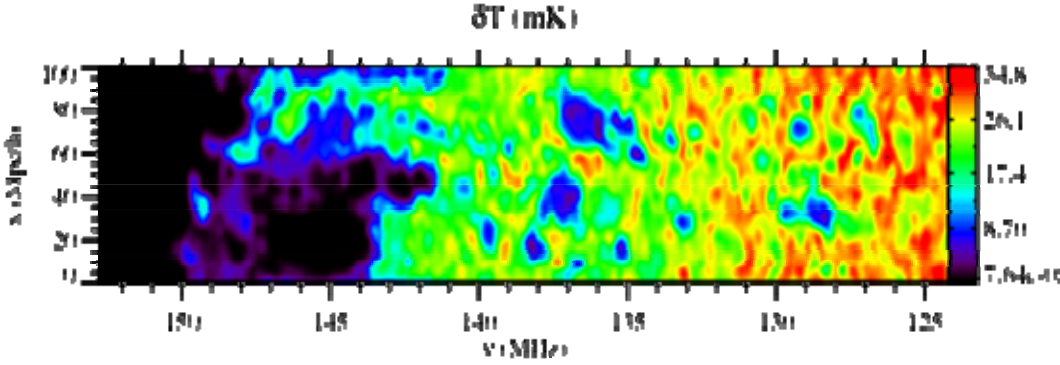

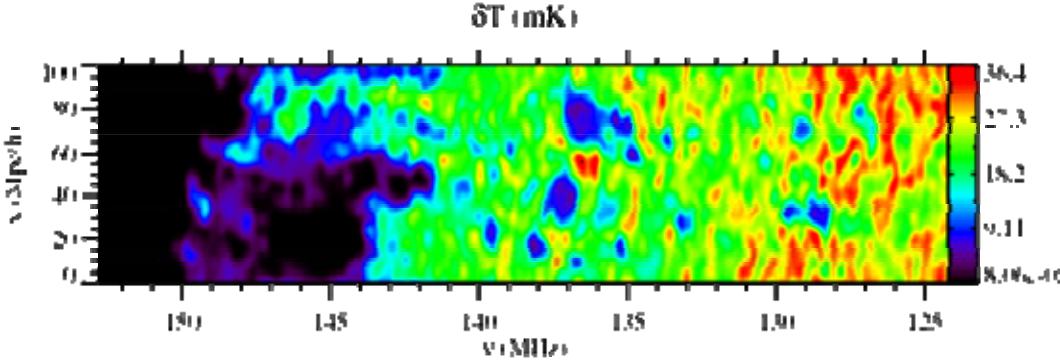

velocity corrected

And Peculiar Velocity ➔ Anisotropy in Fourier Space...

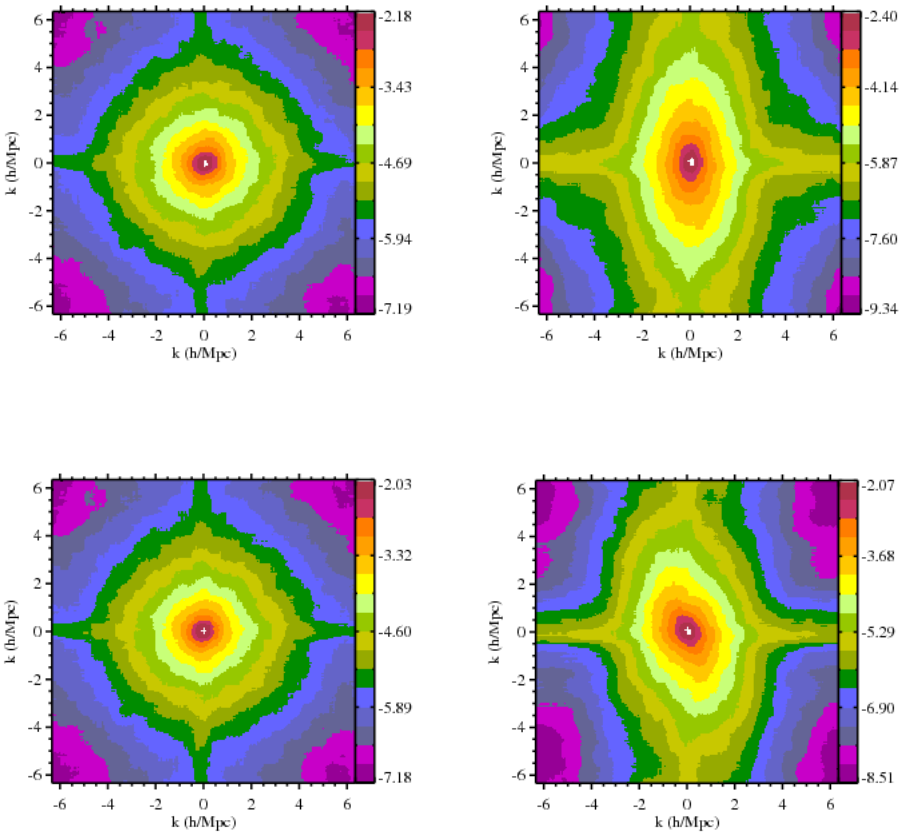

Correlation Length

- Reionization changes the correlation length along the frequency axis in a characteristic way: formation of large H II regions increases correlation length from ~200 kHz to ~1 MHz.
- Still substantially shorter than for the continuum foregrounds, so it could be used as a test for proper foreground subtraction.

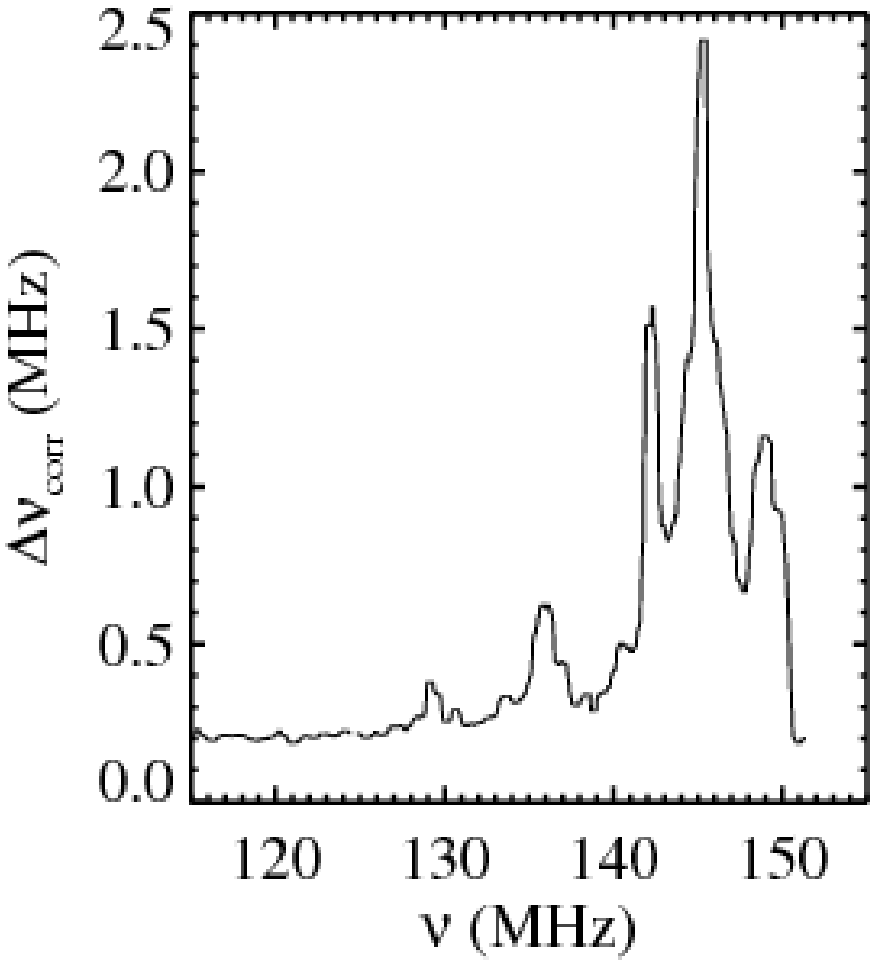

Simulation 100Mpc_f250C_f0_203

Non-Gaussianity

- Probability distribution functions of the 21cm signal are clearly non-Gaussian.
- Limited resolution reduces the effect somewhat, but still noticeable.
- Towards the end of reionization the effect is largest.

Simulation 100Mpc_f250C_f0_203

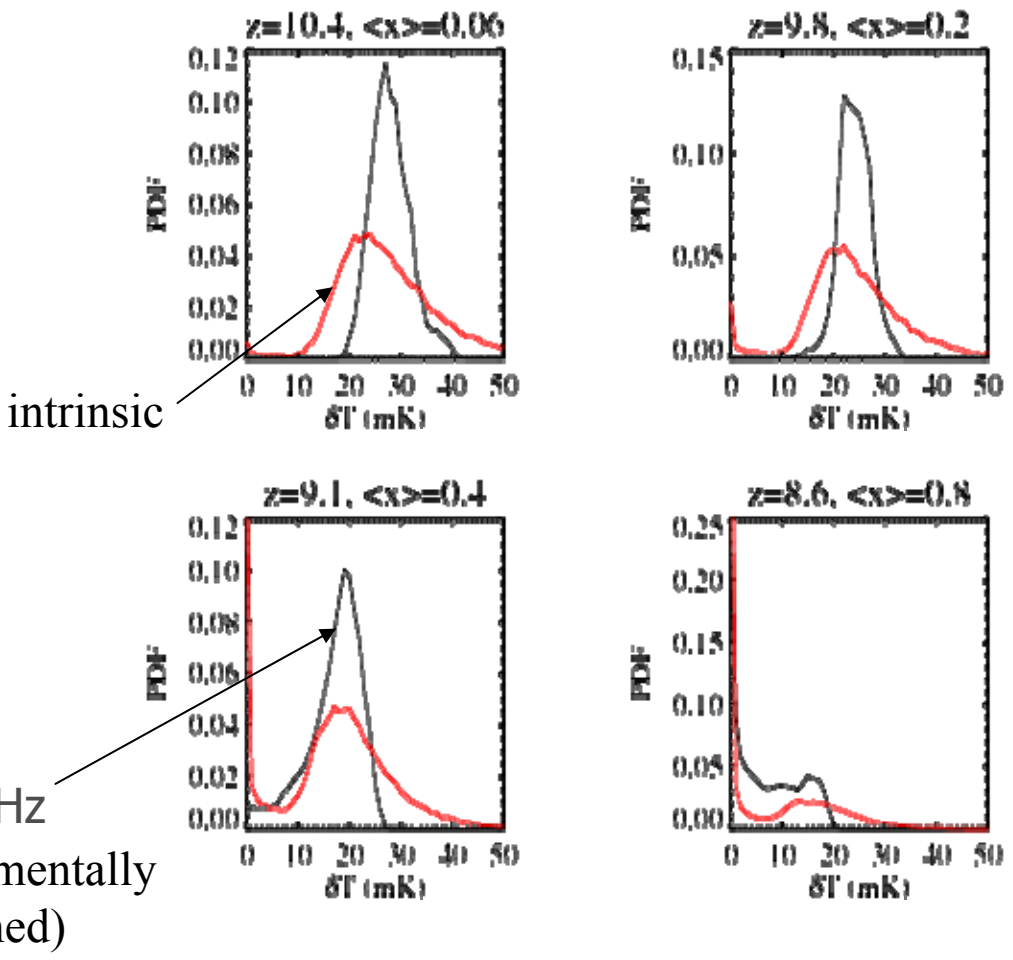

Skewness

- Non-Gaussianity suggests that measuring the skewness could be an interesting diagnostic.
- The simulations show a clear evolution of skewness with increasing ionization.
- Finite resolution modifies skewness, but does not remove it.
- Skewness may offer a good way to detect the signal, if remnants of foreground subtractions and other effects are dominantly Gaussian (cf. Harker et al. 2008).

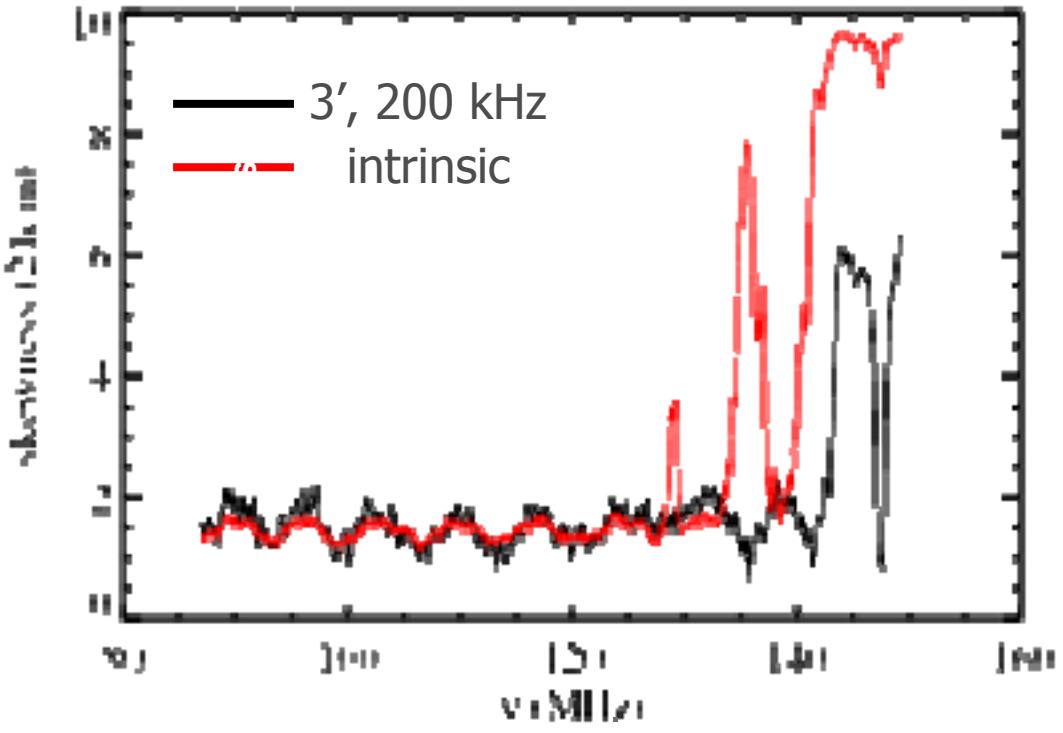

The Fluctuating H_2 Dissociating Background During Reionization

Ahn, Shapiro, Iliev, Mellema, & Pen 2008, ApJ, submitted (astro-ph/0807.2254; 0807.0920)

• Simulations suggest first stars formed inside minihalos of mass $\sim 10^{5-6}$ solar masses at redshift $z >\sim 20$, when H_2 molecules cooled the primordial, metal-free gas and gravitational collapse ensued.

• **But** H_2 Lyman-Werner ("LW") band photons (11.2 – 13.6 eV) dissociate H_2, so too much LW background intensity (i.e. $J_{LW} > (J_{LW})_{threshold}$)

➔ star formation inside minihalos suppressed

The Fluctuating H_2 Dissociating Background During Reionization

Ahn, Shapiro, Iliev, Mellema, & Pen 2008, ApJ, submitted (astro-ph/0807.2254; 0807.0920)

• Simulations suggest first stars formed inside minihalos of mass $\sim 10^{5-6}$ solar masses at redshift $z >\sim 20$, when H_2 molecules cooled the primordial, metal-free gas and gravitational collapse ensued.

• **But** H_2 Lyman-Werner ("LW") band photons (11.2 – 13.6 eV) dissociate H_2, so too much LW background intensity (i.e. $J_{LW} > (J_{LW})_{threshold}$)

➔ star formation inside minihalos suppressed

Q: How much is too much?

The Fluctuating H_2 Dissociating Background During Reionization

Ahn, Shapiro, Iliev, Mellema, & Pen 2008, ApJ, submitted (astro-ph/0807.2254; 0807.0920)

• Simulations suggest first stars formed inside minihalos of mass $\sim 10^{5-6}$ solar masses at redshift $z >\sim 20$, when H_2 molecules cooled the primordial, metal-free gas and gravitational collapse ensued.

• **But** H_2 Lyman-Werner ("LW") band photons (11.2 – 13.6 eV) dissociate H_2, so too much LW background intensity (i.e. $J_{LW} > (J_{LW})_{threshold}$)

➔ star formation inside minihalos suppressed

Q: How much is too much?

A: Early estimates (e.g. Haiman, Abel, and Rees 2000) suggested it depended on minihalo mass and redshift, and to suppress *all* minihalos, $\mathbf{(J_{LW,21})_{threshold} \sim 0.01}$ **to 1**, as z varies from 10 to 50, respectively. Later estimates with more realistic, cosmological initial conditions, 3D, numerical gas dynamics found similar range (e.g. Ricotti et al. 2002; Yoshida et al. 2003; Yoshida et al. 2007; O'Shea and Norman 2007).

The Fluctuating H_2 Dissociating Background During Reionization

Ahn, Shapiro, Iliev, Mellema, & Pen 2008, ApJ, submitted (astro-ph/0807.2254; 0807.0920)

• Simulations suggest first stars formed inside minihalos of mass ~ 10^{5-6} solar masses at redshift $z \gtrsim 20$, when H_2 molecules cooled the primordial, metal-free gas and gravitational collapse ensued.

• **But** H_2 Lyman-Werner ("LW") band photons (11.2 – 13.6 eV) dissociate H_2, so too much LW background intensity (i.e. $J_{LW} > (J_{LW})_{threshold}$)

➔ star formation inside minihalos suppressed

Q: How much is too much?

A: Early estimates (e.g. Haiman, Abel, and Rees 2000) suggested it depended on minihalo mass and redshift, and to suppress *all* minihalos, $\mathbf{(J_{LW,21})_{threshold} \sim 0.01}$ **to 1**, as z varies from 10 to 50, respectively. Later estimates with more realistic, cosmological initial conditions, 3D, numerical gas dynamics found similar range (e.g. Ricotti et al. 2002; Yoshida et al. 2003; Yoshida et al. 2007; O'Shea and Norman 2007).

• **But** during EOR, sources of reionization also emit continuum below 13.6 eV Lyman limit, in the H_2 LW bands ➔ *rising LW background inevitable!*

The Fluctuating H_2 Dissociating Background During Reionization

Ahn, Shapiro, Iliev, Mellema, & Pen 2008, ApJ, submitted (astro-ph/0807.2254; 0807.0920)

• Simulations suggest first stars formed inside minihalos of mass ~ 10^{5-6} solar masses at redshift $z \gtrsim 20$, when H_2 molecules cooled the primordial, metal-free gas and gravitational collapse ensued.

• **But** H_2 Lyman-Werner ("LW") band photons (11.2 – 13.6 eV) dissociate H_2, so too much LW background intensity (i.e. $J_{LW} > (J_{LW})_{threshold}$)

➔ star formation inside minihalos suppressed

Q: How much is too much?

A: Early estimates (e.g. Haiman, Abel, and Rees 2000) suggested it depended on minihalo mass and redshift, and to suppress *all* minihalos, $\mathbf{(J_{LW,21})_{threshold} \sim 0.01}$ **to 1**, as z varies from 10 to 50, respectively. Later estimates with more realistic, cosmological initial conditions, 3D, numerical gas dynamics found similar range (e.g. Ricotti et al. 2002; Yoshida et al. 2003; Yoshida et al. 2007; O'Shea and Norman).

• **But** during EOR, sources of reionization also emit continuum below 13.6 eV Lyman limit, in the H_2 LW bands ➔ *rising LW background inevitable!*

• **How high does it get?**

The Fluctuating H_2 Dissociating Background During Reionization

Ahn, Shapiro, Iliev, Mellema, & Pen 2008, ApJ, submitted (astro-ph/0807.2254; 0807.0920)

- Ionization sources also emit continuum below Lyman limit, in the H_2 Lyman-Werner bands (11.2 – 13.6 eV).
- In IGM, this radiation is attenuated by scattering in H Lyman series lines and downgrading to lower energy photons.
- By transfering this radiation from each source halo thru the IGM, we compute the inhomogeneous LW band intensity field durng reionization.
- e.g. Pop II sources, $f_{esc} = 0.2$, $f_* = 0.2$, $f_\gamma = 250$.

The Fluctuating H_2 Dissociating Background During Reionization

Ahn, Shapiro, Iliev, Mellema, & Pen 2008, ApJ, submitted (astro-ph/0807.2254; 0807.0920)

- Ionization sources also emit continuum below Lyman limit, in the H_2 Lyman-Werner bands (11.2 – 13.6 eV).
- In IGM, this radiation is attenuated by scattering in H Lyman series lines and downgrading to lower energy photons.
- By transfering this radiation from each source halo thru the IGM, we compute the inhomogeneous LW band intensity field durng reionization.
- e.g. Pop II sources, $f_{esc} = 0.2$, $f_* = 0.2$, $f_\gamma = 250$.

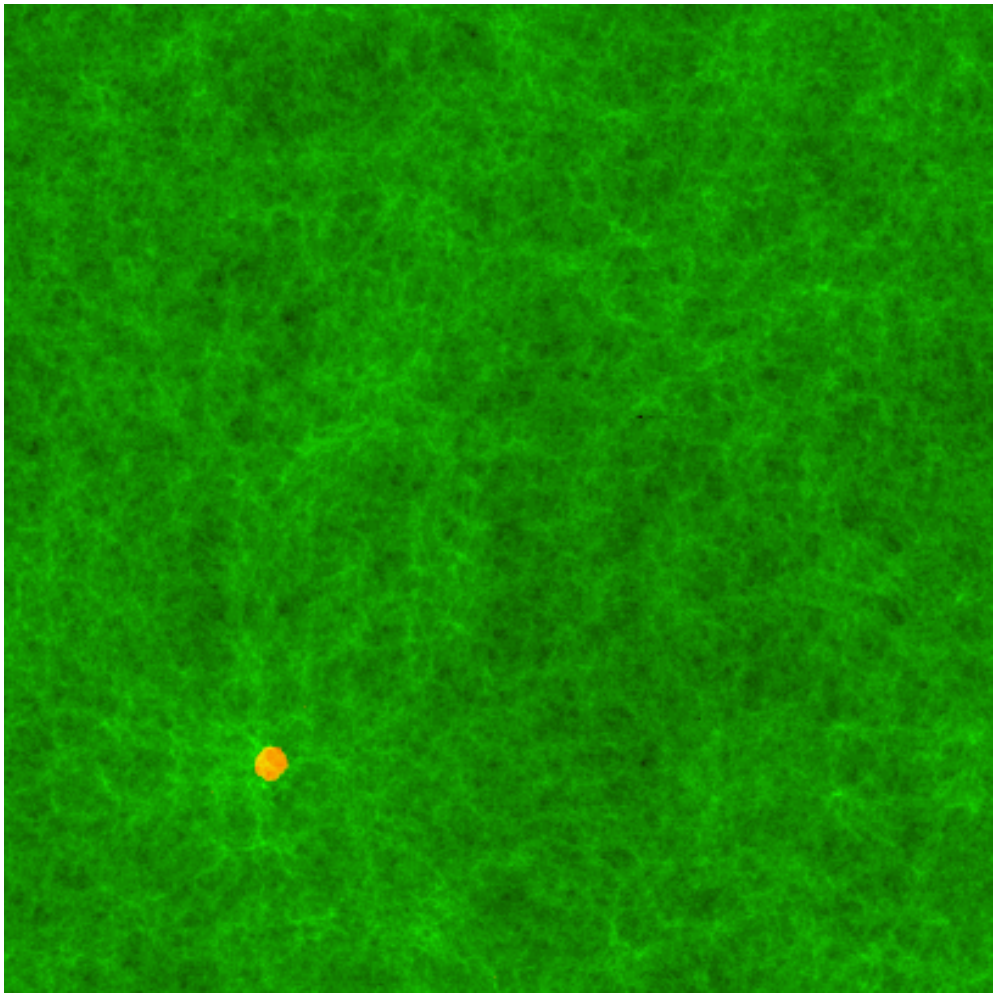

35/h Mpc box

Previous approximation for cosmic mean LW Background during EOR: homogeneous universe ➔ "saw-tooth" modulation

- assume sources of UV emissivity *uniformly* distributed in space (e.g. Haiman et al. 2000; Ricotti et al. 2002; Yoshida et al. 2003)

- assume H_2 dissociating photons, emitted below H Lyman limit, are removed whenever they redshift into an H Lyman series line and are resonantly scattered by the IGM, down-converting them out of LW bands

- uniform IGM opacity filters uniformly distributed LW emitters by "saw-tooth" modulation.

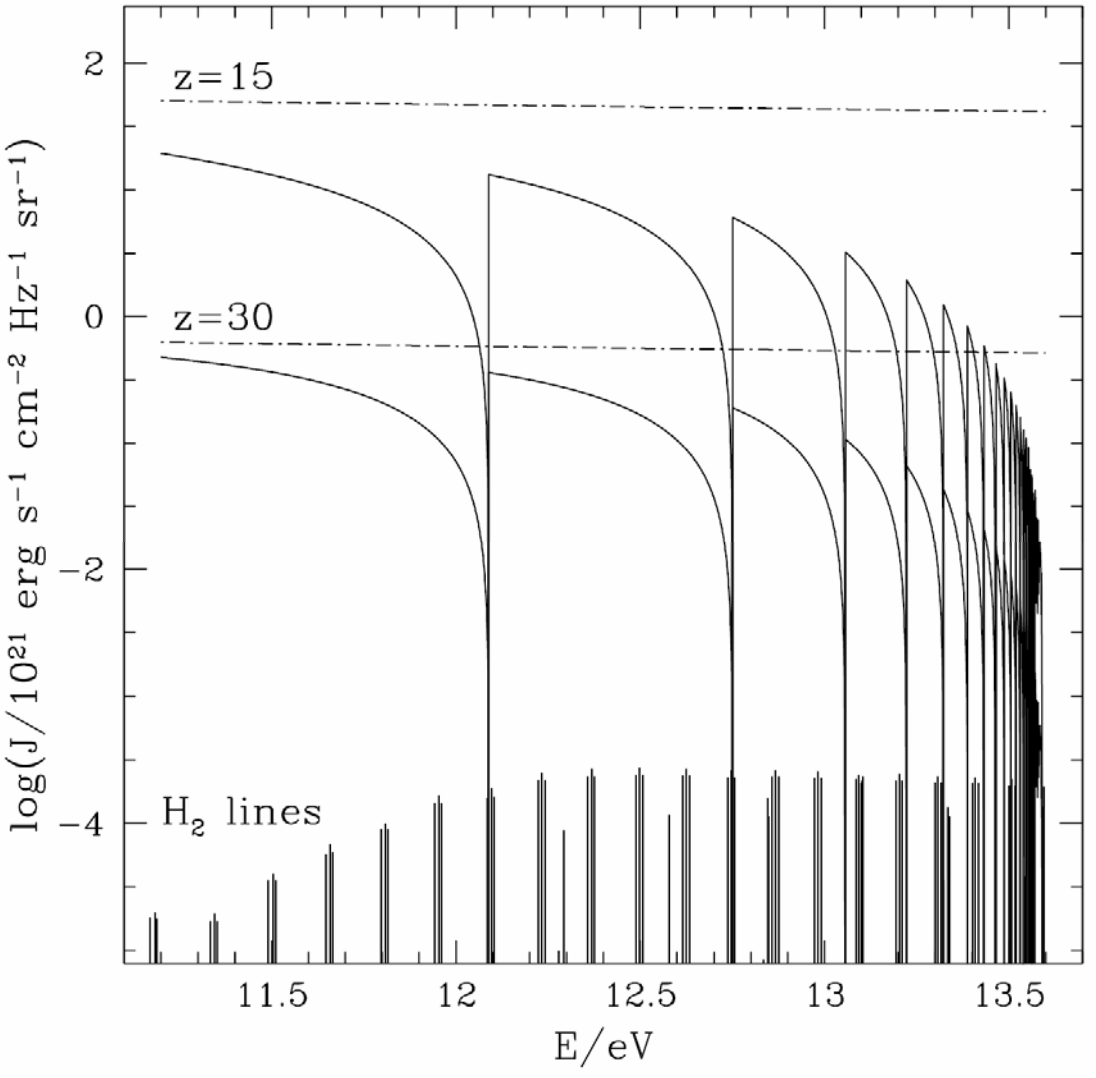

(Haiman, Abel, and Rees 2000)

Attenuation of LW photons from a single source: "picket-fence" modulation

- A source at redshift z_s observed at different distances suffers different amounts of attenuation, dilution, and redshift
- When LW photon redshifts into the nearest lower H Lyman series line, it is scattered and destroyed (converted to lower energy photon).
- Source is completely attenuated at comoving distance

$$r_{cMpc} = 97\,[(1+z)/21]^{-0.5}$$

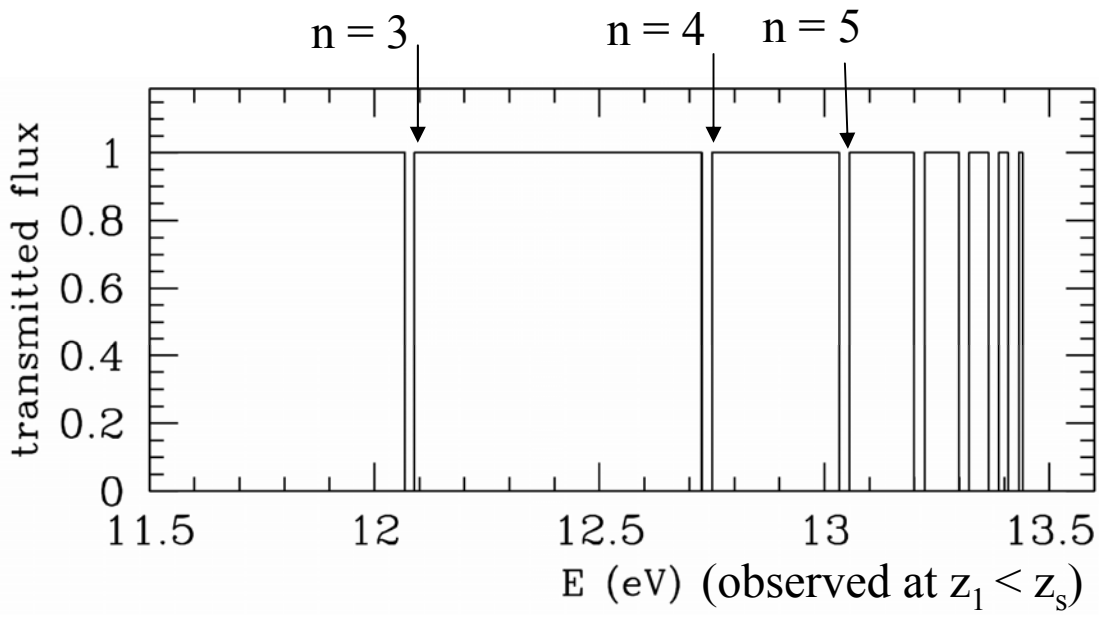

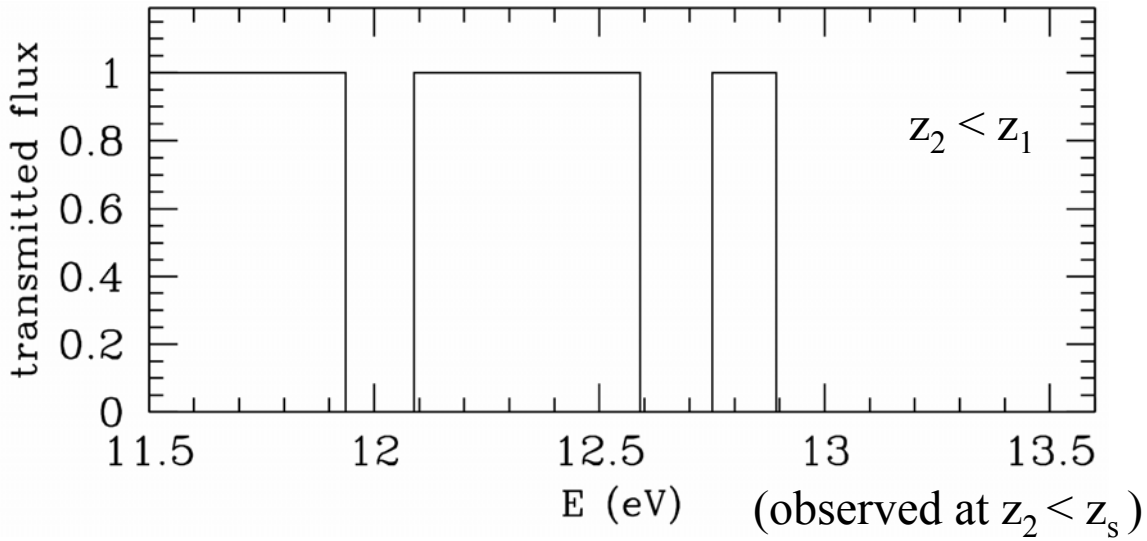

LW background radiative transfer is intrinsically cosmological : sources along the "past light-cone" of every point in space

- Space-time diagram of radiation sources and observer at point P at conformal time τ
- luminosity of each halo source is constant during finite time-step
- observer at point P will see sources whose world lines intersect the past light-cone
- must determine the attenuation, dilution, and redshift of the LW photons emitted at A and received at P

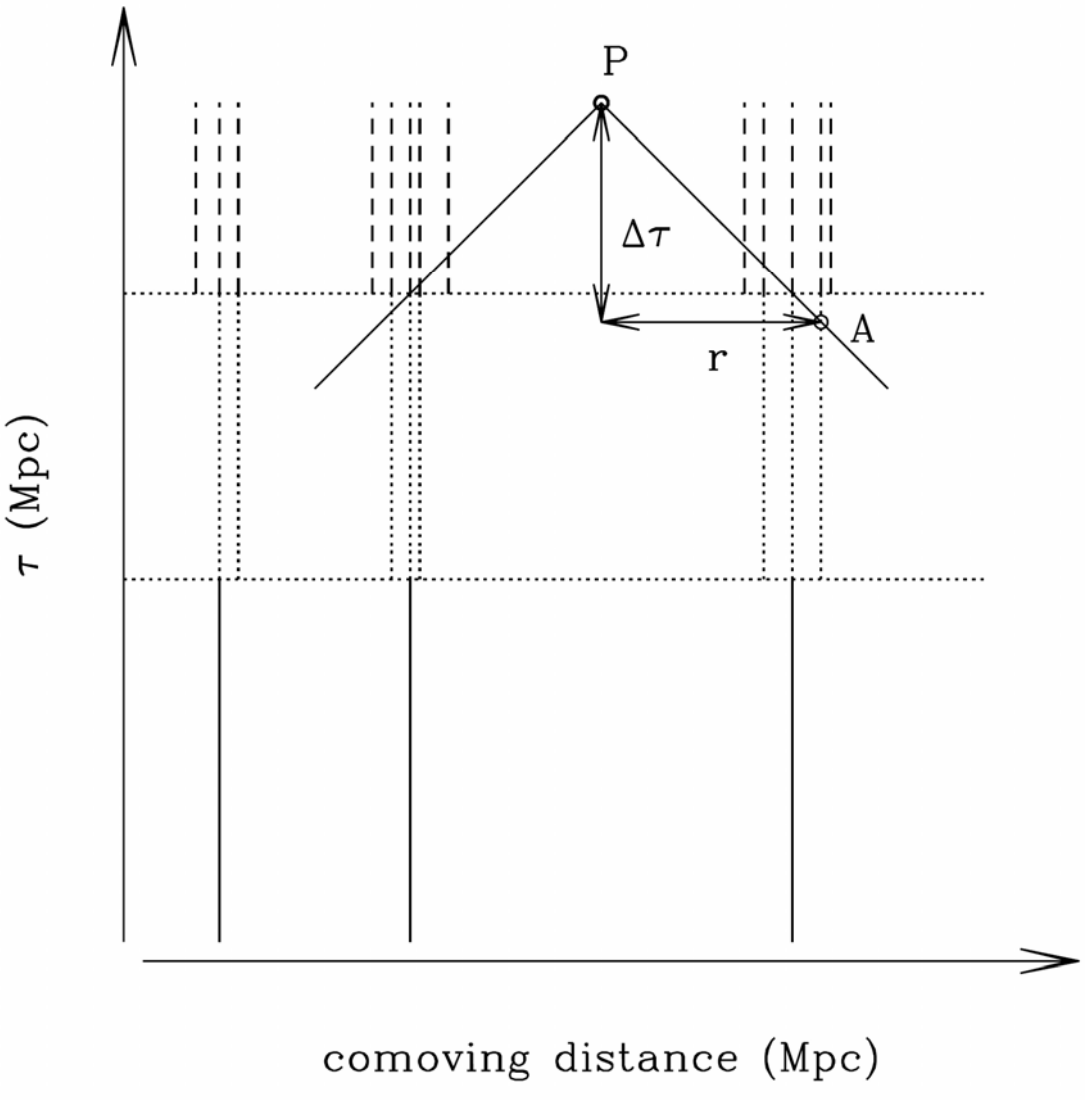

Computational Challenge

$J_\nu(\mathbf{x}_{\rm obs}, z_{\rm obs}, \nu_{\rm obs})$ at observed frequency $\nu_{\rm obs}$ at some comoving position $\mathbf{x}_{\rm obs}$ at redshift $z_{\rm obs}$ is given by

$$J_\nu(\mathbf{x}_{\rm obs}, z_{\rm obs}, \nu_{\rm obs}) = \frac{1}{4\pi} \sum_{\rm s} F_{\nu,\,\rm s}(\mathbf{x}_{\rm obs}, z_{\rm obs}, \nu_{\rm obs}), \tag{5}$$

where $F_{\nu,\,\rm s}$ is the flux received at $(\mathbf{x}_{\rm obs}, z_{\rm obs}, \nu_{\rm obs})$ that was emitted at $(\mathbf{x}_{\rm s}, z_{\rm s}, \nu_{\rm s})$ by a source (denoted by subscript s), where

$$\frac{\nu_{\rm s}}{\nu_{\rm obs}} = \frac{1 + z_{\rm s}}{1 + z_{\rm obs}}. \tag{6}$$

Computational Challenge

The position and redshift, $(\mathbf{x}_{\rm s}, z_{\rm s})$, of a source are related to those of the observer at $(\mathbf{x}_{\rm obs}, z_{\rm obs})$ by the fact that the signal emitted at the epoch $z_{\rm s}$ must reach the position $\mathbf{x}_{\rm obs}$ at the epoch $z_{\rm obs}$, travelling at the speed of light while the universe expands. We express this implicitly by writing the comoving separation, $r_{\rm os}$, of the source and observer as follows:

$$r_{\rm os} = |\mathbf{x}_{\rm obs} - \mathbf{x}_{\rm s}| = \int_{t(z_{\rm s})}^{t(z_{\rm obs})} \frac{cdt}{a(t)} = -\int_{z_{\rm obs}}^{z_{\rm s}} c\frac{dz}{H(z)}. \qquad (7)$$

Computational Challenge

The differential flux, $F_{\nu,s}$, received at $(\mathbf{x}_{\rm obs}, z_{\rm obs}, \nu_{\rm obs})$ from a source of differential luminosity L_ν emitted at $(\mathbf{x}_{\rm s}, z_{\rm s}, \nu_{\rm s})$ is given by

$$F_{\nu,s}(\mathbf{x}_{\rm obs}, z_{\rm obs}, \nu_{\rm obs}) = \frac{L_\nu\left(\nu = \nu_{\rm s}\right)}{4\pi D_L^2(z_{\rm obs}, z_{\rm s})} \cdot \left(\frac{1+z_{\rm s}}{1+z_{\rm obs}}\right) \cdot \exp\left[-\tau_{\nu_{\rm obs}}\right], \tag{9}$$

Here $D_L(z_{\rm obs}, z_{\rm s})$ is
the luminosity distance given by

$$D_L(z_{\rm obs}, z_{\rm s}) \equiv \left(\frac{r_{\rm os}}{1+z_{\rm obs}}\right)\left(\frac{1+z_{\rm s}}{1+z_{\rm obs}}\right), \tag{10}$$

Computational Challenge

The differential flux, $F_{\nu,s}$, received at $(\mathbf{x}_{\rm obs}, z_{\rm obs}, \nu_{\rm obs})$ from a source of differential luminosity L_ν emitted at $(\mathbf{x}_{\rm s}, z_{\rm s}, \nu_{\rm s})$ is given by

$$F_{\nu,s}(\mathbf{x}_{\rm obs}, z_{\rm obs}, \nu_{\rm obs}) = \frac{L_\nu\left(\nu = \nu_{\rm s}\right)}{4\pi D_L^2(z_{\rm obs}, z_{\rm s})} \cdot \left(\frac{1+z_{\rm s}}{1+z_{\rm obs}}\right) \cdot \exp\left[-\tau_{\nu_{\rm obs}}\right], \qquad (9)$$

Here $D_L(z_{\rm obs}, z_{\rm s})$ is the luminosity distance given by

$$D_L(z_{\rm obs}, z_{\rm s}) \equiv \left(\frac{r_{\rm os}}{1+z_{\rm obs}}\right)\left(\frac{1+z_{\rm s}}{1+z_{\rm obs}}\right), \qquad (10)$$

- Expected number of computational operations : $\sim N_{sources} * N_{cells} * N_{frequencies}$
  where $N_{sources} >\sim 10^7$ within the LW horizon of $r_{LW} \sim 100$ cMpc
  $N_{cells} >\sim 10^6$ grid cells for sufficient resolution and statistical accuracy
  $N_{frequencies} >> 1$ for multi-frequency transfer of optically thick Lyman series lines

➔ *full 3D, multi-frequency radiative transfer would be prohibitive!!*

Computational Challenge

The differential flux, $F_{\nu,s}$, received at $(\mathbf{x}_{\rm obs}, z_{\rm obs}, \nu_{\rm obs})$ from a source of differential luminosity L_ν emitted at $(\mathbf{x}_{\rm s}, z_{\rm s}, \nu_{\rm s})$ is given by

$$F_{\nu,s}(\mathbf{x}_{\rm obs}, z_{\rm obs}, \nu_{\rm obs}) = \frac{L_\nu\left(\nu = \nu_{\rm s}\right)}{4\pi D_L^2(z_{\rm obs}, z_{\rm s})} \cdot \left(\frac{1+z_{\rm s}}{1+z_{\rm obs}}\right) \cdot \exp\left[-\tau_{\nu_{\rm obs}}\right], \qquad (9)$$

Here $D_L(z_{\rm obs}, z_{\rm s})$ is the luminosity distance given by

$$D_L(z_{\rm obs}, z_{\rm s}) \equiv \left(\frac{r_{\rm os}}{1+z_{\rm obs}}\right)\left(\frac{1+z_{\rm s}}{1+z_{\rm obs}}\right), \qquad (10)$$

- Expected number of computational operations : $\sim N_{sources} * N_{cells} * N_{frequencies}$
  where $N_{sources} >\sim 10^7$ within the LW horizon of $r_{LW} \sim 100$ cMpc
  $N_{cells} >\sim 10^6$ grid cells for sufficient resolution and statistical accuracy
  $N_{frequencies} >> 1$ for multi-frequency transfer of optically thick Lyman series lines

➔ *full 3D, multi-frequency radiative transfer would be prohibitive!!*

➔ **We solve this by making a grey opacity approximation equivalent to multi-freqency…**

Attenuation of LW photons from a single source: "picket-fence" modulation factor

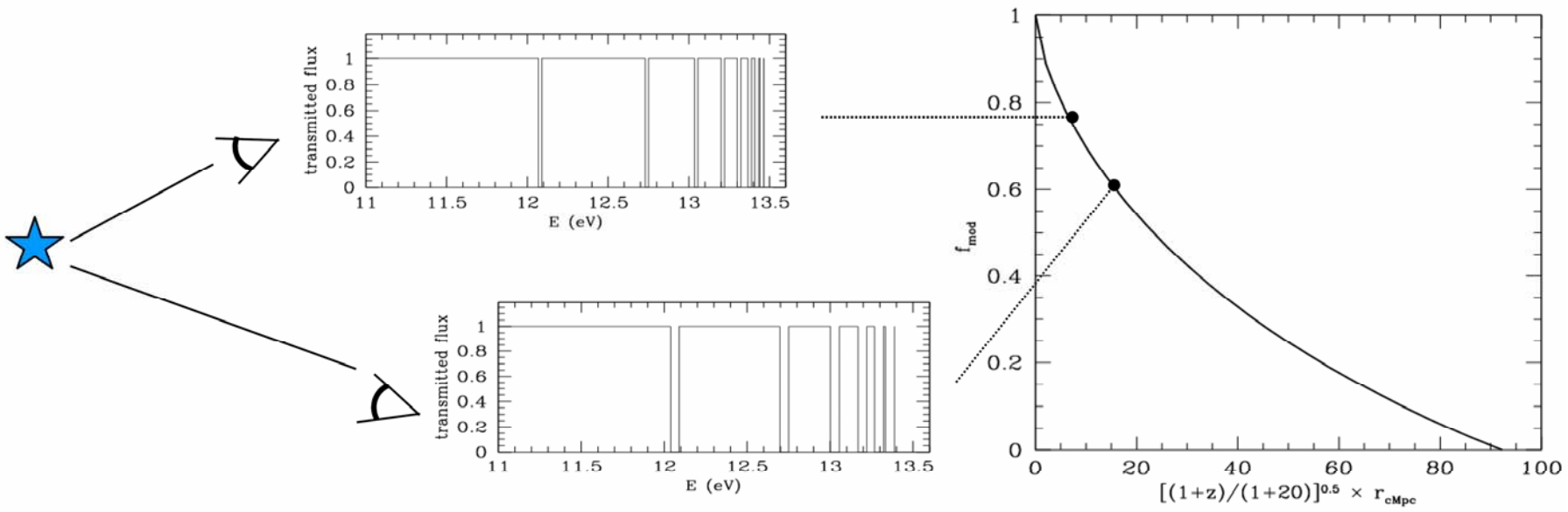

Modulation Factor

LW background radiative transfer is intrinsically cosmological : sources along the "past light-cone" of every point in space

- Space-time diagram of radiation sources and observer at point P at conformal time τ
- luminosity of each halo source is constant during finite time-step
- observer at point P will see sources whose world lines intersect the past light-cone
- must determine the attenuation, dilution, and redshift of the LW photons emitted at A and received at P

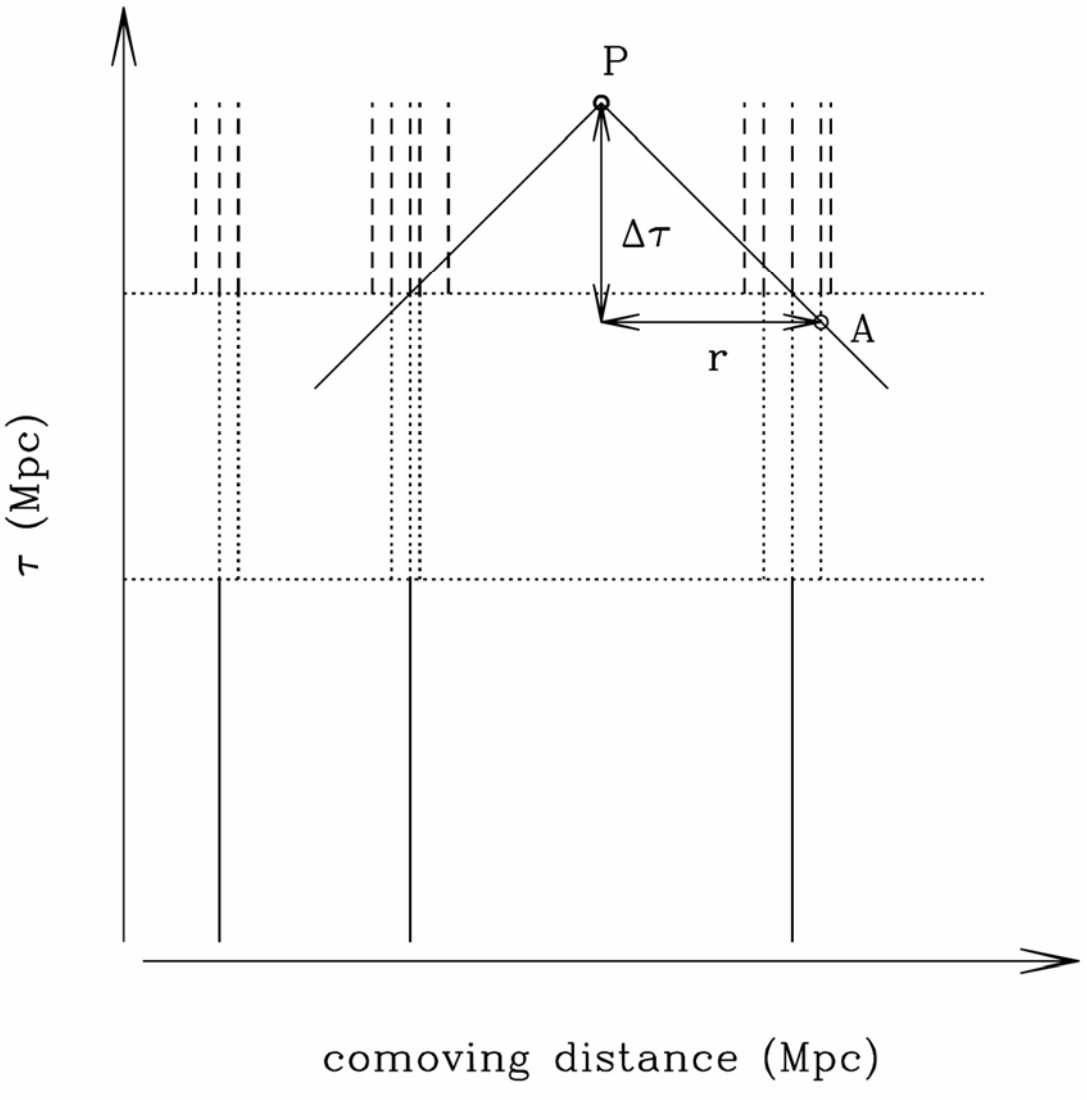

The Fluctuating H_2 Dissociating Background During Reionization

Ahn, Shapiro, Iliev, Mellema, & Pen 2008, MNRAS, submitted (astro-ph/0807.0920)

- LW background radiative transfer code parallelized using MPI for distributed-memory parallel computers;
- e.g. 35/h Mpc reionization simulation has $(203)^3$ cells, $N_{sources}$ = 200,000 by $z = 8$, but must do LW transfer in 5^3 boxes stacked around the central box to fill 100 Mpc LW horizon ➔ $N_{sources}$, total > 20 million!
- Ran for 22 hours, on 320 computing cores, 1.5 GB memory per core, Texas supercomputer *Lonestar* (5200 cores of dual-core Intel Xeon processors, with 11.6 TB aggregate memory).

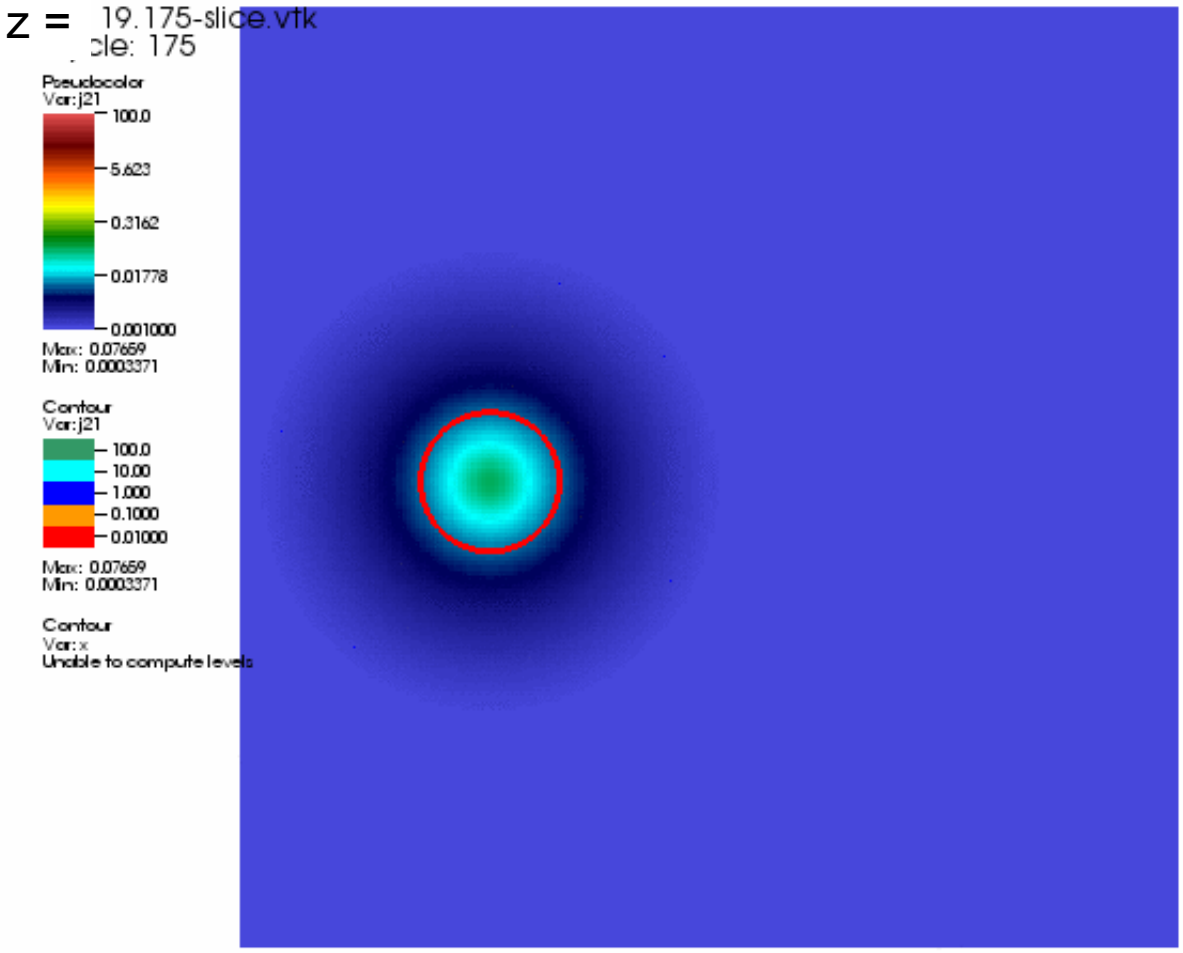

35/h Mpc box

H_2 Dissociating Background during EOR

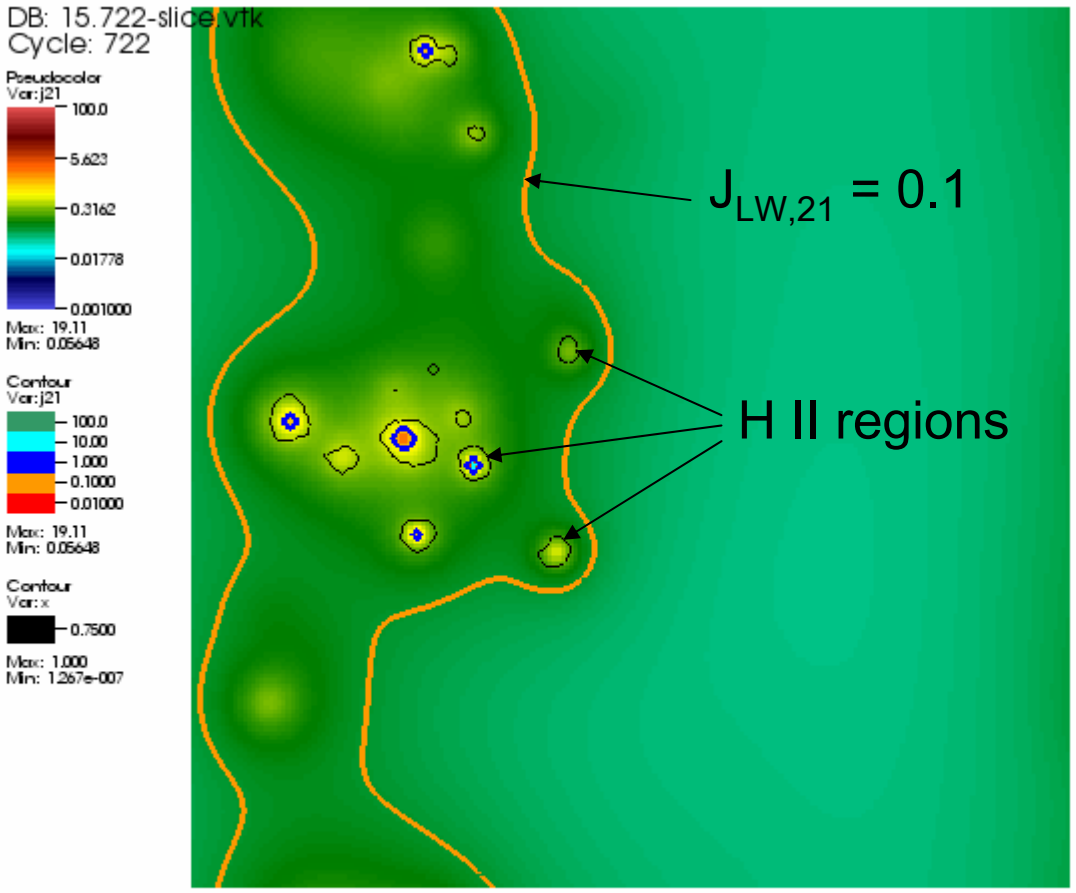

H_2 Dissociating Background during EOR

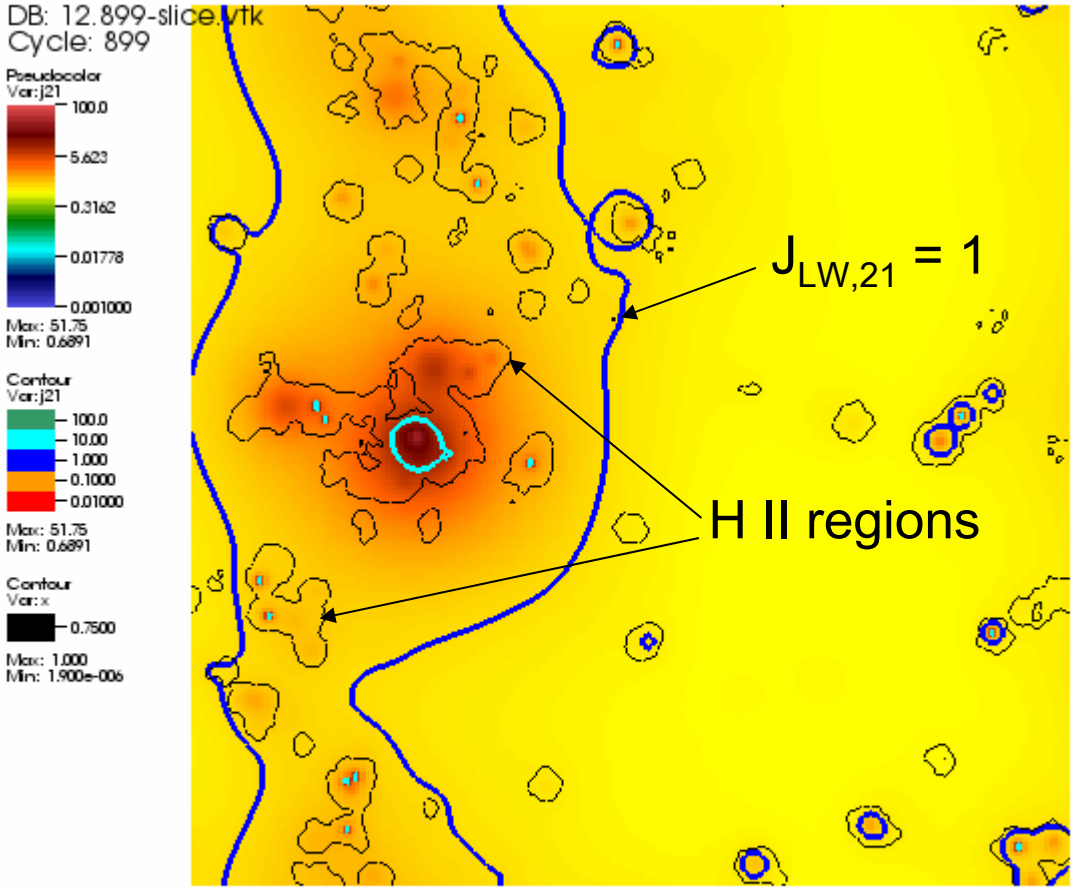

Z=19.175; <x>=10^{-5}

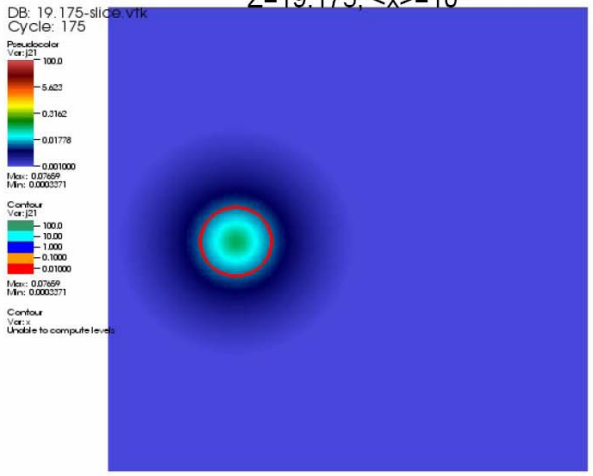

Z=16.602; <x>=10^{-3}

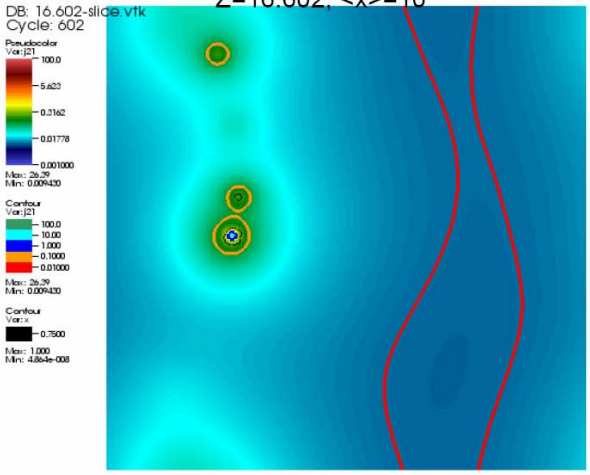

Z=15.722; <x>=10^{-2}

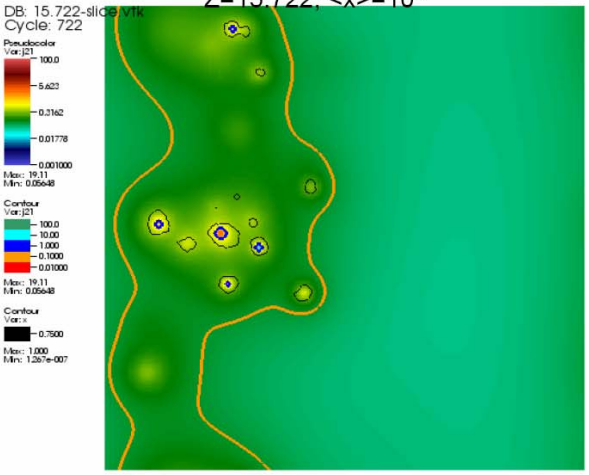

Z=12.899; <x>=10^{-1}

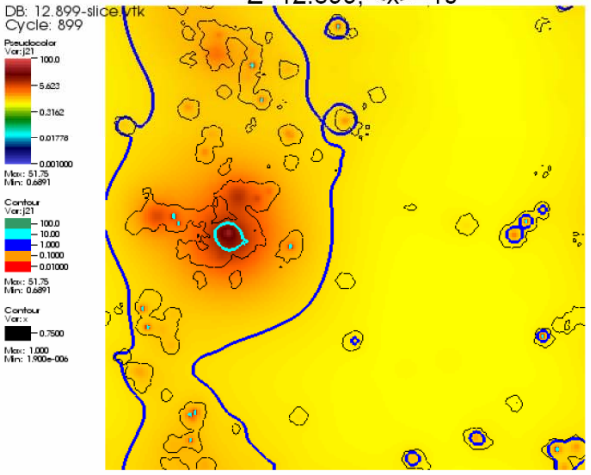

Z=10.279; <x>=0.7

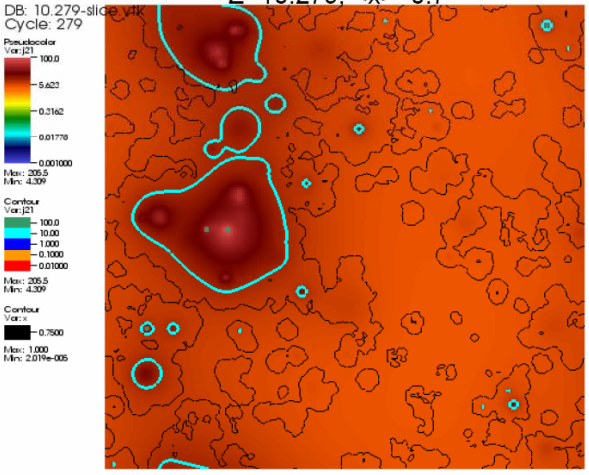

Z=9.625; <x>=0.8

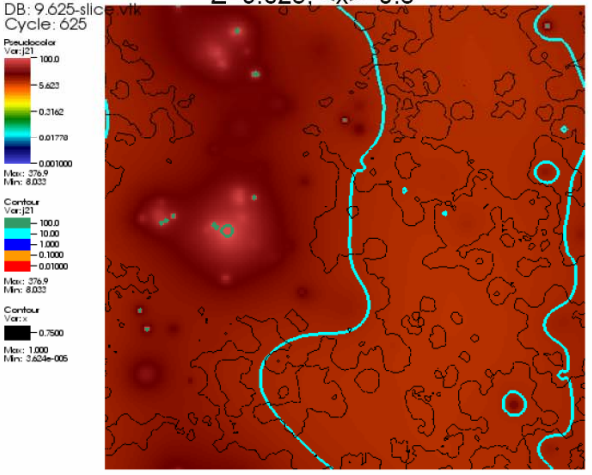

The Mean H_2 Dissociating UV Background During EOR

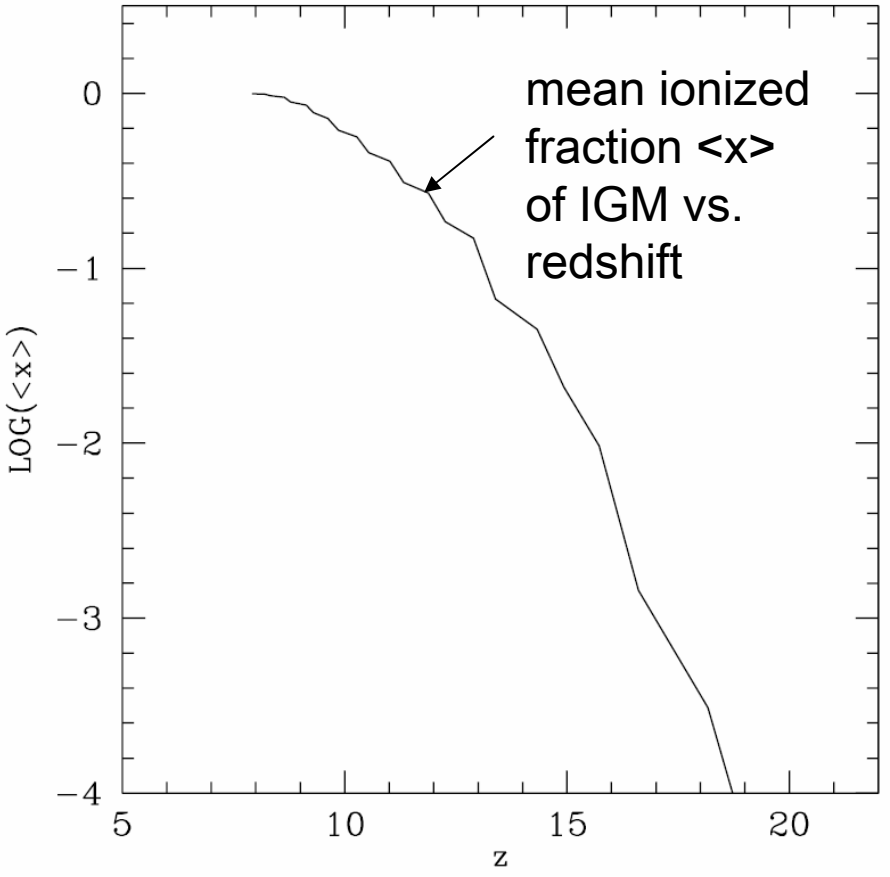

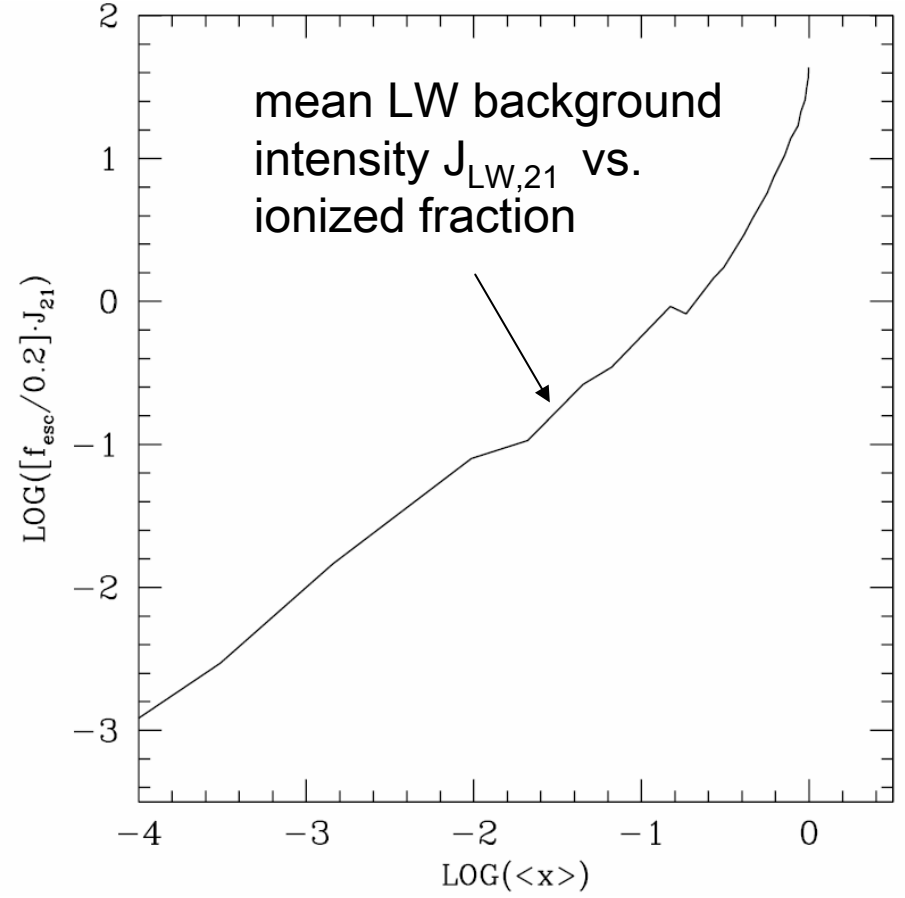

$J_{LW,\,21}$ = J/(10^{-21} erg $s^{-1}cm^{-2}$ Hz^{-1} $ster^{-1}$)

Distribution of Intensity Fluctuations for the LW Background During Reionization

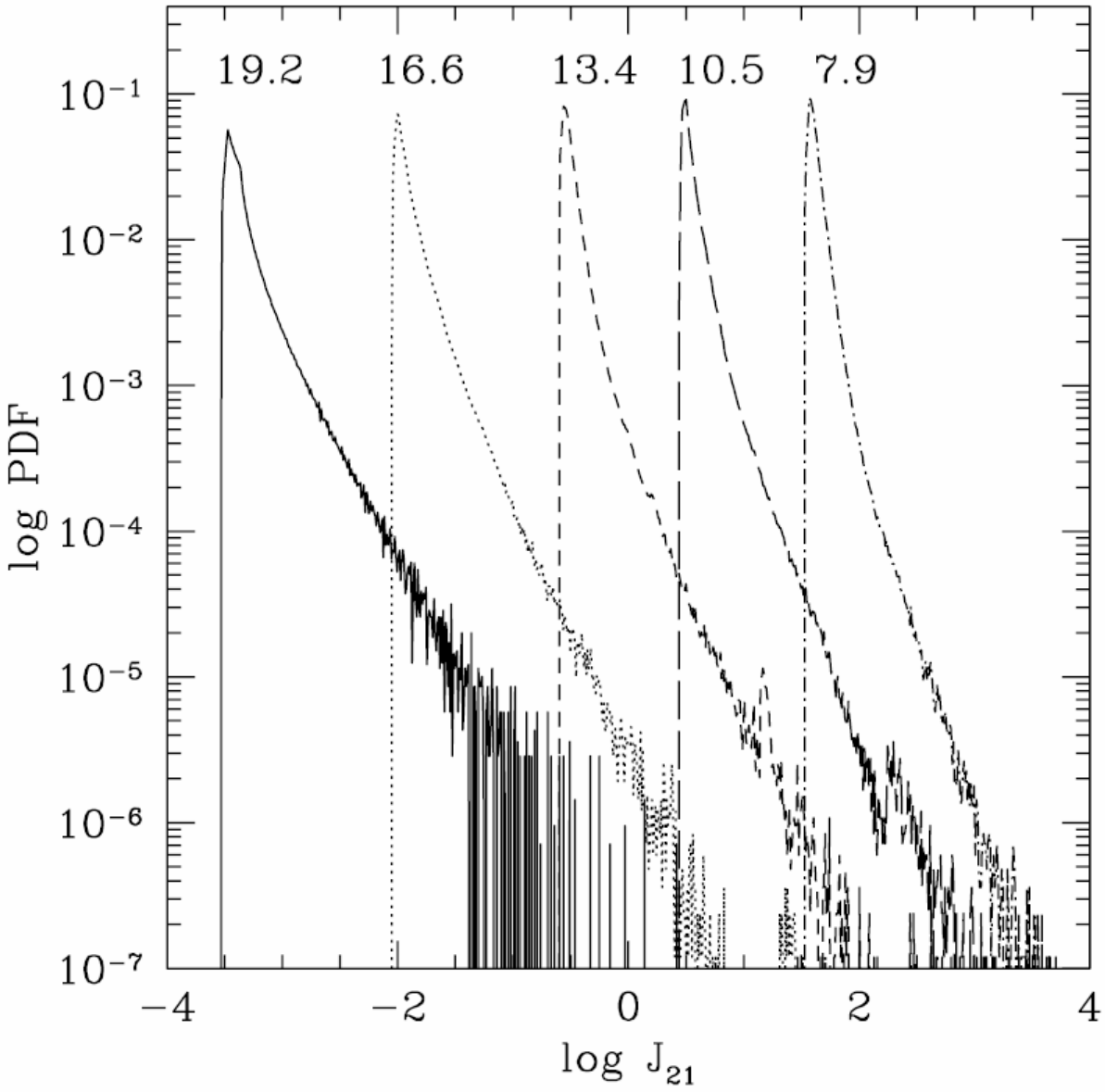

(35/h Mpc box)

What are the dominant sources of the LW background during the EOR?

- Self-regulation of reionization

➔ early LW background is dominated by low-mass sources that are suppressed if they form inside H II regions,

BUT the rise of the small-mass sources saturates long before end of EOR

➔

the high-mass sources eventually dominate the LW background

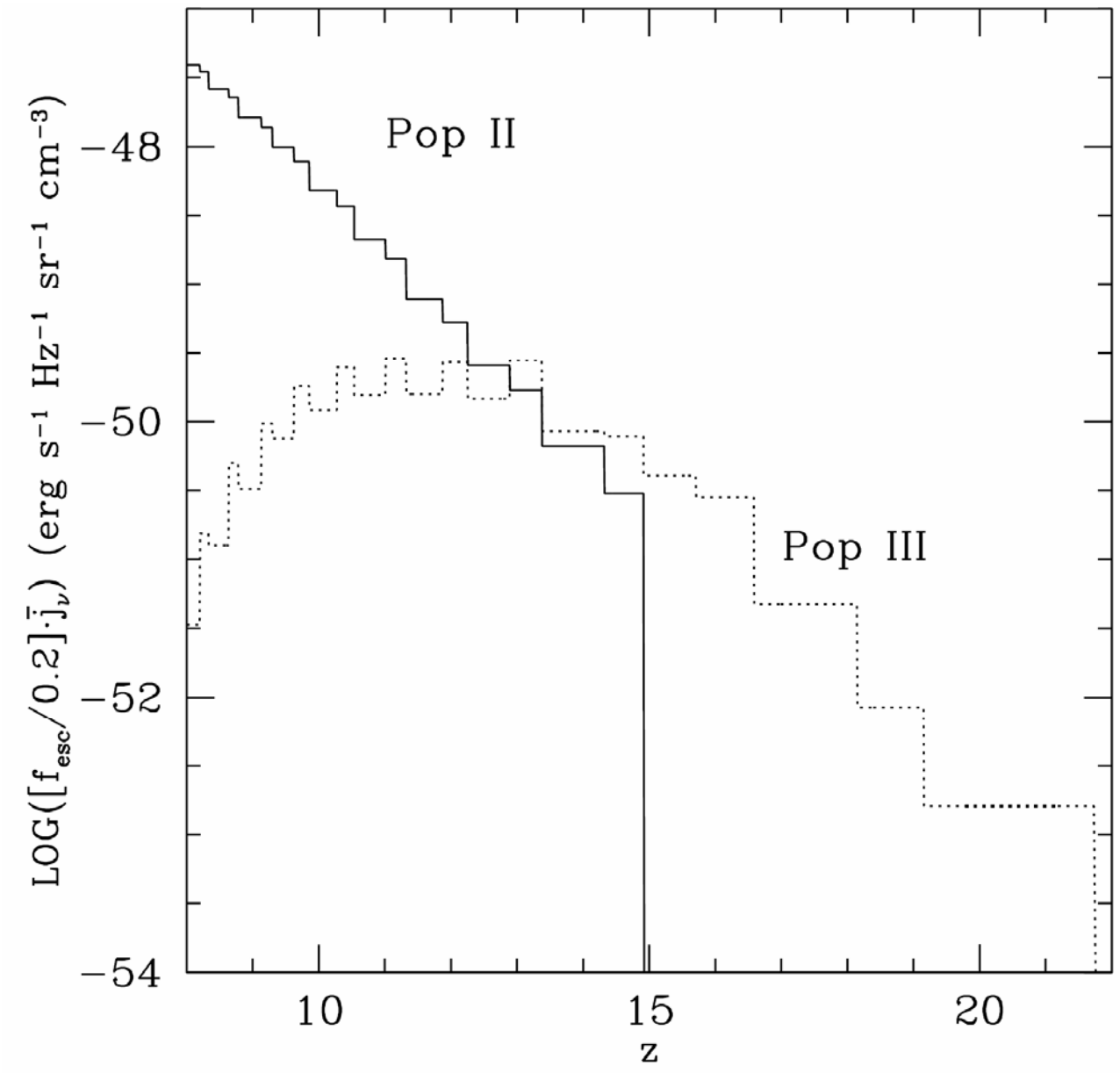

LW background intensity fluctuations in space are correlated with matter density fluctuations

z = 19

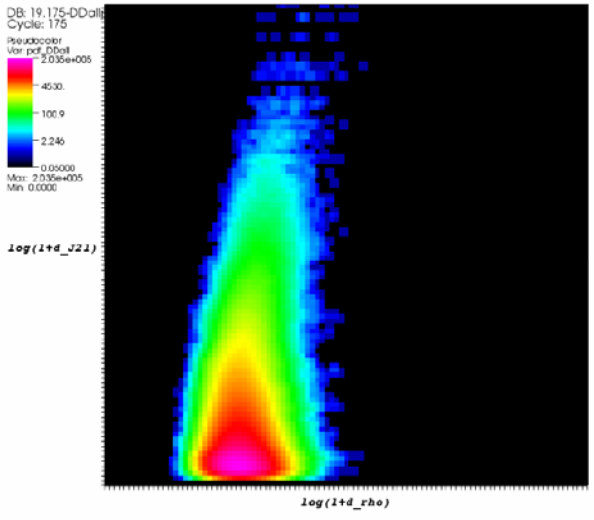

z = 13

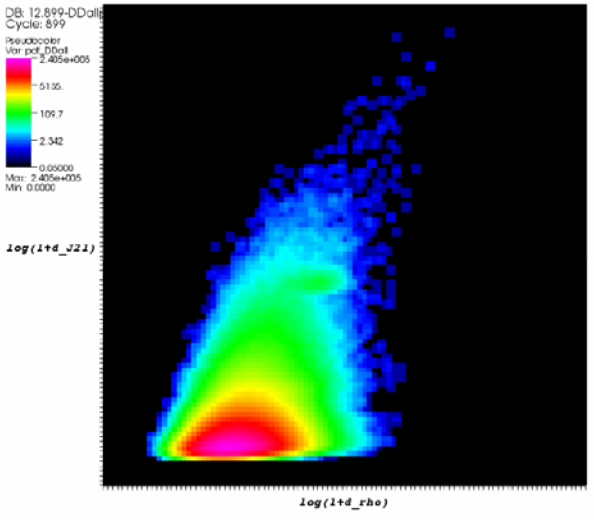

z = 12

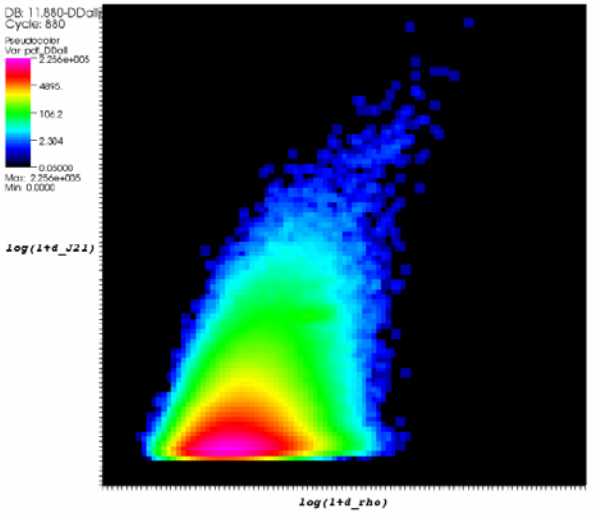

LW Background Conclusions

- Picket-fence modulation of LW background photons
  - makes computation of inhomogeneous LW background tractable

- LW rises above the threshold for suppressing star formation in minihalos long before end of the EOR➔ supports the idea that MHs, on average, not significant reionization source, but

- LW intensity fluctuates significantly in space ➔may be "safe spots" early on, to form Pop III stars in minihalos where LW background minima occur, far from the large-scale H II regions made by clustered dwarf galaxies.

- Fluctuation in LW background comes from source clustering, at a scale of ~10 comoving Mpc

- May contribute to NIR background fluctuations

- Understanding radiative feedback on Pop III star formation in minihalos may be important to complete the theory of reionization

Feedback From First Radiation Sources: H^- Photodissociation

Chuzhoy, Kuhlen, & Shapiro (2007), ApJL, 665, L85 (astro-ph/0704.0426)

- Rate for H_2 formation in primordial gas,

$$H^- + H \rightarrow H_2 + e^-$$

is proportional to abundance of H^- ===> destroying H^- will reduce H_2 formation rate;

- Photodissociation can destroy H^-,

$$H^- + \gamma \rightarrow H + e^- \qquad (\nu \geq 0.755 \text{ eV});$$

- During reionization, as sources release ionizing radiation, they also cause a background of H^- dissociating radiation to build up, which reduces the H_2 formation rate by factor F_s,

$$F_s \sim 1 + 1000\, k_s\, x / (f_{esc}\, \delta) ,$$

where x = cosmic mean ionized fraction, δ = local baryon gas overdensity, and k_s = a constant of order unity which depends on type of radiation source (e.g. recombination radiation, direct stellar or quasar emission, or secondary emission by nonthermal electrons following X-ray background ionization) ;

- Hence, by the time $x \gtrsim 0.1$, H^- photodissociation may significantly reduce H_2 abundance and cooling, and the rate of primordial star formation.

More Feedback From First Radiation Sources: H^- Photodissociation

Chuzhoy, Kuhlen, & Shapiro (2007), ApJL, 665, L85 (astro-ph/0704.0426)

- Rate for H_2 formation in primordial gas,

$$H^- + H \rightarrow H_2 + e^-$$

is proportional to abundance of H^- ===> destroying H^- will reduce H_2 formation rate;

- Photodissociation can destroy H^-,

$$H^- + \gamma \rightarrow H + e^- \qquad (\nu \geq 0.755 \text{ eV});$$

- **During reionization, as sources release ionizing radiation, they also cause a background of H^- dissociating radiation to build up, which reduces the H_2 formation rate by factor F_s,**

$$\mathbf{F_s \sim 1 + 1000\, k_s\, x / (f_{esc}\, \delta)\ ,}$$

where x = cosmic mean ionized fraction, δ = local baryon gas overdensity, and k_s = a constant of order unity which depends on type of radiation source

(e.g. recombination radiation, direct stellar or quasar emission, or secondary emission by nonthermal electrons following X-ray background ionization) ;

- **Hence, by the time x ≳ 0.1, H^- photodissociation may significantly reduce H_2 abundance and cooling, and the rate of primordial star formation.**

Cosmological Radiative Transfer Codes Comparison Project I. : The Static Density Field Tests

Iliev, Ciardi, …, Shapiro, … (2006) MNRAS, 371, 1057